Title
Spatial Regulation of Gene Expression in Neurons During Synapse Formation and Synaptic Plasticity

Author
Kim, Sangmok

Publication Date
2013

Peer reviewed|Thesis/dissertation

UNIVERSITY OF CALIFORNIA

Los Angeles

Spatial Regulation of Gene Expression in Neurons During Synapse Formation and Synaptic Plasticity

A dissertation submitted in partial satisfaction

of the requirements for the degree Doctor of Philosophy

in Neuroscience

by

Sangmok Kim

2013

ABSTRACT OF THE DISSERTATION

Spatial Regulation of Gene Expression in Neurons During Synapse Formation and Synaptic Plasticity

Sangmok Kim

Doctor of Philosophy in Neuroscience

University of California, Los Angeles, 2013

Professor Kelsey C. Martin, Chair

mRNA localization and regulated translation allow individual neurons to locally regulate the proteome of each of their many subcellular compartments. To investigate the spatial regulation of gene expression during synaptic plasticity, we used a translational reporter system to demonstrate synapse- and stimulus-specific translation during long-term facilitation of *Aplysia* sensory-motor synapse. These studies revealed a role for a retrograde signal from the postsynaptic motor neuron in regulating translation in the presynaptic sensory neuron. Additional studies with the translational reporter demonstrated that distinct cis-acting localization elements were involved in targeting mRNA to distal neurites and to synapses. Our studies identified a 66 nucleotide long stem loop structure that directs mRNAs to synapses.

In the final part of my thesis research, I addressed the question of whether and how synaptogenic signals direct mRNA targeting and spatially regulate gene expression

during synapse formation. I cultured a bifurcated *Aplysia* sensory neuron contacting a nontarget motor neuron, with which it did not form chemical synapses, and a target motor neuron, with which it formed glutamatergic synapses, and imaged RNA and protein localization. I find that RNAs and translational machinery are delivered throughout the neuron, but that translation is enriched at sites of synaptic contact. Investigation of the molecular mechanisms that promote local translation revealed a role for netrin1-DCC signaling. Together, my research indicates that the spatial regulation of gene expression during synapse formation and during synaptic plasticity is mediated at the level of translation. This mechanism maximizes neuronal plasticity by rendering each compartment capable of locally changing its proteome in response to local cues.

The dissertation of Sangmok Kim is approved.

_____

Alcino J. Silva

_____

Douglas Black

_____

Thomas J. O'Dell

_____

Kelsey C. Martin, Committee Chair

University of California, Los Angeles

2013

Dedication

To my parents, my wife Yunjung, my daughter Da-In and teachers

TABLE OF CONTENTS

LIST OF FIGURES AND TABLES

Chapter 2

Chapter 3

Chapter 4

ACKNOWLEDGMENTS

First and foremost, I would like to thank Kelsey Martin for giving me the opportunity to encourage and pursue this study and my degree. I never imagine meeting her as my wonderful Mentor. She is really thoughtful and respectable person and also allows me to do whatever I want to do. I learned a lot of things from her. She taught me how I can do science and be a good scientist. I couldn't finish my research without her efforts and considerations. Also, I will always keep in my mind her word "Little is better than nothing" for my future work as long as I can.

Many thanks to my committee member: Alcino Silva, Doug Black and Tom O'Dell who also advised and helped to finish this thesis. All the time, they encouraged and directed me throughout this project with wonderful discussions.

I would like to acknowledge all previous my mentors: Professor Sanghwa Han who was my first mentor and taught me how to learn a science, Professor Paul Worley and David Linden whom I started to learn neuroscience and interested in.

I would like to thank all of Martin's lab members who make me to be humble with their insights and friendships. I'd like to acknowledge Ohtan Wang who is the first author of Chapter II and III and initiated this project when I rotated and also Elliott Meer who is the first author of Chapter III.

I would like to acknowledge my friends, Besim Uzgil and Yong-Seok Lee for support, both scientifically and personally, and also sincerely friendships in the field in the Saturday morning.

Finally, I would like to thank my parents, Man-soo and Soonsub, for their continued support throughout my life. And a special thanks to my wife, Yunjung and daughter, Da-In. There are no words to express how I am grateful.

VITA

2001	B.S., Biochemistry Kangwon National University, Korea
2003	M.S., Biochemistry Kangwon National University, Korea
2003-2004	Research Associate, Biology Kyong-Hee University, Korea
2004-2006	Visiting Scientist, Neuroscience John Hopkins University, Maryland

PUBLICATIONS AND PRESENTATIONS

Meer EJ, W.D., **Kim S**, Barr I, Guo F, Martin KC. (2012). Identification of a cis-acting element that localizes mRNA to synapses. Proc Natl Acad Sci U S A *109*, 4639-4644.

Hu JH, P.J., Park S, Xiao B, Dehoff MH, **Kim S**, Hayashi T, Schwarz MK, Huganir RL, Seeburg PH, Linden DJ, Worley PF. (2010). Homeostatic scaling requires group I mGluR activation mediated by Homer1a. Neuron *68*, 1128-1142.

Wang DO, **Kim S**, Zhao Y, Hwang H, Miura SK, Sossin WS, Martin KC. (2009). Synapse- and stimulus-specific local translation during long-term neuronal plasticity. Science *324*, 1536-1540.

Park S, P.J., **Kim S**, Kim JA, Shepherd JD, Smith-Hicks CL, Chowdhury S, Kaufmann W, Kuhl D, Ryazanov AG, Huganir RL, Linden DJ, Worley PF. (2008). Elongation factor 2 and fragile X mental retardation protein control the dynamic translation of Arc/Arg3.1 essential for mGluR-LTD. Neuron *59*, 70-83.

Kim SM, H.S. (2003). Tyrosinase scavenges tyrosyl radical. Biochem Biophys Res Commun *312*, 642-649.

Lee YK, **Kim S**, Han S. (2003). Ozone-induced inactivation of antioxidant enzymes. Biochimie *85*, 947-952.

(Hu JH, 2010; Kim SM, 2003; Lee YK, 2003; Meer EJ, 2012; Park S, 2008; Wang DO, 2009)

CHAPTER ONE

INTRODUCTION

INTRODUCTION

mRNA localization and local translation mediate spatial regulation of gene expression in asymmetric cells

Synapse formation is an intricate process that occurs during brain development and during activity-dependent rewiring of neural circuits. The formation of stable synapses requires new RNA and protein synthesis, and many studies have shown that messenger RNA (mRNA) localization as well as local translation permits compartmentalized changes in the synaptic proteome during this process. mRNA localization and local translation play important roles in the posttranscriptional regulation of gene expression within specific subcellular compartments and thus provide a mechanism for spatially restricting gene expression in asymmetric cells (Martin et al., 2009; Shav-Tal et al., 2005). In neurons, this process allows subcellular compartments such as growth cones and dendrites to undergo localized changes in protein composition in response to stimuli, and has been shown to be critical to axon guidance, synapse formation, synaptic plasticity and regeneration following axonal injury (Sutton and Schuman, 2006; Willis and Twiss, 2006; Jung et al., 2012). Studies of mRNA localization and local translation have revealed that a large number of transcripts localize to subcellular compartments, subserving a wide and diverse range of cellular functions (Moccia et al., 2003; Poon et al., 2006; Eberwine et al., 2002; Cajigas et al., 2012).

In the early 1990s, studies of mRNA localization in a variety of asymmetric cell types revealed the existence of distinct mechanisms of localization including diffusion,

local entrapment, and active transport. In budding yeast, the mRNA encoding the translational repressor ASH1 is localized to the bud tip of the dividing cell using a directed transport mechanism (Paquin and Chartrand, 2008). During early development in *Drosophila melanogaster*, the localization of *gurken, oskar, bicoid, and nanos* mRNAs is required for the establishment of morphogenetic gradients in the developing embryo. While *bicoid* mRNA localization involves directed targeting, *nanos* mRNA involves locally regulated stabilization as well as diffusion and entrapment mechanisms (Johnstone and Lasko, 2001; Becalska and Gavis, 2009).

In the mammalian nervous system, specific mRNAs localize to neuronal axons and/or dendrites. For example, the mRNA encoding Tau is selectively targeted to axons in developing neuron while the mRNA encoding CamKIIα and MAP2 localize to dendrites in mature neurons (Litman et al., 1993; Mayford et al., 1996). The mRNA encoding β-Actin localizes to both growth cone in axons and filopodial protrusions in dendrites in developing neurons (Bassell et al., 1998). The local translation of β-actin mRNA mediates chemoattactive growth cone turning in response to neutrophic factors such as BDNF or Netrin-1 (Yao et al., 2006; Leung et al., 2006). This process of axon guidance is essential to the formation of precise functional circuits.

Recent studies showed that the disruption of β-actin mRNA localization and local translation abolished BDNF-induced growth cone turning (Yao et al., 2006) and netrin-1-induced guidance (Welshhans et al., 2011), demonstrating the critical role of regulated translation in the growth cone to axon guidance.

mRNA localization and local translation during synaptic plasticity

As discussed in the previous paragraph, long-lasting learning-related synaptic plasticity also requires new translation and transcription for its persistence (Martin et al., 1997, 2000; Kandel, 2001) and can occur in a synapse-specific manner (Martin et al., 1997; Frey et al., 1997 and Casadio et al., 1999). One mechanism that has been proposed to mediate this spatial restriction of gene expression during neuronal plasticity involves the regulated translation of localized mRNAs at stimulated synapses (Martin, 2004; Sutton et al., 2006). Many results support idea that local translation at synapses is required during synaptic plasticity. First, all of the machinery required for translation is present in neuronal processes, including polyribosomes (Steward et al., 1982; Ostroff et al., 2002), translation factors (Tang et al., 2002), and a subpopulation of mRNAs (Moccia et al., 2003 and Lecuyer et al., 2007). Second, studies using protein synthesis inhibitors have revealed an essential role for local translation during long-lasting synaptic plasticity (Martin et al., 1997; Kang et al., 1996 and Huber et al., 2000).

mRNA localization depends on cis- and trans-acting elements

The localization of mRNA in subcellular compartments mediates multiple processes. The active transport and asymmetric distributions of mRNAs depend on intrinsic mRNA targeting elements known as localization element or zipcode sequences, initially described for β–actin mRNA. These *cis*-acting elements are frequently located within the 3'UTR of a localized mRNA and, less frequently within the 5'UTR and coding sequences. The redundancy of localization elements has also been identified in vertebrate

cell. For example, a 54-nt zipcode sequence and a 43-nt zipcode sequence have been identified within the 3'UTR of β-actin mRNA, both of which can mediate mRNA localization (Kislauskis et al., 1994).

In mature neurons, dendritically localized CamKIIα mRNA has been found four elements including a 94-nt, 1200-nt, a cytoplasmic polyadenylation element(CPE) and G-quadruplex structure, all within 3'UTR (Mori et al., 2000; Blichenberg et al., 2001; Huang et al., 2003; Subramanian et al., 2011). Any of these four localization elements were by themselves sufficient to target mRNA to dendrites.

The secondary structure of mRNA is often a critical component of the localization element that directs mRNA into specific subcellular compartments. For example, localization of ASH1 mRNA in budding yeast depends on secondary stem-loop structures formed by localization elements (Chartand et al., 1999).

These *cis*-acting elements recruit specific trans-acting RNA binding protein to form ribonucleoprotein particles (RNPs), which then assemble into RNA transport granules. Numerous studies have demonstrated that localized mRNAs are transported by motor proteins along cytoskeletal elements to their final destinations in the cell. For example, the recruitment of multiple Myo4p myosin motor protein to the localization element increases the efficiency of ASH1 mRNA transport in yeast (Chung et al., 2010). The RNA-binding protein FMRP has been shown to correlate with dendritic mRNA transportation, and to bind to kinesin light chain (KLC) as well as to the dynein-interacting protein BicD protein (Dictenberg et al., 2008; Bianco et al., 2010)

Aplysia sensory-motor neuron cultures as a model for studying mRNA localization and local translation

The marine mollusk *Aplysia* has proven to be a useful preparation for studying mechanisms underlying synapse formation and synaptic plasticity. In *Aplysia*, the cellular and molecular mechanisms of different phases of behavioral memory have been extensively studied. Studies of the gill-withdrawal reflex in *Aplysia* have provided insights into short-term and long-term learning processes. This simple behavior exhibits three learning-related forms of plasticity familiar in vertebrates: habituation, sensitization, and classical conditioning (Abrams and Kandel, 1988; Glanzman, 1995; Lechner and Byrne, 1998).

The best characterized form of learning-related plasticity in *Aplysia* is sensitization, in which a behavioral reflex response elicited by a weak stimulus becomes greater in magnitude and duration following a noxious stimulus to the tail. A weak stimulus (single tail shock) induces short-term sensitization that last for few minutes but a repeated strong shock produces long-lasting sensitization that can persist for days or even weeks. Long-term sensitization differs from short-term sensitization in its requirement for new RNA and protein synthesis. The circuit underlying the gill-withdrawal reflex can be reconstituted *in vitro* by culturing a single sensory neuron together with motor neuron, with which the sensory neuron will form glutamatergic synapses. Long-term facilitation of these synaptic connections mirrors long-term sensitization of the gill-withdrawal reflex and can be induced by repeated application of the neurotransmitter serotonin (5-HT). A single application of 5-HT induces short-term facilitation (STF) lasting minutes, but five

spaced 5-HT pulses induce long-term facilitation (LTF) lasting at least 24 hours. This form of LTF is synapse-specific, and has been shown to depend on the regulated translation of synaptically localized mRNAs (Martin et la., 1997; Moccia et al., 2003).

The 5-HT application, but not the FMRFamide, induced *de-novo* translation of Dendra2, but only when the SN was contacting a target MN. If the SN was cultured together with a nontarget MN, no new translation resulted from the stimuli (Wang et al., 2009). Furthermore, SNs only form chemical synapses with appropriate target MNs (Lyles et al., 2006; Glanzman et al., 1989), allowing local translation to be studied in the presence or absence of synapses.

Netrins, a retrograde signal to regulate translation during synapse formation

Netrins has been shown to regulate the attraction or repulsion of commissural axonal growth cones and to serve as a guidance cue for migrating neuron (Kennedy et al., 1994; Alcantara et al., 2000). The first reported member of the netrin family, uncoordinated-6 (UNC-6), was identified as a gene product that regulates neural development in *Caenorhaditis* elegans(C.elegans) (Ishii et al., 1992). Netrins have been identified and studied in both vertebrate and invertebrate species. In mammals, there are three secreted netrins: netrin 1, 3 and 4, as well as two membrane-tethered glycophosphatidylinositol (GPI)-linked netrins, netrin G1 and G2.

Netrin-1 is the evolutionarily conserved vertebrate homolog of the *C.elegans* UNC-6 protein. It is involved in axon guidance and cell migration (Livesey, 1999) and is expressed in regions of the both developing and mature nervous systems, including the

optic disc, forebrain, cerebellum and spinal cord (Deiner et al., 1997; Hamasaki et al., 2001; Kennedy et al., 1994 Livesey and Hunt, 1997). Netrin-1 is also highly expressed in various non-neuronal tissues including the developing heart, lung, pancreas, intestine and mammary gland (Liu et al., 2004; Shin et al., 2007; Srinivasan et al., 2003; Yebra et al., 2003; Zhang and Cai, 2010).

While netrins are widely expressed in various tissues, they have primarily been studied in the context of axon guidance during neural development. The results of many studies support the idea that netrins play a role as long-range chemotropic guidance cues for growth cone in the embryonic vertebrate CNS where they also regulate axon branching. For example, netrin-1 promotes *de novo* axon branch formation by rapidly inducing Ca^{2+} transients, polymerization of F-actin, and the formation of filopodial protrusions that may become a branch point (Dent et la., 2004; Tang et al., 2005).

In mammals, netrin receptors include deleted in colorectal cancer (DCC), the DCC paralogue neogenin, the UNC-5 homologues UNC5A-D and Down syndrome cell adhesion molecule (DSCAM) (Fearon et al., 1990; Cho et al., 1994; Leonardo et al., 1997; Andrews et al., 2008). DCC was first identified in humans as a candidate tumor suppressor associated with allelic deletion of chromosome 18q21in colon cancer (Fearon et al., 1990). More recent studies defined a role for DCC in axon growth and guidance (Keino-Masu et al., 1996; Fazeli et al., 1997). DCC has also been shown to localize postsynaptically in dendrites (Parent et al., 2005). In addition, Flanagan and colleagues reported that DCC forms a complex containing both multiple translation components, including translation initiation factors and ribosomal subunits, with netrin binding

triggering disassociation of translation components from DCC promote translation (Tcherkezian et al., 2010).

Objective of Thesis

In this thesis, I asked the following questions: 1) how do neurons regulate the local synaptic proteome during synapse formation and synaptic plasticity? And if so, 2) how are RNAs synaptically localized during synapse formation? And 3) is the spatial restriction of gene expression is mediated primarily at the level of mRNA targeting or translational regulation?

A localized transcript is regulated in a synape- and stimulus-specific manner.

To study how neurons change the local proteome during synaptic plasticity, I developed a translational reporter consisting of the photoconvertible fluorophore Dendra2, fused to the 5' and 3' UTRs of sensorin mRNA, which found were sufficient for synaptic localization of the mRNA (Wang et al., 2009). This part of the thesis work was done in collaboration with post-doctoral fellow Dr. Dan Ohtan Wang, We first determined that the sensorin mRNA 3'UTR was sufficient for localization to neurites, whereas addition of the 5'UTR was required for synaptic localization, so in subsequent experiment for this part of the thesis, we used Dendra2 fused to both the 3'UTR and 5'UTR. We expressed the Dendra2-sensroin 5'3'UTR in sensory neurons in *Aplysia* SN-MN cocultures, and used.

Described above, we gave five spaced applications of serotonin (5X5HT) to induce transcription-dependent long-term facilitation (LTF) of SN-MN or five spaced application of the neuropeptide FMRFamide(5XFMRFamide) to induce transcription-dependent long-term depression (LTD). LTF induced in this manner parallels long-term sensitization of the gill-withdrawal reflex (Kandel, 2001), whereas FMRFamide induced a LTD that parallels long-term habituation of the gill-withdrawal reflex (Castellucci et al., 1990; Mackey et al., 1987). Synapse-specific, transcription-dependent LTF of SN-MN synapses is blocked by perfusion of translational inhibitors to distal SN neurites (Martin et al., 1997).

Finally, we showed that local translation of reporter RNA during long-term facilitation requires postsynaptic calcium. This finding indicates that a retrograde signal from the motor neuron is required for serotonin-induced translation in the sensory neuron.

A stem-loop structure in the sensorin 5'UTR directs this mRNA to synapses

We next wanted to find out what aspects of the sensorin 5'UTR mediated synaptic localization of the mRNA. This part of my thesis was collaboration with Dr. Dan Ohtan Wang and graduate student Elliot Meer in Martin lab. We were interested in finding out whether it was the nucleotide sequence or the secondary structure of the 5'UTR that conferred synaptic targeting. To do this, we generated a series of deletion and point mutations in the 5'UTR, some that resulted in a different nucleotide sequence but the same general secondary structure, and some where the secondary structure were collapsed but different part of the nucleotide sequence retained. We identified a 66-nt-

long-stem-loop cis-element in the sensorin 5'UTR that was required for synaptic localization during synapse formation.

Spatially regulated gene expression is achieved by local translation, not by mRNA targeting

Studies showing highly specific patterns of subcellular mRNA localization in asymmetric cells have suggested that mRNA targeting mediates protein localization (Lecuyer et al., 2007). Similarly, studies of activity-dependent localization of *Arc* mRNA in hippocampal dentate granule cell dendrites following perforant pathway stimulation have suggested that mRNA targeting locally regulates gene expression during synapse-specific forms of neuronal plasticity (Steward et al., 2001). On the other hand, studies of synaptic tagging during neuronal plasticity have suggested that the products of gene expression are targeted throughout the neuron, and can be captured at any synapse with subsequent subthreshold stimulation (Casadio et al., 1997; Fonseca et al., 2004). These findings are more consistent with cell-wide distribution of transcripts, with regulated translation controlling local gene expression.

Using the *Aplysia* sensory-motor culture system, I set out to directly determine whether spatial regulation of gene expression during synapse formation was mediated primarily by mRNA localization or by local translation. Second, using a translational reporter protein, consisting of a localized transcript (sensorin mRNA) fused to the photoconvertible protein Dendra2, I investigated the regulation of local translation at the synapse during synaptic plasticity and during synapse formation.

To study mRNA localization during synapse formation, I cultured a single bifurcated sensory neuron with a target (L7) neuron, with which it forms a glutamatergic synapse, and a nontarget (L11) neuron, with which it fasciculates but does not form a chemical synapse (Glanzman et al., 1989). I then asked whether and how synaptogenic stimuli regulate RNA and protein localization and concentration by analyzing the distribution of ribosomal RNA (rRNA), messenger RNA (mRNA), RNA binding proteins and translation factors. I find that rRNA, mRNA, ribosomal proteins and translation factors are delivered throughout the sensory neuron, to both synaptic and non-synaptic sites, but that translation is significantly enriched at sites of synaptic contact. These results indicate that the spatial regulation of gene expression in neurons is mediated at the level of translation rather than at the level of RNA localization.

In investigating the nature of the synaptic signals that stimulate translation during synapse formation, I find that netrin-1, a chemoattractant known to promote translation in growth cones during axon guidance (Campbell and Holt, 2001), is sufficient to promote translation of localized mRNAs at nonsynaptic sites. My findings are thus consistent with neurons delivering transcripts and translational machinery throughout the neuron, but with a synaptically restricted netrin-1-dependent signal triggering localized translation at synapses.

Summary

The studies described in Chapter Two of this thesis provide direct evidence that local translation occurs at synapses in response to stimuli that induce transcription-

dependent, learning-related synaptic plasticity. First, translational regulation of the reporter is stimulus-specific, occurring during 5HT-induced LTF but not during FMRFamide-induced LTD. Second, 5HT does not regulate translation of all localized transcripts (because translation of the 3′UTR reporter is not stimulated), indicating that translational regulation is transcript-specific. Finally, stimulus-induced translation of the reporter requires calcium signaling in the postsynaptic MN, suggesting that a trans-synaptic retrograde signal is required for the regulation of local translation during neuronal plasticity.

The studies described in Chapter Three of my thesis identify a cis-acting localization element that mediates localization of mRNA to neuronal synapses.

Finally, in Chapter Four, I describe studies using a single bifurcated Aplysia sensory neuron with an L7 target and an L11 non-target motor neuron to address the question of whether changes in the local proteome is regulated primarily at the level of translation rather than mRNA targeting during synapse formation. My results show that localized transcripts, ribosomes and translational machinery are evenly distributed in neuron, but that translation is specifically enhanced at synaptic contact sites that receive synaptogenic signals. I further show that netrin-1 may serve as a retrograde signaling molecule to regulate translation during synapse formation. In addition, my studies show that localized translation occurs in a synapse-specific manner during long-term plasticity in a manner that is dependent on postsynaptic calcium. I hypothesize that postsynaptic calcium is required for the release of retrograde signaling molecules, such as Netrin-1, during synaptic plasticity.

Localized translation as a mechanism of gene regulation during synapse formation and during synaptic plasticity poses considerable advantages to the wiring and activity-dependent rewiring of the nervous system because it renders every subcellular compartment, from dendrites and axons to synapses and growth cones, capable of locally changing their proteome, and hence their structure and function, in response to local stimuli.

REFERENCES

Abrams TW, K.E. (1988). Is contiguity detection in classical conditioning a system or a cellular property? Learning in Aplysia suggests a possible molecular site. Trends Neurosci *11*, 128-135.

Alcántara S, R.M., De Castro F, Soriano E, Sotelo C. (2000). Netrin 1 acts as an attractive or as a repulsive cue for distinct migrating neurons during the development of the cerebellar system. Development *127*, 1359-1372.

Andrews GL, T.S., Farmer WT, Morin S, Brotman S, Berberoglu MA, Price H, Fernandez GC, Mastick GS, Charron F, Kidd T. (2008). Dscam guides embryonic axons by Netrin-dependent and -independent functions. Development *135*, 3839-3848.

Becalska AN, G.E. (2009). Lighting up mRNA localization in Drosophila oogenesis. Development *136*, 2493-2503.

Cajigas IJ, T.G., Will TJ, tom Dieck S, Fuerst N, Schuman EM. (2012). The local transcriptome in the synaptic neuropil revealed by deep sequencing and high-resolution imaging. Neuron *74*, 453-466.

Campbell DS, H.C. (2001). Chemotropic responses of retinal growth cones mediated by rapid local protein synthesis and degradation. Neuron *32*, 1013-1026.

Casadio A, M.K., Giustetto M, Zhu H, Chen M, Bartsch D, Bailey CH, Kandel ER. (1999). A transient, neuron-wide form of CREB-mediated long-term facilitation can be stabilized at specific synapses by local protein synthesis. Cell *99*, 221-237.

Casadio A, M.K., Zhu H, Yaping E, Rose JC, Chen M, Bailey CH, Kandel ER. (1997). Synapse-specific, long-term facilitation of aplysia sensory to motor synapses: a function for local protein synthesis in memory storage. Cell *91*, 927-938.

Cho KR, O.J., Simons JW, Hedrick L, Fearon ER, Preisinger AC, Hedge P, Silverman GA, Vogelstein B. (1994). The DCC gene: structural analysis and mutations in colorectal carcinomas. Genomics *19*, 525-531.

Deiner MS, K.T., Fazeli A, Serafini T, Tessier-Lavigne M, Sretavan DW. (1997). Netrin-1 and DCC mediate axon guidance locally at the optic disc: loss of function leads to optic nerve hypoplasia. Neuron *19*, 575-589.

Dent EW, B.A., Tang F, Kalil K. (2004). Netrin-1 and semaphorin 3A promote or inhibit cortical axon branching, respectively, by reorganization of the cytoskeleton. J Neurosci *24*, 3002-3012.

Eberwine J, B.B., Kacharmina JE, Miyashiro K. (2002). Analysis of subcellularly localized mRNAs using in situ hybridization, mRNA amplification, and expression profiling. Neurochem Res *27*, 1065-1077.

Fazeli A, D.S., Hermiston ML, Tighe RV, Steen RG, Small CG, Stoeckli ET, Keino-Masu K, Masu M, Rayburn H, Simons J, Bronson RT, Gordon JI, Tessier-Lavigne M, Weinberg RA. (1997). Phenotype of mice lacking functional Deleted in colorectal cancer (Dcc) gene. Nature *386*, 796-804.

Fearon ER, C.K., Nigro JM, Kern SE, Simons JW, Ruppert JM, Hamilton SR, Preisinger AC, Thomas G, Kinzler KW, et al. (1990). Identification of a chromosome 18q gene that is altered in colorectal cancers. Science *247*, 49-56.

Fonseca R, N.U., Morris RG, Bonhoeffer T. (2004). Competing for memory: hippocampal LTP under regimes of reduced protein synthesis. Neuron *44*, 1011-1020.

Frey U, M.R. (1997). Synaptic tagging and long-term potentiation. Nature *385*, 533-536.

Glanzman DL (1995). The cellular basis of classical conditioning in Aplysia californica--it's less simple than you think. Trends Neurosci *18*, 30-36.

Glanzman DL, K.E., Schacher S. (1990). Target-dependent structural changes accompanying long-term synaptic facilitation in Aplysia neurons. Science *249*, 799-802.

Hamasaki T, G.S., Nishikawa S, Ushio Y. (2001). A role of netrin-1 in the formation of the subcortical structure striatum: repulsive action on the migration of late-born striatal neurons. J Neurosci *21*, 4272-4280.

Huber KM, K.M., Bear MF. (2000). Role for rapid dendritic protein synthesis in hippocampal mGluR-dependent long-term depression. Science *288*, 1254-1257.

Ishii N, W.W., Stern BD, Culotti JG, Hedgecock EM. (1992). UNC-6, a laminin-related protein, guides cell and pioneer axon migrations in C. elegans. Neuron *9*, 873-881.

Johnstone O, L.P. (2001). Translational regulation and RNA localization in Drosophila oocytes and embryos. Annu Rev Genet *35*, 365-406.

Jung H, Y.B., Holt CE. (2012). Axonal mRNA localization and local protein synthesis in nervous system assembly, maintenance and repair. Nat Rev Neurosci *13*, 308-324.

Kandel ER (2001). The molecular biology of memory storage: a dialogue between genes and synapses. Science *294*, 1030-1038.

Kang H, S.E. (1996). A requirement for local protein synthesis in neurotrophin-induced hippocampal synaptic plasticity. Science *273*, 1402-1406.

Keino-Masu K, M.M., Hinck L, Leonardo ED, Chan SS, Culotti JG, Tessier-Lavigne M. (1996). Deleted in Colorectal Cancer (DCC) encodes a netrin receptor. Cell *87*, 175-185.

Kennedy TE, S.T., de la Torre JR, Tessier-Lavigne M. (1994). Netrins are diffusible chemotropic factors for commissural axons in the embryonic spinal cord. Cell *78*, 425-435.

Lécuyer E, Y.H., Parthasarathy N, Alm C, Babak T, Cerovina T, Hughes TR, Tomancak P, Krause HM. (2007). Global analysis of mRNA localization reveals a prominent role in organizing cellular architecture and function. Cell *131*, 174-187.

Lechner HA, B.J. (1998). New perspectives on classical conditioning: a synthesis of Hebbian and non-Hebbian mechanisms. Neuron *20*, 355-358.

Leonardo ED, H.L., Masu M, Keino-Masu K, Ackerman SL, Tessier-Lavigne M. (1997). Vertebrate homologues of C. elegans UNC-5 are candidate netrin receptors. Nature *386*, 833-838.

Litman P, B.J., Rindzoonski L, Ginzburg I. (1993). Subcellular localization of tau mRNA in differentiating neuronal cell culture: implications for neuronal polarity. Neuron *10*, 627-638.

Liu Y, S.E., Oliver T, Li Y, Brunken WJ, Koch M, Tessier-Lavigne M, Hogan BL. (2004). Novel role for Netrins in regulating epithelial behavior during lung branching morphogenesis. Curr Biol *14*, 897-905.

Livesey FJ (1999). Netrins and netrin receptors. Cell Mol Life Sci *56*, 62-68.

Livesey FJ, H.S. (1997). Netrin and netrin receptor expression in the embryonic mammalian nervous system suggests roles in retinal, striatal, nigral, and cerebellar development. Mol Cell Neurosci *8*, 417-429.

Martin KC (2004). Local protein synthesis during axon guidance and synaptic plasticity. Curr Opin Neurobiol *14*, 305-310.

Martin KC, B.M., Kandel ER. (2000). Local protein synthesis and its role in synapse-specific plasticity. Curr Opin Neurobiol *10*, 587-592.

Martin KC, C.A., Zhu H, Yaping E, Rose JC, Chen M, Bailey CH, Kandel ER. (1997). Synapse-specific, long-term facilitation of aplysia sensory to motor synapses: a function for local protein synthesis in memory storage. Cell *91*, 927-938.

Martin KC, E.A. (2009). mRNA localization: gene expression in the spatial dimension. Cell *136*, 719-730.

Mayford M, B.D., Podsypanina K, Kandel ER. (1996). The 3'-untranslated region of CaMKII alpha is a cis-acting signal for the localization and translation of mRNA in dendrites. Proc Natl Acad Sci U S A *93*, 13250-13255.

Moccia R, C.D., Lyles V, Kapuya E, E Y, Kalachikov S, Spahn CM, Frank J, Kandel ER, Barad M, Martin KC (2003). An unbiased cDNA library prepared from isolated Aplysia sensory neuron processes is enriched for cytoskeletal and translational mRNAs. J Neurosci *23*, 9409-9417.

Ostroff LE, F.J., Allwardt B, Harris KM, (2002). Polyribosomes redistribute from dendritic shafts into spines with enlarged synapses during LTP in developing rat hippocampal slices. Neuron *35*, 535-545.

Paquin N, C.P. (2008). Local regulation of mRNA translation: new insights from the bud. Trends Cell Biol *18*, 105-111.

Parent AT, B.N., Taniguchi Y, Thinakaran G, Sisodia SS. (2005). Presenilin attenuates receptor-mediated signaling and synaptic function. J Neurosci *25*, 1540-1549.

Poon MM, C.S., Jamieson CA, Geschwind DH, Martin KC. (2006). Identification of process-localized mRNAs from cultured rodent hippocampal neurons. J Neurosci *26*, 13390-13399.

Shav-Tal Y, S.R. (2005). RNA localization. J Cell Sci *118*, 4077-4081.

Shin SK, N.T., Jung BH, Matsubara N, Kim WH, Carethers JM, Boland CR, Goel A. (2007). Epigenetic and genetic alterations in Netrin-1 receptors UNC5C and DCC in human colon cancer. Gastroenterology *133*, 1849-1857.

Srinivasan K, S.P., Valdes A, Shin GC, Hinck L. (2003). Netrin-1/neogenin interaction stabilizes multipotent progenitor cap cells during mammary gland morphogenesis. Dev Cell *4*, 371-382.

Steward O, L.W. (1982). Preferential localization of polyribosomes under the base of dendritic spines in granule cells of the dentate gyrus. J Neurosci *2*, 284-291.

Sutton MA, S.E. (2006). Dendritic protein synthesis, synaptic plasticity, and memory. Cell *127*, 49-58.

Tang F, K.K. (2005). Netrin-1 induces axon branching in developing cortical neurons by frequency-dependent calcium signaling pathways. J Neurosci *25*, 6702-6715.

Tang SJ, R.G., Kang H, Gingras AC, Sonenberg N, Schuman EM. (2002). A rapamycin-sensitive signaling pathway contributes to long-term synaptic plasticity in the hippocampus. Proc Natl Acad Sci U S A *99*, 467-472.

Tcherkezian J, B.P., Thomas F, Roux PP, Flanagan JG. (2010). Transmembrane receptor DCC associates with protein synthesis machinery and regulates translation. Cell *141*, 632-644.

Welshhans K, B.G. (2011). Netrin-1-induced local β-actin synthesis and growth cone guidance requires zipcode binding protein 1. J Neurosci *31*, 9800-9813.

Willis DE, T.J. (2006). The evolving roles of axonally synthesized proteins in regeneration. Curr Opin Neurobiol *16*, 111-118.

Yao J, S.Y., Wen Z, Bassell GJ, Zheng JQ. (2006). An essential role for beta-actin mRNA localization and translation in Ca2+-dependent growth cone guidance. Nat Neurosci *9*, 1265-1273.

Yebra M, M.A., Diaferia GR, Kaido T, Silletti S, Perez B, Just ML, Hildbrand S, Hurford R, Florkiewicz E, Tessier-Lavigne M, Cirulli V. (2003). Recognition of the neural chemoattractant Netrin-1 by integrins alpha6beta4 and alpha3beta1 regulates epithelial cell adhesion and migration. Dev Cell *5*, 695-707.

Zhang J, C.H. (2010). Netrin-1 prevents ischemia/reperfusion-induced myocardial infarction via a DCC/ERK1/2/eNOS s1177/NO/DCC feed-forward mechanism. J Mol Cell Cardiol *48*, 1060-1070.

CHAPTER TWO

SYNAPSE- AND STIMULUS-SPECIFIC LOCAL TRANSLATION DURING LONG-TERM NEURONAL PLASTICITY

(Wang et al., Science 2009)

INTRODUCTION

Long-lasting forms of learning-related synaptic plasticity require transcription for their persistence (*1-3*) and yet can occur in a synapse-specific manner (*4-7*). One mechanism that has been proposed to mediate this spatial restriction of gene expression during neuronal plasticity involves the localization and regulated translation of mRNAs at stimulated synapses (*8-10*).

Many findings support the existence of local translation at synapses. First, all of the machinery required for translation is present in neuronal processes, including polyribosomes (*11, 12*), translation initiation and elongation factors (*13*), and an increasingly large but select population of mRNAs (*14-18*). Second, studies using pharmacological inhibitors of protein synthesis have indicated a central role for local translation during long-lasting synaptic plasticity (*5, 19, 20*). Third, translation of specific transcripts has been visualized in dendrites of cultured neurons following stimulation with BDNF (*21*), KCl (*22*), or following inhibition of sodium channels, NMDA receptor or the mTOR signaling pathway (*9, 23, 24*). What is lacking, however, is direct evidence that a specific mRNA is translated at stimulated synapses during a transcription-dependent form of learning-related synaptic plasticity.

To directly visualize synaptic translation at the level of individual synapses during long-term, learning-related neuronal plasticity, we turned to the *Aplysia* sensory neuron (SN)-motor neuron (MN) culture system (*2*). The monosynaptic connection formed between SNs and MNs, a central component of the gill-withdrawal reflex in *Aplysia*, can

be reconstituted in culture, where well-characterized stimuli elicit forms of plasticity that have direct correlates in the behavior of the animal. Specifically, five spaced applications of serotonin (5HT) induce a transcription-dependent long-term facilitation (LTF) of SN-MN synapses that parallels long-term sensitization of the gill-withdrawal reflex (*2*), while five spaced applications of the neuropeptide FMRFamide induce a transcription-dependent long-term depression (LTD) of SN-MN synapses that parallels long-term habituation of the gill-withdrawal reflex (*25, 26*).

Synapse-specific, transcription-dependent LTF of SN-MN synapses is blocked by perfusion of translational inhibitors to distal SN neurites (*5*). An additional advantage of this culture system is that SNs only form chemical synapses with appropriate target MNs (*27, 28*), allowing local translation to be studied in the presence or absence of synapses.

RESULTS

Sensorin translational reporter

To monitor translation in sensory neurites during neuronal plasticity, we generated translational reporters of sensorin, a SN-specific peptide neurotransmitter whose mRNA localizes to distal neuronal processes (*15, 29*). This localization is further regulated by synapse formation such that the mRNA is distributed diffusely throughout neuronal processes of SNs that do not form synapses (e.g. in isolated SNs), but concentrates at synapses in SNs paired with MNs (*27*). Translation of sensorin is required for the formation and/or stabilization of synapses between sensory and motor neurons (*27*) and both translation and secretion of sensorin are required for 5HT-induced LTF of *Aplysia* sensory-motor synapses (*30*).

To generate sensorin translational reporters, we fused the 5' and 3' UTRs of sensorin to the coding region of the photoconvertible fluorescent protein dendra2 (*31*). Dendra2 switches irreversibly from a green fluorescent protein to a red fluorescent protein following brief UV illumination, allowing newly synthesized proteins (green) to be differentiated from proteins synthesized prior to photoconversion (red). As shown in Fig 2.1A and Fig 2.2, addition of the 5' and 3'UTRs of sensorin to the dendra2 coding sequence generates a reporter whose localization is indistinguishable from endogenous sensorin mRNA measured as colocalization coefficient using double-labeling fluorescence *in situ* hybridization (FISH). Specifically, it localizes to neurites of isolated SNs, and concentrates at synapses in SNs paired with MNs. Ectopic labeling of

presynaptic terminals by expression of VAMP-mCherry in the SN further confirmed that these concentration sites are indeed synapses (Fig 2.1B). Analysis of reporters containing either the 3'UTR or the 5'UTR alone revealed that the 3'UTR was sufficient for localization to neuronal processes, while the 5'UTR was required for targeting to synapses, indicating that distinct *cis*-acting elements mediate neuritic and synaptic mRNA localization (Fig 2.3 and data not shown).

We first set out to visualize local translation of the reporter during LTF induced by bath application of 5X5HT. To do this, we expressed the reporter in SNs forming synapses with MNs, removed the SN soma, and photoconverted the dendra2 from green to red (see protocol in fig 2.4, and supporting information for detailed methods). Any newly synthesized (green) protein had to result from local translation in the neurite since the soma was no longer present. Of note, while 5x5HT induces transcription-dependent LTF, the 24 hr (but not the 48 hr) facilitation has been shown to occur in the absence of a SN soma, indicating that the initial events involved in persistent LTF can be monitored in SNs that lack cell bodies (*32*). We imaged red and green channels before the first application and immediately after the fifth application of 5HT. Control cultures were stimulated with five spaced applications of vehicle (5X artificial seawater, ASW), or were untreated following photoconversion. As shown in Fig 2.5, very little green signal but robust red signal was detected following UV illumination, indicating efficient photoconversion. After the fifth pulse of 5HT, however, we observed a dramatic increase in green dendra signal at multiple sites within the neurite. The increase was completely blocked by the translational inhibitor anisomycin (10 μM, fig 2.5, fig 2.6). Modest but

significant increases in green dendra fluorescence were observed in control cultures following application of 5XASW, and these were also blocked by anisomycin (10 μM, fig 2.5, fig 2.6). This modest increase in green dendra fluorescence represents ongoing basal translation since it was also observed in untreated cultures (fig 2.5, fig 2.6). Immediately following imaging, we fixed the cells and performed FISH for the reporter mRNA. Comparison of the live cell imaging results with FISH signals from the same cells revealed that 143 of 147 (97%) of sites with new translation were also sites of reporter mRNA concentration (yellow arrowheads in Fig 2.5).

Thus the subcellular localization of new translation correlated with the subcellular localization of reporter mRNA with remarkable accuracy. Since we have shown that the reporter mRNA specifically concentrates in VAMP-positive synapses (fig. 2.1 and fig 2.3, (*27*)), these results indicate that the reporter is indeed being translated at synapses. We quantified new translation as ΔF/F (x100 = % change), normalized to the red dendra2 signal (which serves as a volume control, see supporting information). When stimuli were applied in the presence of anisomycin, there was no significant change in green signal, and thus no translation (2.3±3.4% for Ani+5XASW; -8.9±4.9% for Ani+5X5HT). In untreated cultures, we observed a 41.2±3.7% increase in newly translated reporter. Following 5XASW, we observed a 43.5±3.6% increase, and following stimulation with 5X5HT, we observed a 155.9±18.7% increase in translation. These results indicate that there is a basal level of constitutive sensorin translation that occurs in neurites, and that this translation is significantly increased following stimuli (5x5HT) that induce LTF (***$p<0.001$, ANOVA with Bonferroni's multiple comparison test).

Spatial specificity of translation

To determine the spatial specificity of stimulus-induced local translation, we locally perfused 5X5HT onto a subset of synapses made by a given sensory neuron onto a motor neuron (Fig 2.7, see also fig 2.8 and 2.9). This protocol has been shown to produce synapse-specific long-term facilitation of sensory-motor synapses (*5, 7*). Images were acquired from both stimulated (perfused) and unstimulated (non-perfused) sites within the same sensory neuron at the beginning and end of local perfusion. In control experiments, we locally perfused 5XASW and detected modest increases in newly synthesized green dendra2 at both perfused and non-perfused synapses (27.4±5.6% and 20.2±8.2%, respectively). However, when 5X5HT was perfused onto a subset of synapses, robust increases in new green dendra2 signal were detected at stimulated sites (54.7±10.9%) with only modest increases at non-perfused sites (16.6±4.9%). For each neuron, we calculated the ratio of the ΔF/F at the perfused site to the average ΔF/F at non-perfused sites. In cultures locally perfused with 5XASW (Fig 2.7D and fig 2.10), this ratio was 1.0±0.1, indicating no significant difference between perfused and non-perfused sites. In contrast, in cultures locally perfused with 5X5HT (Fig 2.7A), the ratio was 1.3±0.1, indicating a significant increase in new translation at perfused as compared to non-perfused sites (***$p<0.001$, paired Student's t-test). Thus local serotoninergic stimulation induced translation in a spatially restricted manner within an individual neuron. FISH analysis revealed equivalent reporter mRNA at all synapses under all conditions (Fig 2.7 and fig 2.10, 2.11). Further, no significant difference in basal translation was observed at non-perfused synapses between 5XASW and 5X5HT groups

(fig 2.11). Finally, imaging of the red channel revealed that 5x5HT did not induce significant structural changes between the initial and final imaging times (fig 2.9).

Stimulus specificity

Five spaced applications of the peptide neurotransmitter FMRFamide produces transcription-dependent LTD of *Aplysia* SN-MN synapses, and local perfusion of 5xFMRFamide has been shown to produce synapse-specific LTD (*33*).

To ask whether the 5HT-induced translation of the reporter was stimulus-specific, we locally perfused 5xFMRFamide and monitored the effect on reporter translation. As shown in figure 2.7C, the ratio of translation between 5xFMRFamide perfused and non-perfused sites was 1.0±0.1, indicating that FMRFamide does not stimulate sensorin translation, consistent with previous studies of sensorin immunoreactivity (*34*) (Fig 2.7D and fig 2.11, 2.12). Basal levels of translation at non-perfused synapses, and concentrations of reporter RNA were equivalent to those in cultures locally perfused with 5x5HT or 5xASW (Fig 2.7 and fig 2.10, 2.11). Together, these results indicate that translational regulation of the sensorin reporter is stimulus-specific, being triggered by 5x5HT (which induces LTF) but not by 5xFMRFamide (which induces LTD).

Transcript specificity

We had previously shown, using metabolic labeling and TCA precipitation, that global translation in sensory neurites is increased three-fold in response to serotonin (*5*). To ask whether 5HT stimulates global increases in translation in neurites, or whether it

regulates translation of a specific subset of transcripts, we took advantage of a reporter we made containing the 3'UTR of sensorin (and 5'UTR of SV40) which localizes to distal sensory neurites and is present but not concentrated in synapses (Fig 2.3). We expressed this reporter in SNs making synapses with MNs, and asked whether local perfusion of 5x5HT stimulated its translation. As shown in Fig 2.7, we did not detect any increase in translation of this reporter at synapses stimulated with 5X5HT (ratio of ΔF/F at perfused versus non-perfused sites = 1.0 ± 0.1). Importantly, the 3'UTR reporter was present in SN processes and translation was quantified at sites containing equivalent amounts of 3'UTR or 5'3'UTR reporter (fig 2.11). These results demonstrate that 5HT does not regulate the translation of all process-localized mRNAs.

Translational regulation requires a synapse

We next investigated the role of synaptic connectivity in translational regulation by 5HT. Specifically, we asked whether local perfusion of 5x5HT stimulated translation of the reporter in isolated sensory neurons (which do not form autapses or chemical synapses with each other) or in SNs paired with a non-target motor neuron, with which it does not form chemical synapses. As shown in Fig 2.13 and 2.14, local perfusion of 5x5HT did not increase translation of the reporter in isolated SNs (ratio of perfused to non-perfused = 1.0 ± 0.1), despite abundant reporter mRNA. Notably, basal translation of the reporter in isolated SN was not significantly different from basal translation in SNs paired with MNs (Fig 2.15 and fig 2.16). These results indicate that 5HT-induced translation of sensorin only occurs in SNs forming chemical synapses with MNs.

Translational regulation requires postsynaptic calcium

To further test the requirement for chemical synapses, we cultured SNs with a non-target MN, L11, with which SNs fasciculate but do not make chemical synapses (*27, 28*). As shown in Fig 2.13, local perfusion of 5x5HT did not increase reporter translation (ratio of perfused to non-perfused sites = 1.0 ± 0.1). Again, reporter mRNA was localized at the perfused sites (Fig 2.13, and fig. 2.16) and basal translation of the reporter did not differ from basal translation in SNs forming chemical synapses with target MNs (Fig 2.15 and fig 2.16).

Together, these results indicate that 5HT stimulates sensorin reporter translation only in the context of a chemical synapse. To begin to explore the nature of the signal provided by the MN, we asked whether it involved calcium signaling in the postsynaptic compartment. To do so, we microinjected the calcium chelator BAPTA (50mM) into the motor neuron and, 1-2 hrs later, monitored translation of the reporter in the SN. BAPTA injection into the MN has recently been reported to block LTF of SN-MN synapses as well as increases in sensorin immunoreactivity, in the SN, without affecting basal synaptic transmission (*35*). Using Fluo4 imaging, we confirmed that BAPTA injection blocked depolarization-induced increases in intracellular Ca++ in the MN (Fig 2.17A). We further found that BAPTA did not alter the synaptic localization of endogenous sensorin or reporter mRNA (Fig 2.17B), and did not alter the morphology of varicosities (Fig 2.18 and data not shown). While these results indicate that BAPTA injection did not perturb the structure of the synapse, it completely blocked translation of the reporter in the SN (ratio of $\Delta F/F$ at perfused versus non-perfused sites = 1.0 ±0.0). In control

experiments, vehicle injection into MN did not inhibit translation of the reporter in the SN (ratio of ΔF/F at perfused versus non-perfused sites = 1.2 ± 0.0). These results indicate that a calcium-dependent trans-synaptic signal is required for translational regulation of the reporter in the presynaptic neuron by 5HT.

CONCLUSION

In this study, we use a photoconvertible fluorescent protein translational reporter to visualize local translation in live *Aplysia* SN-MN synapses during 5-HT induced LTF. Our results provide direct evidence that local translation occurs at synapses in response to stimuli that induce transcription-dependent, learning-related synaptic plasticity. They demonstrate that mRNA localization does in fact serve to localize protein synthesis (since new translation precisely correlates with reporter mRNA localization) and that stimuli can regulate translation in a spatially restricted manner within a single neuron—i.e. at stimulated but not at unstimulated synapses. We have previously reported that branch-specific LTF is accompanied by the growth of new synaptic contacts at the stimulated branch (*5*) and that newly synthesized sensorin is required during synaptogenesis (*27*). Together with the finding that release of sensorin is required for LTF (*30*), our results suggest that the highly localized translation of sensorin at stimulated synapses functions to restrict the growth and/or stabilization of new synaptic growth, and to thereby promote LTF, precisely at these sites. Our results provide a number of additional insights into the regulation of local translation in neurons. First they show that translation of the reporter is stimulus specific, occuring during 5HT-induced LTF but not during FMRFamide-induced LTD. Second, they demonstrate that 5HT does not globally upregulate translation of all localized transcripts (since translation of the 3'UTR reporter is not stimulated), indicating that translational regulation is transcript-specific. Finally, they reveal that stimulus-induced translation of the reporter requires calcium signaling in the

postsynaptic motor neuron, suggesting that a trans-synaptic retrograde signal is required for the regulation of local translation during neuronal plasticity.

EXPERIMENTAL PROCEDURE

Reporter Constructs:

pDendra2-N (Evrogen, Moscow, Russia) coding sequence (including stop codon) was PCR-amplified and cloned into pNEX3 as a XbaI/BamHI fragment (pNEX-Dendra). The 3'UTR of sensorin was cloned from an Aplysia sensory neuron process library (1) and PCR-amplified as a BamHI/BamHI fragment, The 5'UTR was obtained from a 5'RACE cDNA library and PCR-amplified as a SalI/SalI fragment (see fig S1 for sensorin 5'UTR, 3'UTR sequences, and for maps of constructs). The two UTR fragments were then independently inserted into pNEX3-Dendra to generate chimeric reporters: pNEX3-Dendra-3'UTR, and pNEX3-5'UTR-dendra-3'UTR. mCherry and VAMP coding sequences were PCR-amplified and independently subcloned into pNEX3 (XbaI/SmaI) to generate a single reading frame as pNEX3-VAMP-mCherry.

Aplysia cell culture, microinjection, electrophysiology, stimulation and pharmacological treatments:

A detailed protocol for Aplysia SN-MN culture preparation can be found at http://www.gonda.ucla.edu/researchlabs/martin/protocols.htm. SN and LFS MNs were obtained from 80—100 gram Aplysia (Alacrity, Redondo Beach, CA). L11 motor neurons were microdissected from the abdominal ganglion of juvenile Aplysia (1-4 g, National Aplysia Resource, University of Miami, FL).

During culturing, the MN and SN cell bodies were carefully positioned so that the

MN would not suffer any mechanical damage when SN cell body was removed during the experimental protocol. Reporter plasmids were microinjected into SNs 24-36 hours after plating. Two days later, reporter expression was monitored in the SNs by fluorescence microscopy, and the cell bodies of dendra-expressing SNs were removed along with ~50 microns of proximal axon segment with a sharp electrode as described in (2). Cultures were excluded from further experiments if any visible damage to MN occurred during cell body removal process.

Synaptic connectivity was assayed by measuring EPSP amplitude between SN and target MN. SN and MN were impaled with sharp glass electrodes (20–40 mΩ resistance) filled with 1.5 M K-acetate, 0.5 M KCl, and 0.01 M HEPES (pH 7.2). MNs were held at -80 mV, and SNs were held at -50 mV. EPSPs were evoked by intracellular stimulation of the sensory neuron (1–3 nA for 5 ms) with a Grass (West Warwick, RI) S88 stimulator. EPSPs were recorded and measured with Axoscope 8.2 and pCLAMP 8 software (Axon Instruments, Union City, CA).

To elicit cell-wide long-term facilitation (LTF) of SN-MN synapses, cultures received five spaced applications of 5HT according the following protocol: five 5 min applications of 5HT (10 μM) with four intervening 20 min washes of 50% L15/50% ASW, with a total stimulation time of 1hr 45 min.

To induce synapse-specific LTF and LTD, we locally perfused 5HT or FMRFamide as described in Martin, 1997 and Guan, 2001, respectively(2, 3). Briefly, 100μM 5HT or 10μM FMRFamide in 50% L15/50% ASW containing 0.05% fast green was applied to a subset of synapses using a perfusion electrode (approximately 1MΩ

resistance). The electrode was connected to a picospritzer (World Precision Instruments, Sarasota, FL) and very low pressure (approximately 1psi) was used to apply five 5s pulses of drugs at 10s interval as one stimulation (perfusion is illustrated in fig. S3). Air pressure and bulk flow in the bath (approximately 1ml/min) were adjusted so that most of synapses in a 63X objective field were locally perfused, without any perfusion of synapses in other fields. The stimulation was repeated five times, with four intervening 10 min bath perfusions of 50% L15/50% ASW, for a total stimulation time of 50 min. Anisomycin (10μM; Calbiochem, San Diego, CA) was present for 30 min before and during stimulation. 5HT-creatine was from Sigma (Saint Louis, MO) and FMRFamide was from Calbiochem (San Diego, CA). L15 was purchased from Sigma (Saint Louis, MO), and ASW consisted of NaCl 27.89g, CaCl2H2O 1.62g, KCl 0.738g, MgCl2 6H2O 11.18g, HEPES 2.38g in 1L nanopure water. All solutions were filtered through 0.2μm filters before use. BAPTA tetraacetic acid was purchased from Sigma (San Louis, MO) and dissolved in 1.5M K-acetate, 0.5M KCl, 0.01M HEPEs (pH 7.2) at injecting concentration of 50mM.

Live cell imaging and image analysis:

All confocal images were taken on Zeiss Pascal scanning laser microscope (Zeiss, Germany). We began image acquisition 18 hrs after removal of the SN cell body to allow time for recovery from injury.

To photoconvert dendra, samples were illuminated with UV light from a 100 W Hg lamp (using a 409 nm filter) for approximately 2” at 100% power through a 63X oil

Apochromat objective. Native, unphotoconverted (green) dendra protein was excited with a 488nm Argon laser at 2.5mW and collected through BP 505-600 filter. Fluorescence signals from photoconverted dendra was excited with a 543nm He-Ne laser at 0.8mW and collected through LP560 filter; the pinhole was set at 1 airy unit for images acquired both at 10X and 63X magnification, with slice intervals of 6.4μm and 0.8μm respectively.

VAMP-mCherry was excited with a 543nm He-Ne laser and Alexa Fluor 647 was excited with a 633nm He-Ne laser. Two-dimensional projections of equal number of slices were made, using maximum transparency mode to allow pixel intensities along the same Z-axis to collapse into one illuminated image. The red fluorescence signal from photoconverted dendra served as an important control to monitor i) the original level of expression of dendra; ii) cell integrity (dramatic decreases in red fluorescence indicate leakiness of the plasma membrane); and iii) morphological changes that occurred over the course of imaging. Note that the growth of new synaptic connections that occurs with this stimulation protocol does not occur until 12-18 hrs following 5HT application (4, 5). Cells in which there was greater than a 20% decrease in red fluorescence were excluded from analysis; the mean ratio (as Fend/Fstart) in red fluorescence across all experiments was 1.0 ± 0.003. To optimize neuronal health and protect neurons from phototoxicity during photoconversion and imaging, Trolox (Tokyo Chemical Industry, Japan), a Vitamin E derivative, was included in the media.

To measure new translation, total fluorescence (both green and red) as well as the total RNA intensity of each synaptic site that had reporter mRNA cluster, were measured by a "blind" observer as mean intensity X area (μm2). All measurements were done using

LSM software. New translation was estimated as the total pixel intensity in the green channel after stimulation minus the total intensity in the green channel before stimulation, divided by the total intensity in the green channel before stimulation, (Fend-Fstart)/Fstart, or ΔF/F. To correct for volume changes, Fend/Fstart for the green signal was normalized to Fend/Fstart for red signal. To quantify the difference between new translation at stimulated (perfused) and unstimulated (non-perfused) synapses within a single neuron, we acquired images at 3-4 non-perfused sites, which were chosen on the basis of their morphological similarity to the perfused site. We quantified new translation at each synaptic site within a field (perfused or non-perfused) and calculated the mean new translation (ΔF/F). The difference was then quantified as the ratio of mean new translation at perfused sites to mean new translation at multiple non-perfused sites. Note that the mean new translation at the 3-4 non-perfused fields per neuron were averaged to generate the mean ΔF/F for non-perfused sites.

To validate this approach, we compared the mean new translation between two non-perfused sites within the same neuron, and found that the ratio was 1.0. Fluorescence in situ hybridization (FISH): Immediately after live cell imaging, cells were fixed with 4%PFA/30% sucrose in PBS and processed for FISH. The dendra2 coding sequence was amplified and cloned into pCR4. Antisense riboprobes (750 bp) were generated by in vitro transcription from the T7 promoter (Roche, Indianapolis, IN). In control experiments, the sense riboprobe did not produce any background signal (data not shown). The integrity of the riboprobes was tested by agarose gel electrophoresis and the efficiency of DIG incorporation was estimated by dot blotting on nylon membranes and

comparing to standard RNA probes (Roche, Indianapolis, IN). FISH detection using the TSA amplification system was done exactly as previously described by Lyles et al, 2006(6), with hybridization at 580C. . Since dendra2 protein fluorescence does not persist following processing of samples for FISH, we manually aligned RNA images to live cell images based on the morphology of SN and MN. To simultaneously detect reporter mRNA and endogenous sensorin in SNs, we made DIG labeled dendra2 riboprobes and Biotin labeled reporter mRNA riboprobes (and vice versa). Sensorin riboprobes were made as described in Lyles et al., 2006(6). Both riboprobes were included in one hybridization step. The FISH detection protocol was modified so that anti-DIG-peroxidase and anti-Biotin-peroxidase antibody detections were carried out sequentially with a H2O2 incubation step added in between to quench the peroxidase activity of the first antibody.

Statistical analysis

Prism Graphpad software (La Jolla, CA) was used for all statistical analysis. Paired and unpaired Students' t-tests were performed when data distribution passed normality tests, otherwise Wilcoxon-Mann-Whitney nonparametric tests were used. When three or more groups were compared, data were analyzed by One-Way ANOVA and Bonferroni's multicomparison tests.

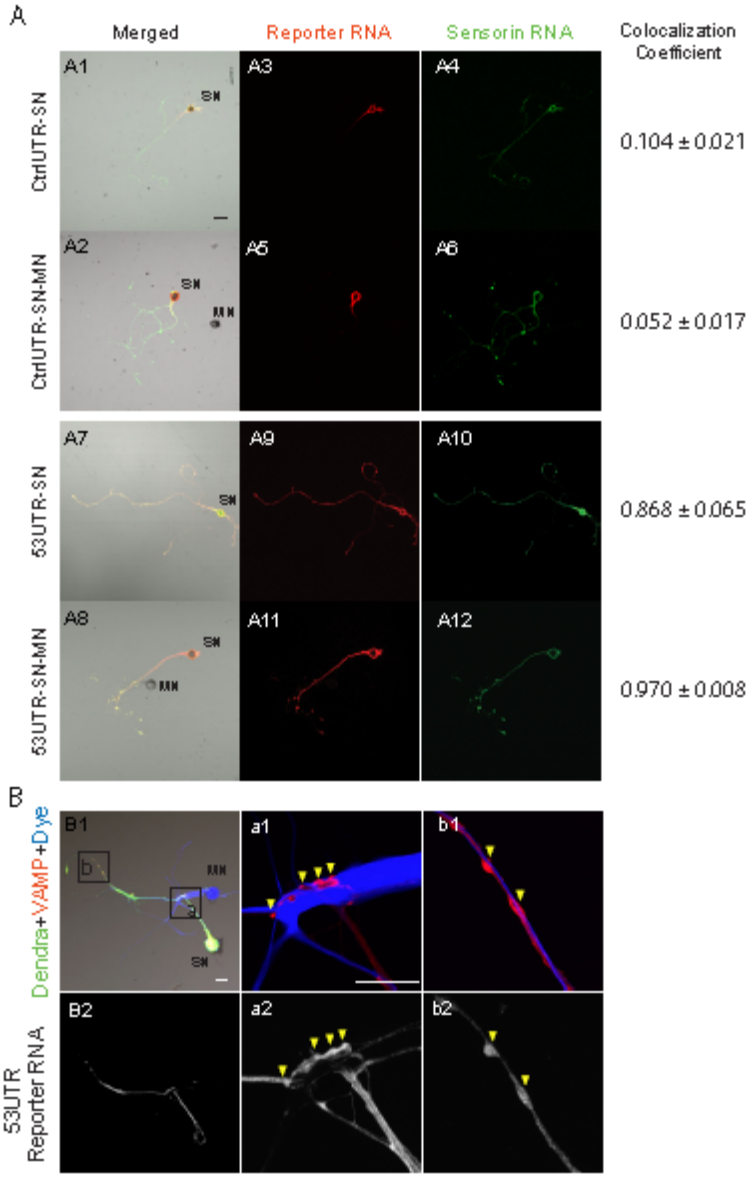
A
Merged
Reporter RNA
Sensorin RNA
Colocalization Coefficient
CtrlUTR-SN
CtrlUTR-SN-MN
53UTR-SN
53UTR-SN-MN
A1
A2
A3
A4
A5
A6
A7
A8
A9
A10
A11
A12
SN
MN
0.104 ± 0.021
0.052 ± 0.017
0.868 ± 0.065
0.970 ± 0.008
B
Dendra+VAMP+Dye
53UTR Reporter RNA
B1
B2
a1
a2
b1
b2

Figure 2.1. Translation reporter mRNA colocalizes with endogenous sensorin mRNA at synapses.
(A) Colocalization of 5'3'UTR sensorin reporter mRNA and endogenous sensorin mRNA. Expression vectors encoding the control (CtrlUTR) or sensorin (5'3'UTR) translational reporter were microinjected into *Aplysia* sensory neurons (SNs, isolated, or co-cultured with motor neurons, MNs) on DIV2. Cultures were fixed 48 hrs later and processed for double label fluorescence *in situ* hybridization (FISH) using DIG-labeled dendra riboprobes and biotin-labeled sensorin probes. Representative confocal images of DIC/merged (A1, 2, 7 and 8), dendra reporter mRNA in red (A3, 5, 9 and 11) and endogenous sensorin mRNA in green (A4, 6, 10 and 12). FISH signals are shown in isolated SNs (A3, 4, 9 and 10) and in SNs paired with MNs (A5, 6, 11 and 12). Scale bar: 50μm. Colocalization was quantified as colocalization coefficient (0, no colocalization; 1, perfect colocalization); **(B)** VAMP-mCherry and reporter were co-expressed in SN, and the MN was labeled with Alexa 647. Synapses are detected as VAMP-mCherry varicosities contacting the MN. B1: Low magnification images of reporter protein (green), VAMP-mCherry (red) and MN (blue) with boxes of higher magnification images in a1 and b1. Cells were fixed after imaging and processed for FISH for reporter mRNA in B2, a2 and b2. Scale bar: 50μm.

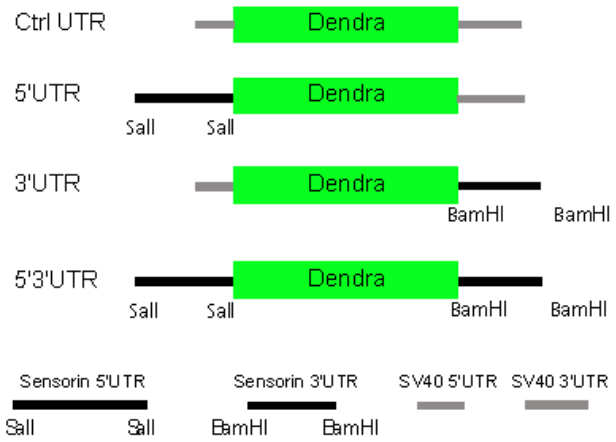

Sensorin 5'UTR

```
  1 CCACTGTGGC GACAGGGCTT GGCACGATAC GACACACTCA CAATTTTGCG GGTGAACCAC
 61 GTGGCCCCTT CCTCGCTGAT TTTCACGCTT GCGGATTCGT GCTCAAAAGA CAGGGCCAGG
121 GGTGCACTTT TGAGGAAACA CAGGTGCTAA TTTATTGCCC TGTCACTTTT ACGTATAAAA
181 CGCAGGCCGC TTTGCTCGAA CATTTAGAAT AGAGAACTGA GAGCTCAAAG ATACATTCCA
241 GTCTTGAAAC AGAAACAGTC TTTCCCCGAT CCCAAAAACT AACACAGATA AGTGAGCAAC//
```

Sensorin 3'UTR

```
  1 CGGTCATTTT CAGACAGGTC CAAGTCTTTT GAGTCTTCTG GACGGCTTCC CTTCGCCTGA
 61 GCCGTGATCA ACAAATTAAT ACTTCGAAAA ATTCTGCTGA TTTGGTTAAT CTTTTTCTGA
121 CAAAAATTAC ATAAAGCTTT TTTCCAAGTT GAAAAAAAAA AAAAAAAAAA AAAAAAAA//
```

Figure 2.2. Sequences of 5’ and 3’ UTRs of sensorin; maps of translational reporter constructs.

Shown are cartoons of the constructs used in the study, containing the control UTRs from SV40, 5’, 3’ or 5’ and 3’ UTRs of sensorin. Constructs were made in pNEXδ3 vector (*7*). Also shown are the 5’ and 3’ UTR sequences of sensorin.

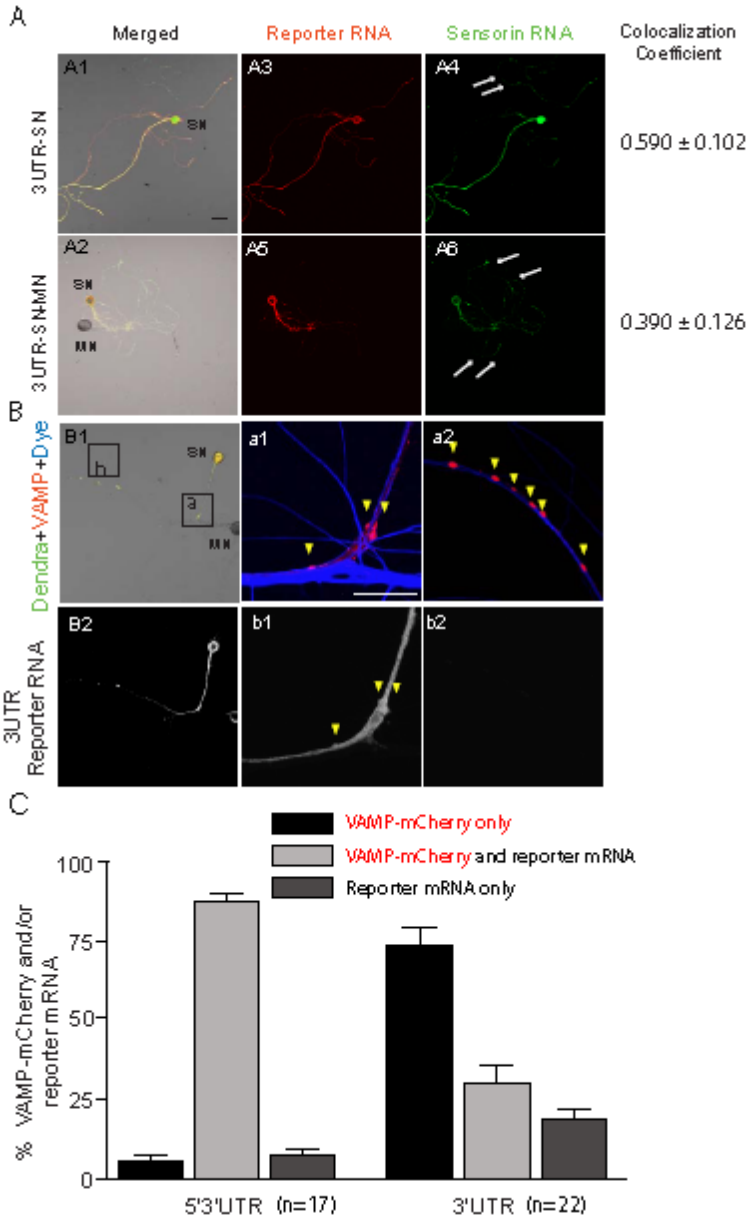
A
Merged
Reporter RNA
Sensorin RNA
Colocalization Coefficient
3 UTR-SN
3 UTR-SN-MN
A1
A2
A3
A4
A5
A6
SN
MN
0.590 ± 0.102
0.390 ± 0.126
B
Dendra+VAMP+Dye
3UTR Reporter RNA
B1
B2
a1
a2
b1
b2
h
a
C
VAMP-mCherry only
VAMP-mCherry and reporter mRNA
Reporter mRNA only
% VAMP-mCherry and/or reporter mRNA
100
75
50
25
0
5'3'UTR (n=17)
3'UTR (n=22)

Figure 2.3. The 3'UTR of sensorin targets reporter mRNA to neuronal processes but does not promote concentration at synapses.
(A) Colocalization of 3'UTR sensorin reporter mRNA and endogenous sensorin mRNA. Expression vectors encoding the sensorin (3'UTR) translational reporter were microinjected into *Aplysia* sensory neurons (SNs, isolated, or co-cultured with motor neurons, MNs) on DIV2. Cultures were fixed 48 hrs later and processed for double label fluorescence *in situ* hybridization (FISH) using DIG-labeled dendra riboprobes and biotin-labeled sensorin probes. Representative confocal images of DIC/merged (A1, 2), dendra reporter mRNA in red (A3, 5) and endogenous sensorin mRNA in green (A4, 6). FISH signals are shown in isolated SNs (A1, 3, 4) and in SNs paired with MNs (A2, 5, 6). Arrows point to areas where only endogenous sensorin mRNA was observed. Note that the 3'UTR is sufficient to transport the reporter RNA to distal neurites (A3). Scale bar: 50μm. Colocalization was quantified as colocalization coefficient (0, no colocalization; 1, perfect colocalization); **(B)** VAMP-mCherry and reporter were co-expressed in SN, and the MN was labeled with Alexa 647. Synapses were detected as VAMP-mCherry varicosities contacting the MN. B1: Low magnification images of reporter protein (green), VAMP-mCherry (red) and MN (blue) with boxes of higher magnification images in a1 and b1. Cells were fixed after imaging and processed for FISH for reporter mRNA in B2, a2 and b2. Scale bar: 50μm. **(C)** Quantification of percent of sites that contained VAMP-mCherry and/or reporter mRNA.

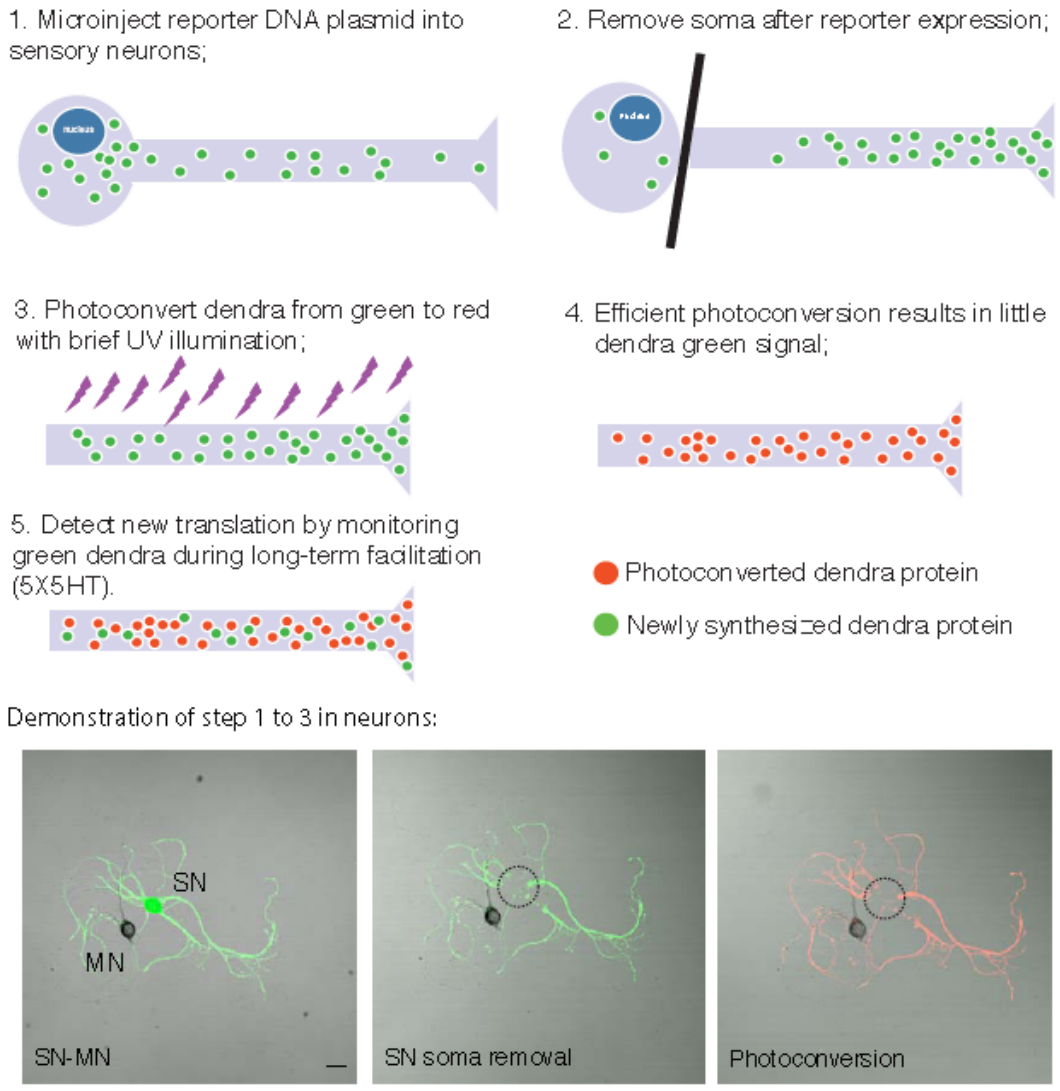

Figure 2.4. Top cartoon illustrates experimental strategy for using dendra-based translational reporters. Confocal images in bottom panel show cultured SN-MN with SN expressing dendra2 reporter (left), SN soma removal (middle), and photoconversion of dendra2 throughout the entire neuronal arbor before treatment (right). Scale bar: 50μm.

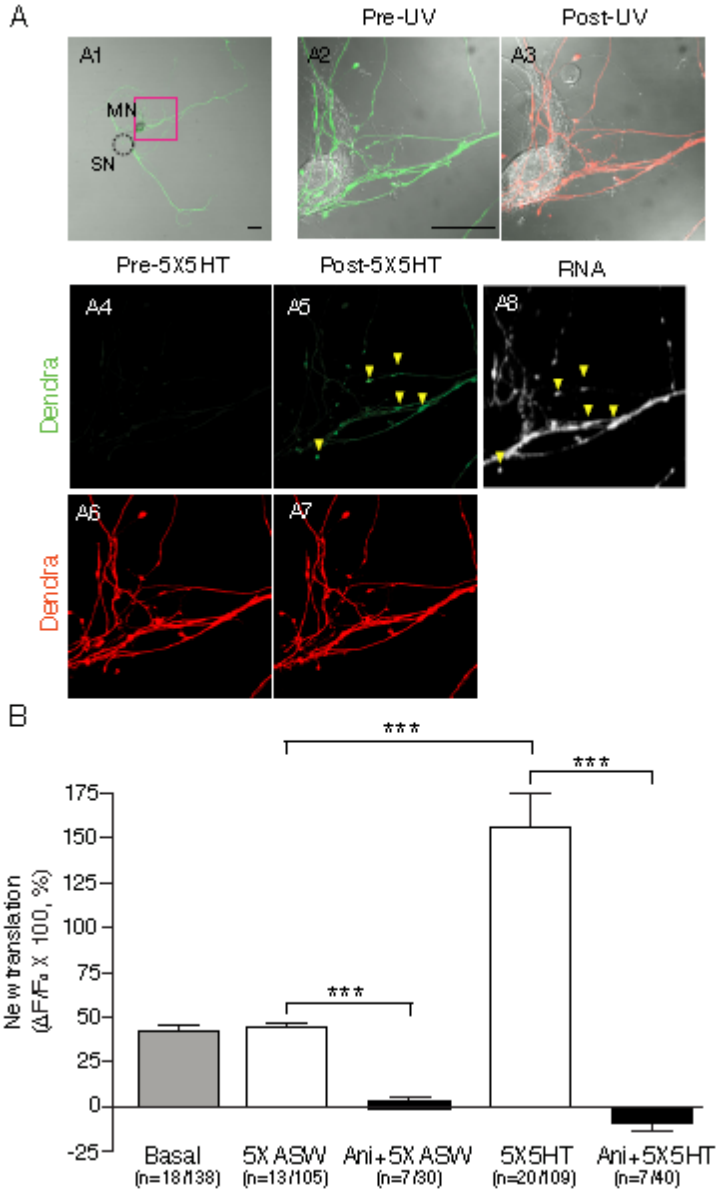
A
Pre-UV
Post-UV
A1
MN
SN
A2
A3
Pre-5X5HT
Post-5X5HT
RNA
A4
A5
A6
Dendra
A6
A7
Dendra
B
***
***
***
175
150
125
100
75
50
25
0
-25
New translation
(ΔF/F0 X 100, %)
Basal
(n=18/138)
5X ASW
(n=13/105)
Ani+5X ASW
(n=7/30)
5X5HT
(n=20/109)
Ani+5X5HT
(n=7/40)

Figure 2.5. Bath application of 5X5HT stimulates translation of reporter mRNA at synaptic contact sites.
Sensorin translational reporter was expressed in *Aplysia* sensory neurons (SNs) co-cultured with motor neurons (MNs), the SN soma was removed and dendra was photoconverted from green to red throughout the neuronal arbor by UV illumination. **(A1)** Low magnification image of dendra-reporter expressing SN in SN-MN coculture. The dashed circle outlines the location of the removed soma. **(A2 and A3)** High magnification DIC/merged image of area outlined by the red box in A1, showing synaptic contacts between SN and MN before (A2) and after (A3) UV photoconversion. **(A4 and A5)** Green dendra signal remaining following photoconversion, before (A4) and after (A5) serotonin stimulation (5X5HT). Lack of green dendra indicates efficient photoconversion; new green dendra reveals significant new translation post 5x5HT. **(A6 and A7)** Photoconverted red dendra signal before (A6) and after (A7) 5x5HT shows SN volume. A8: Cells were fixed at the end of the experiment and processed for fluorescence *in situ* hybridization (FISH) with antisense dendra riboprobes. Arrowheads in A5 and A8 point to the sites of new (green) dendra protein synthesis colocalizing with reporter mRNA clusters. Scale bar: 50μm. See fig 2.6 for Basal, 5XASW, Ani+5X5HT, Ani+5XASW results. **(B)** Quantification of new translation as ΔF/F, ***$p<0.001$, ANOVA and Bonferroni multiple comparison test.

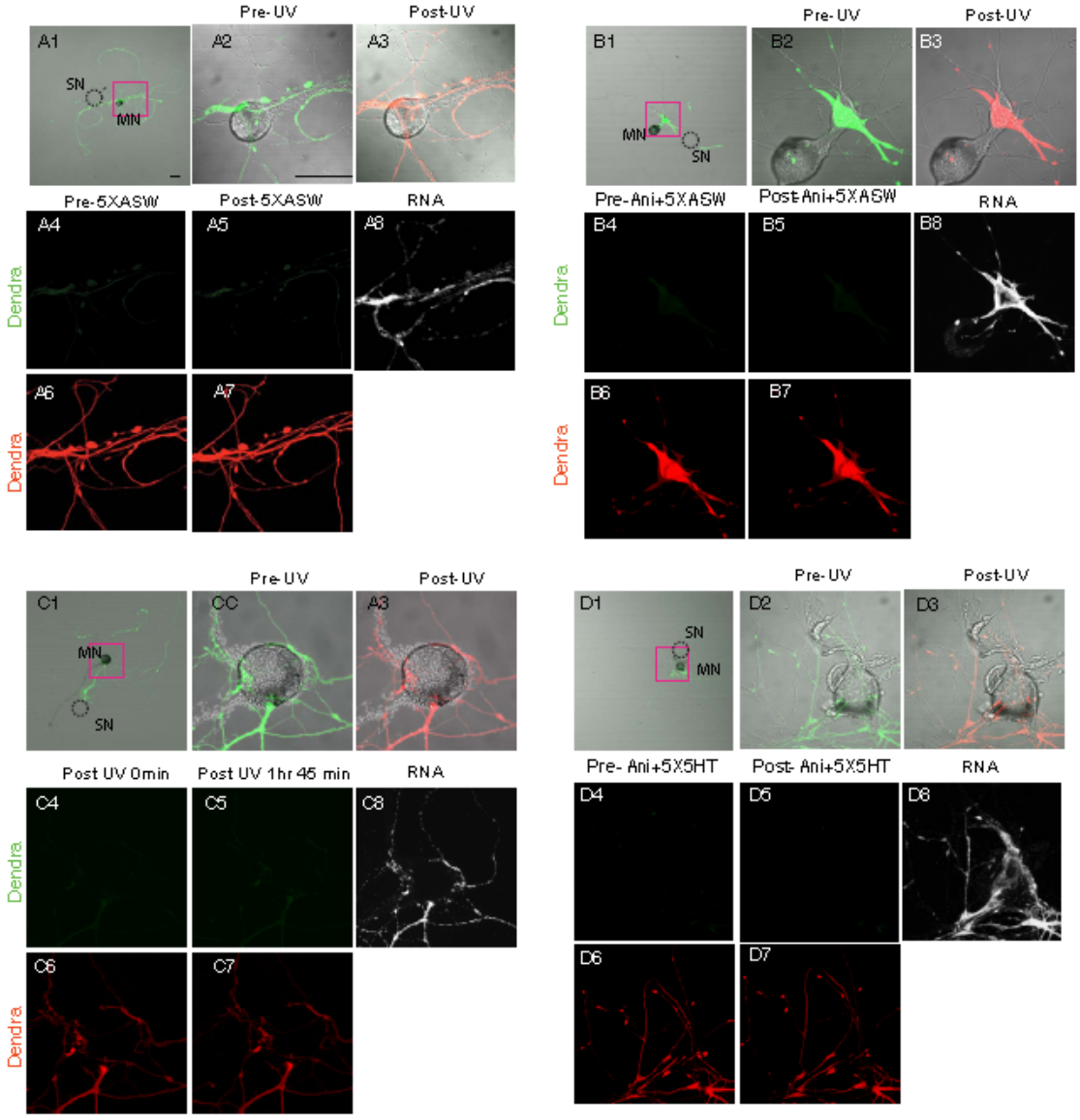
Pre-UV
Post-UV
A1
A2
A3
SN
MN
Pre-5XASW
Post-5XASW
RNA
A4
A5
A8
Dendra
A6
A7
Dendra
Pre-UV
Post-UV
B1
B2
B3
MN
SN
Pre-Ani+5XASW
Post-Ani+5XASW
RNA
B4
B5
B8
Dendra
B6
B7
Dendra
Pre-UV
Post-UV
C1
CC
A3
MN
SN
Post UV 0min
Post UV 1hr 45 min
RNA
C4
C5
C8
Dendra
C6
C7
Dendra
Pre-UV
Post-UV
D1
D2
D3
SN
MN
Pre- Ani+5X5HT
Post- Ani+5X5HT
RNA
D4
D6
D8
D6
D7

Figure 2.6. Control experiments for fig 2.5: representative images of reporter translation in 5XASW vehicle control, untreated control, and cultures treated with 5XASW and 5X5HT in the presence of the protein synthesis inhibitor anisomycin. **(A1)** Low magnification image of a SN expressing the dendra-reporter in a SN-MN coculture. The dashed circle outlines the location of the removed soma. **(A2 and A3)** High magnification DIC/merged image of area outlined by the red box in A1, showing synaptic contacts between SN and MN before (A2) and after (A3) UV photoconversion. **(A4 and A5)** Green dendra signal remaining following photoconversion, before (A4) and after (A5) vehicle stimulation (5XASW). Lack of green dendra indicates efficient photoconversion, new green dendra reveals modest new translation post 5xASW. **(A6 and A7)** Photoconverted red dendra signal before (*A6*) and after (*A7*) 5xASW shows SN volume. (A8) Cells were fixed at the end of the experiment and processed for FISH with antisense dendra riboprobes. **(B1-7)** 5XASW treatment in the presence of anisomycin (10 μm). **(C1-7)** Control images taken from untreated cultures. **(D1-7)** 5X5HT treatment in the presence of anisomycin (10 μM). Modest increases in green dendra signal were detected following 5xASW (A4-5) and in untreated control cultures, reflecting basal translation; no increase in green dendra signal was observed in the presence of anisomycin (B4-5 and D4-5), demonstrating that the new green signal resulted from new translation. **(A8, B8, C8, D8)** RNA staining at the end of experiments reveals equivalent RNA intensity acrossexperiments. Scale bar: 50μm.

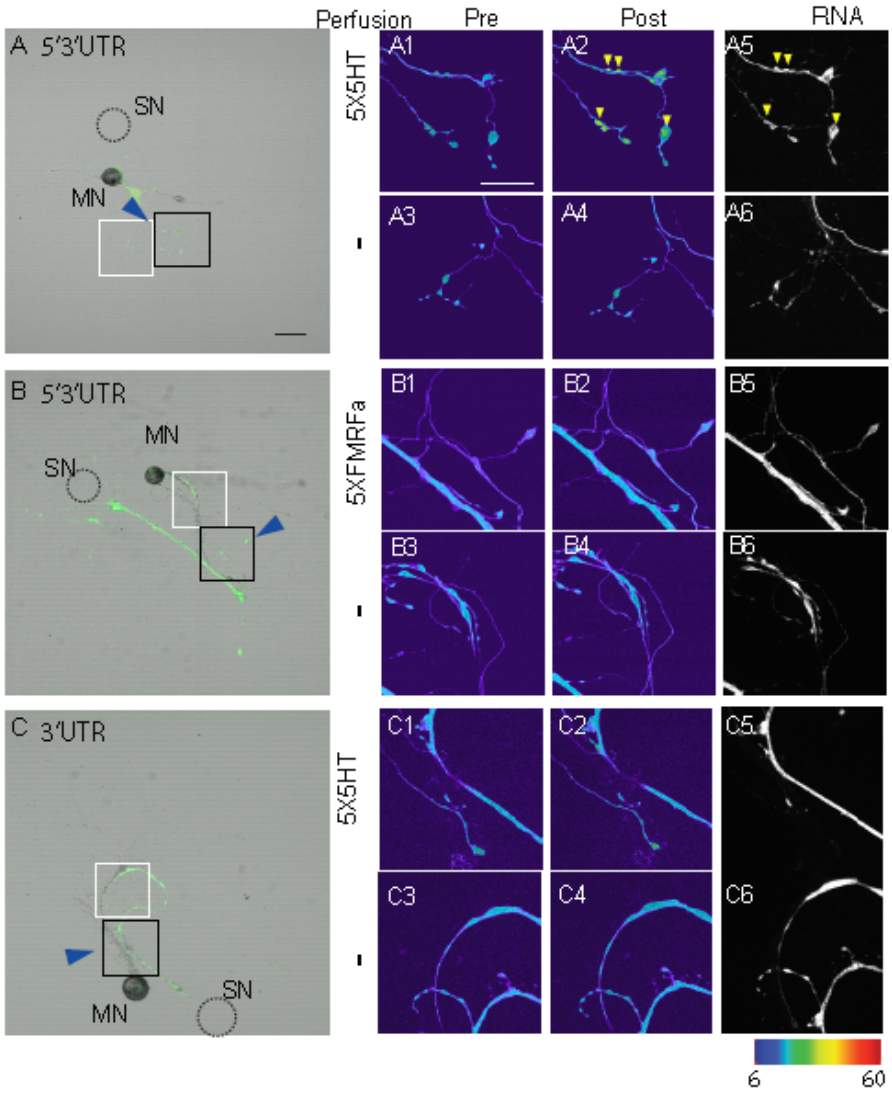
Perfusion
Pre
Post
RNA
A 5'3'UTR
SN
MN
5X5HT
A1
A2
A5
A3
A4
A6
B 5'3'UTR
MN
SN
5XFMRFa
B1
B2
B5
B3
B4
B6
C 3'UTR
5X5HT
C1
C2
C5
C3
C4
C6
MN
SN
6
60

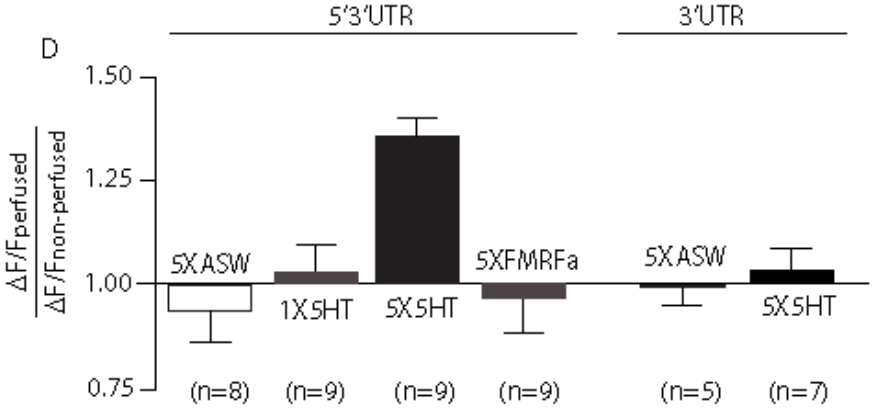
D
5'3'UTR
3'UTR
ΔF/Fperfused / ΔF/Fnon-perfused
1.50
1.25
1.00
0.75
5XASW
1X5HT
5X5HT
5XFMRFa
5XASW
5X5HT
(n=8)
(n=9)
(n=9)
(n=9)
(n=5)
(n=7)

Figure 2.7. Synapse-, stimulus- and transcript-specific translation.
Sensorin translational reporter was expressed in *Aplysia* sensory neurons (SNs) co-cultured with motor neurons (MNs), the SN soma was removed and dendra was photoconverted from green to red by UV illumination. Perfusion electrodes were used to locally apply compounds to subsets of synapses formed between SN and MN. **(A, B, C)** Low magnification image of dendra-reporter expressing SN in SN-MN coculture. Dashed circle indicates removed soma; blue arrowheads indicate direction of perfusion flow; black squares denote regions imaged before and after local perfusion; white squares denote imaged non-perfused regions. **(A-C panels 1-4)** Pseudocolored images of green dendra signal after photoconversion and before (pre) and after (post) local perfusion. **(A-C panels 5 and 6)** Fluorescence *in situ* hybridization for reporter mRNA. Arrowheads in A2 and A5 point to new translation colocalizing with reporter mRNA. A: 5'3'UTR reporter, local perfusion of 5x5HT. B: 5'3'UTR reporter, local perfusion of 5xFMRFa. C: 3'UTR, localperfusion of 5x5HT. See fig 9 and 10 for images of pre-UV green and post-UV red photoconverted dendra signal, 5XASW controls, and 1X5HT stimulation. Scale bar: 50μm; **(D)** Quantification of translation as ratio of ΔF/F at perfused compared to non-perfused sites reveals translation occurs only with 5x5HT. ***p<0.0001, Wilcoxon-Mann Whitney test (also see fig 2.11 for group data).

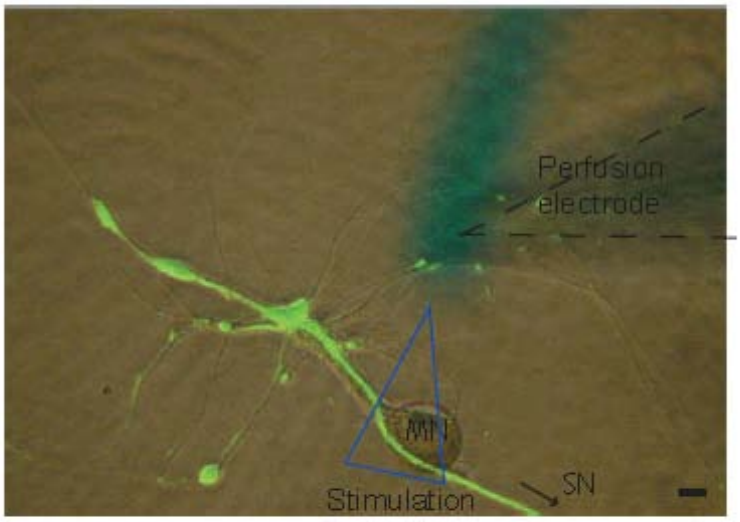

Figure 2.8. Photomicrograph illustrating local perfusion.

Neurites of a SN expressing the green dendra reporter (the SN cell soma has been removed), in contact with an LFS MN. A perfusion electrode (dotted line) was used to locally deliver stimuli (5XASW, 1X5HT, 5x5HT, or 5XFMRFa) to a subset of synapses, with bulk flow (blue triangle) in the bath directing the flow away from the rest of the neuronal arbor. Fast green dye was included to visualize the perfused area (green-blue stream). Scale bar: 50μm.

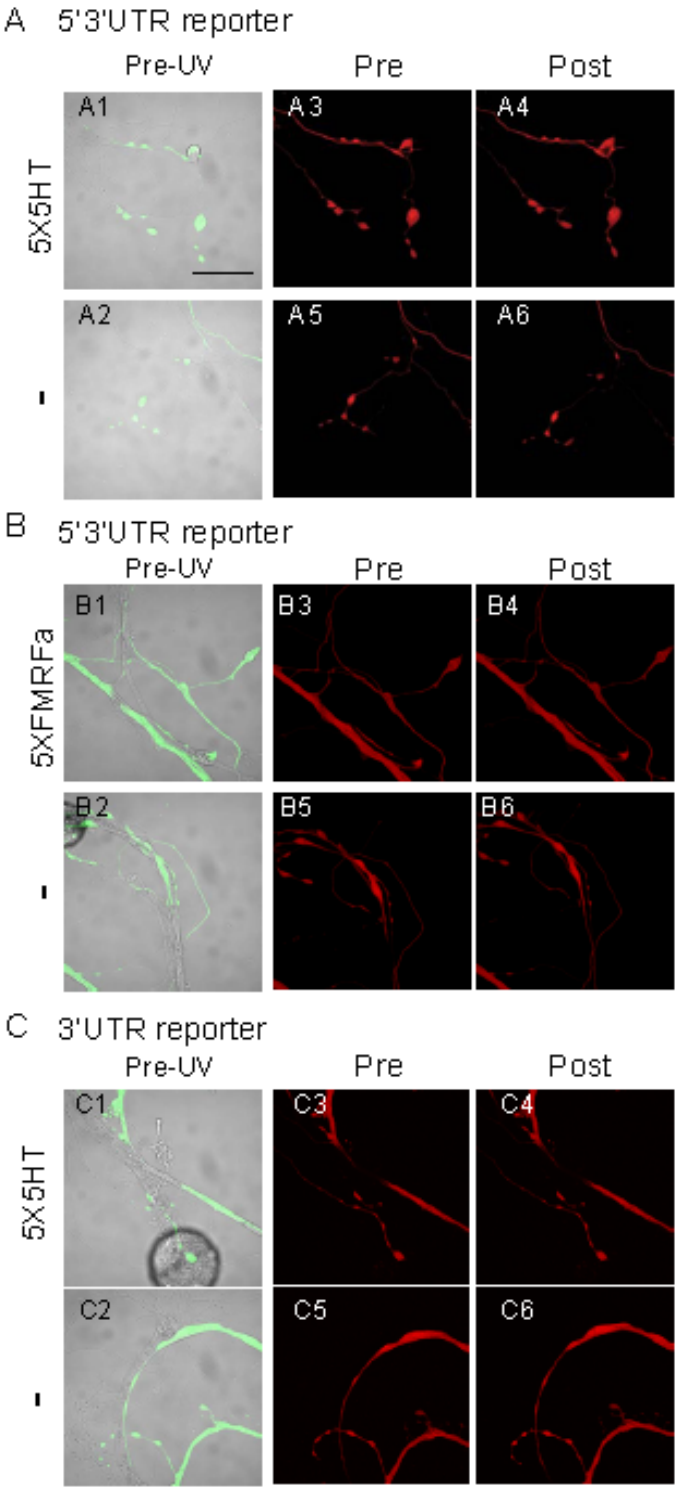
A 5'3'UTR reporter
Pre-UV
Pre
Post
A1
A3
A4
5X5HT
A2
A5
A6
-
B 5'3'UTR reporter
Pre-UV
Pre
Post
B1
B3
B4
5XFMRFa
B2
B5
B6
-
C 3'UTR reporter
Pre-UV
Pre
Post
C1
C3
C4
5X5HT
C2
C5
C6
-

Figure 2.9. Pre-photoconversion images and photoconverted (red) dendra images to accompany fig 3.

(A-C panels 1 and 2) Merged DIC, green and red images of boxed regions (from fig 2.7) showing sites of synaptic contact before UV photoconversion. (A-C panels 3-6) Confocal images of red dendra signal after photoconversion and before (pre) and after (post) local perfusion. Note that no significant morphological changes occurred during the stimulation, as indicated by the lack of change in the red dendra signal. Scale bar: 50μm.

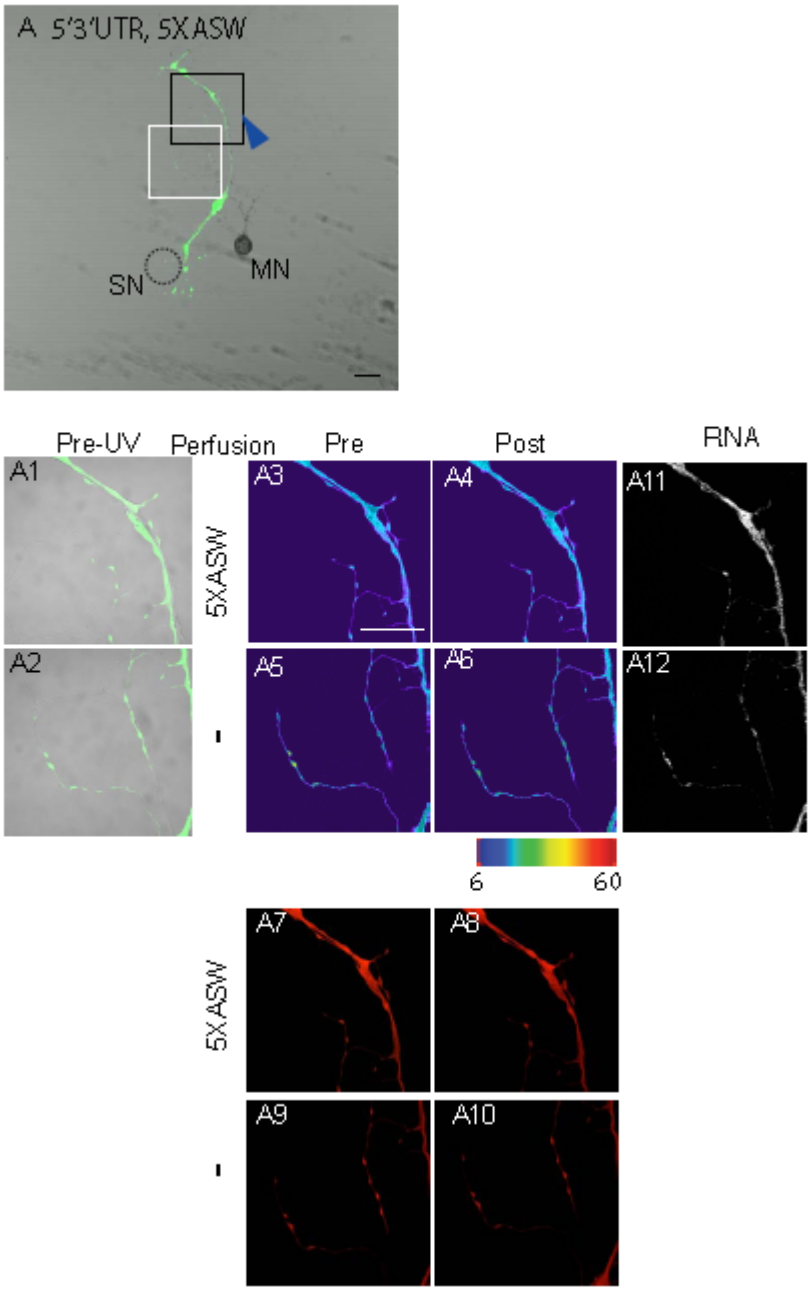
A 5'3'UTR, 5XASW
SN
MN
Pre-UV
Perfusion
Pre
Post
RNA
A1
A2
A3
A4
A5
A6
A7
A8
A9
A10
A11
A12
5XASW
5XASW
6
60

Figure 2.10. Local perfusion of 5XASW does not stimulate translation of 5'3'UTR reporter.
(A) Low magnification images indicating perfused region (black box), non-perfused region (white box), removed SN soma (dashed circle), and direction of local perfusion (blue arrow). **(Panels A1 and A2)** Merged DIC, green and red images of boxed regions showing sites of synaptic contact before UV photoconversion. **(Panels A3-6)** Pseudocolored confocal images of green dendra signal after photoconversion and before (pre) and after (post) local perfusion. **(Panels A7-10)** Confocal images of red dendra signal after photoconversion and before (pre) and after (post) local perfusion. **(Panels A11 and A12)** RNA staining at the end of experiments reveals equivalent RNA intensity in both perfused and non-perfused sites. Note that no significant morphological changes occurred during the stimulation, as indicated by the lack of change in the red dendra signal. Scale bars: 50μm.

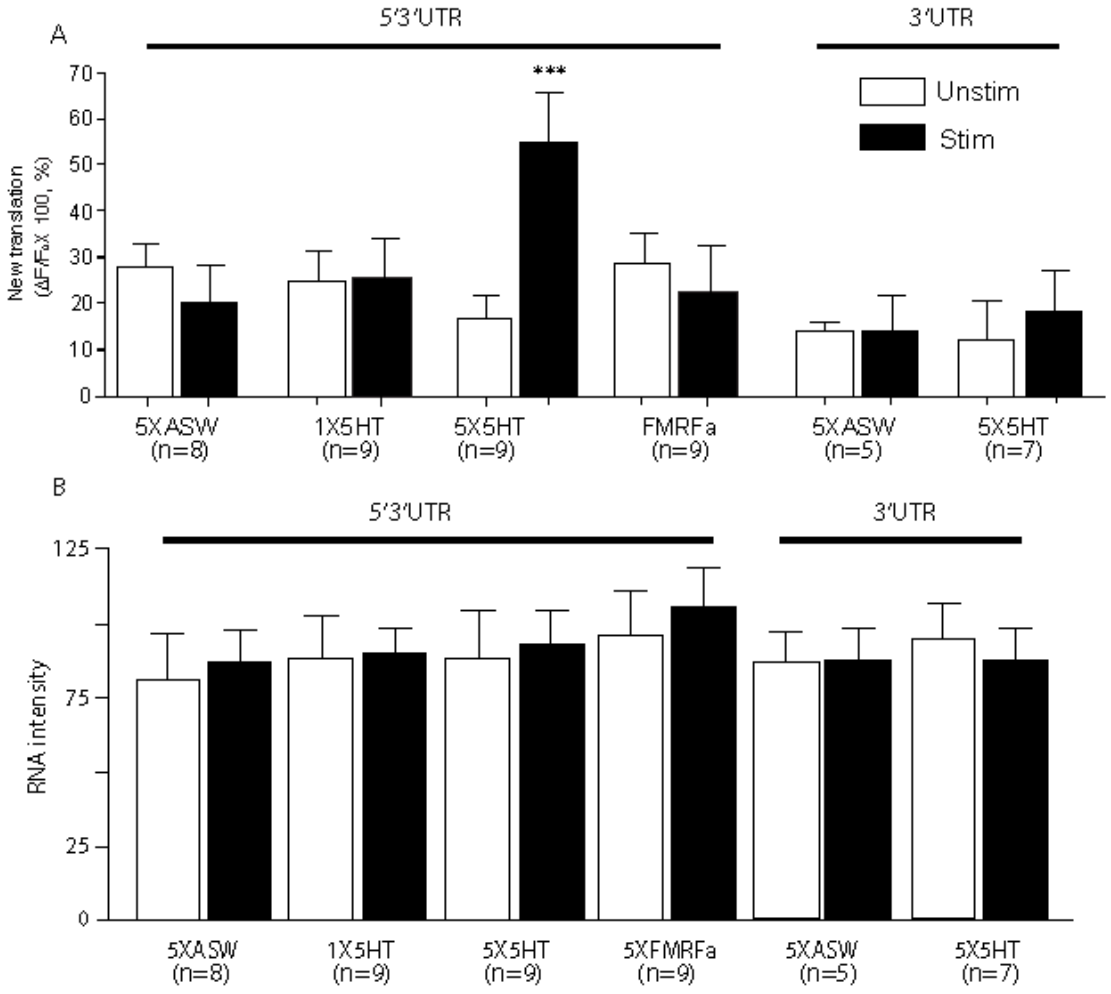

Translation at perfused and nonperfused sites measured as ΔF/F

Figure 2.11. Quantification of new translation and RNA intensity in local stimulation experiments.
New translation was quantified as described in the supporting online methods section, and results were grouped across experiments. Note that the analysis of the differences in figure 2.7, 2.12 and 2.18 was measured in each neuron (intraneuron comparison) and the results are presented as a ratio between ΔF/F at perfused and non-perfused sites. Here, we present the group data by showing the mean ΔF/F at perfused sites and at non-perfused sites (instead of showing them as a ratio of perfused/non-perfused) **(A)** Group analysis accompanying fig 2.7. New translation at non-perfused synapses and at synapses perfused wtih 5XASW, 1X5HT, 5X5HT, or 5XFMRFa. There was no significant difference in translation at non-perfused synapses. Only synapses perfused with 5X5HT showed significantly higher translation (***p<0.001, Wilcoxon-Mann-Whitney test). **(B)** Analysis of mean RNA intensity for each imaged field showed that there was no significant difference in the concentration of RNA between perfused and non-perfused regions, or between cells treated with different stimuli. Thus, the increase in translation with local application of 5x5HT cannot be attributed to differences in RNA concentrations.

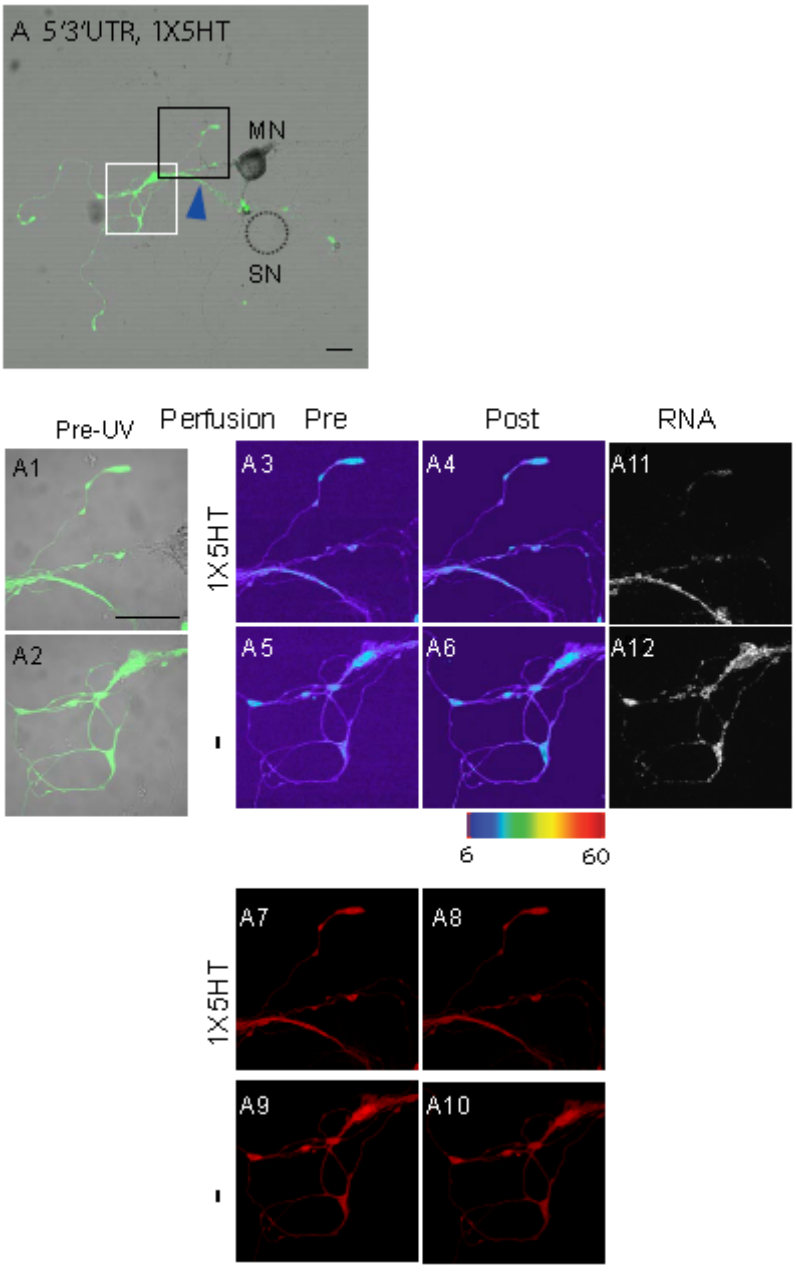
A 5'3'UTR, 1X5HT
MN
SN
Pre-UV
Perfusion
Pre
Post
RNA
A1
A2
A3
A4
A5
A6
A11
A12
1X5HT
-
6
60
A7
A8
A9
A10
1X5HT
-

Figure 2.12. 1X5HT followed by 4XASW, which produces short-term facilitation, does not stimulate translation of the 5'3'UTR reporter.
(A) Low magnification images indicating perfused region (black box), non-perfused region (white box), removed SN soma (dashed circle), and direction of local perfusion (blue arrow). **(Panels A1 and A2)** Merged DIC, green and red images of boxed regions showing sites of synaptic contact before UV photoconversion. **(Panels A3-6)** Pseudocolored confocal images of green dendra signal after photoconversion and before (pre) and after (post) local perfusion. **(Panels A7-10)** Confocal images of red dendra signal after photoconversion and before (pre) and after (post) local perfusion. **(Panels A11 and A12)** RNA staining at the end of experiments reveals equivalent RNA intensity in both perfused and non-perfused sites. Note that no significant morphological changes occurred during the stimulation, as indicated by the lack of change in the red dendra signal. Scale bars: 50μm.

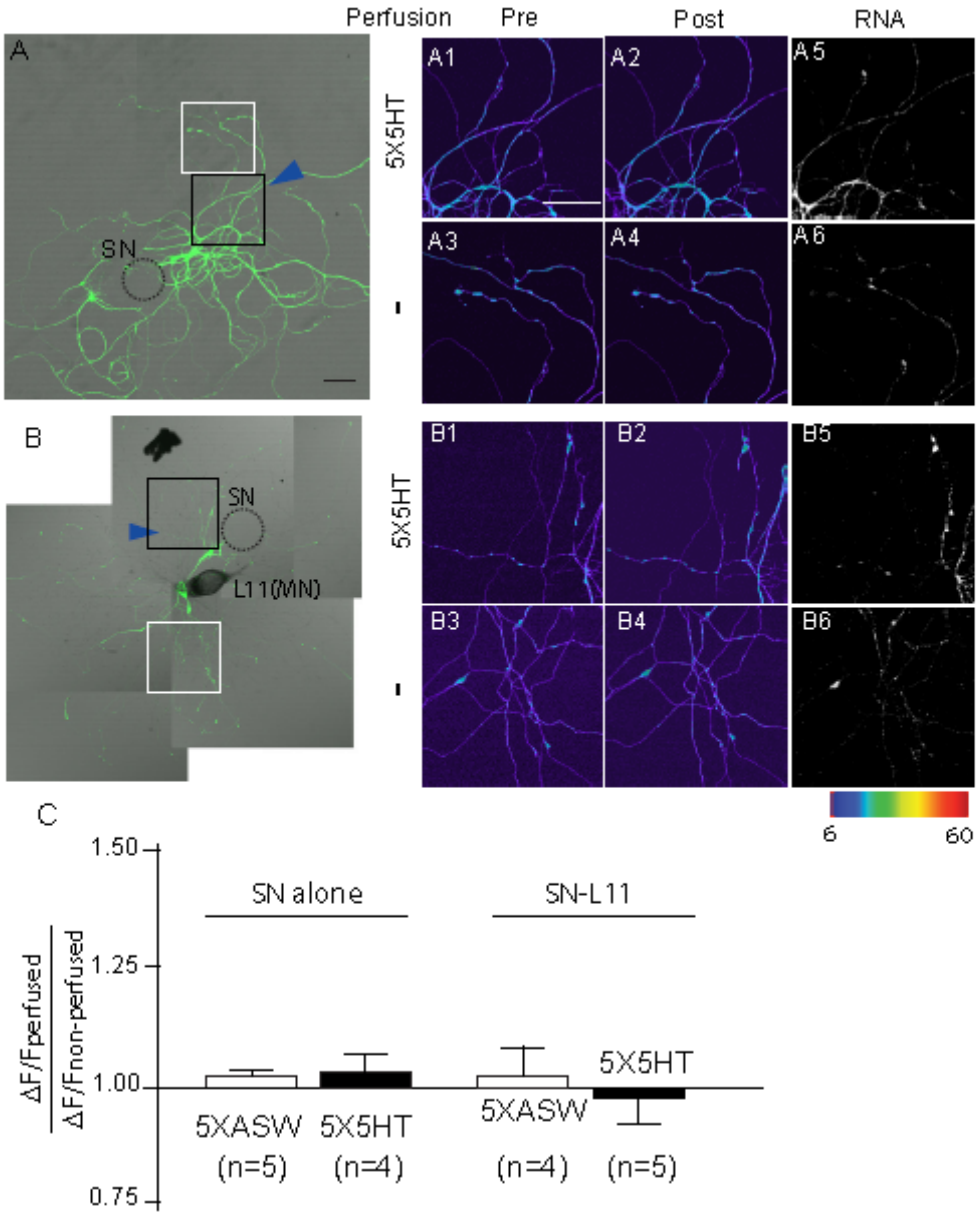
Perfusion
Pre
Post
RNA
A
SN
5X5HT
A1
A2
A5
A3
A4
A6
B
SN
L11(MN)
5X5HT
B1
B2
B5
B3
B4
B6
6
60
C
1.50
1.25
1.00
0.75
ΔF/Fperfused
ΔF/Fnon-perfused
SN alone
SN-L11
5X5HT
5XASW
5X5HT
5XASW
(n=5)
(n=4)
(n=4)
(n=5)

Figure 2.13. Local stimulation with 5X5HT does not stimulate translation of sensorin reporter in isolated SNs or in SNs paired with non-target MNs.
Sensorin translational reporter was expressed in isolated *Aplysia* sensory neurons (SNs, which do not form autapses or chemical synapses with one another, A), or (B) in SNs cocultured with nontarget L11 motor neurons (MNs), with which SNs do not form chemical synapses. Local perfusion of 5X5HT was applied as described in Fig 2.7. **(A, B)** Low magnification image of dendra-reporter expressing SNs. Dashed circle indicates removed soma; blue arrowheads indicate direction of perfusion flow; black squares denote regions imaged before and after local perfusion; white squares denote imaged non-perfused regions. **(A and B panels 1-4)** Pseudocolored images of green dendra signal after photoconversion and before (pre) and after (post) local perfusion. **(A and B panels 5 and 6)** FISH for reporter mRNA. Scale bar: 50μm; **(C)** Quantification of translation as ratio of ΔF/F at perfused compared to non-perfused sites reveals no increase in translation with either 5X5HT or 5XASW (Wilcoxon-Mann-Whitney test; also see group data and RNA intensity quantification in fig 2.16).

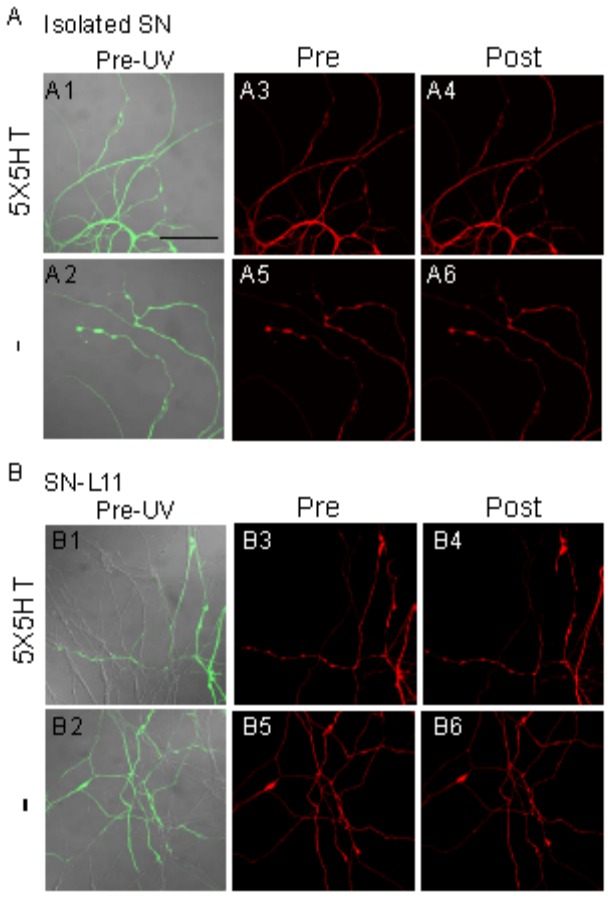

Figure 2.14. Pre-photoconversion images and photoconverted (red) dendra images to accompany fig 2.4.
(A-B panels 1 and 2) Merged DIC, green and red images of boxed regions (from fig. 2.7) showing sites of synaptic contact before UV photoconversion. **(A-B panels 3-6)** Confocal images of red dendra signal after photoconversion and before (pre) and after (post) local perfusion. Note that no significant morphological changes occurred during the stimulation, as indicated by the lack of change in the red dendra signal. Scale bar: 50μm.

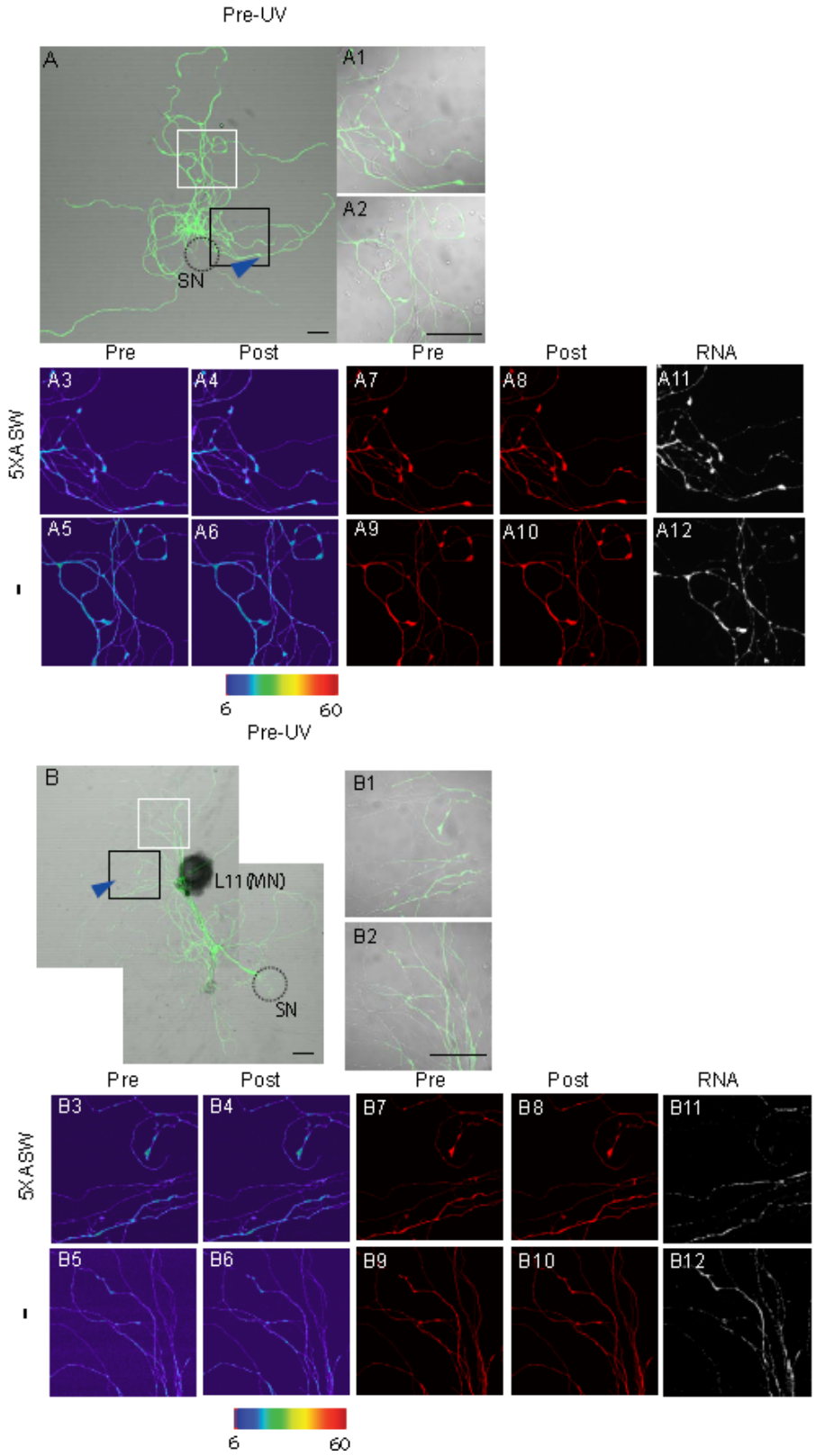
Pre-UV
A
A1
A2
SN
Pre
Post
Pre
Post
RNA
5XA SW
A3
A4
A7
A8
A11
A5
A6
A9
A10
A12
6
60
Pre-UV
B
B1
B2
L11 (MN)
SN
Pre
Post
Pre
Post
RNA
5XA SW
B3
B4
B7
B8
B11
B5
B6
B9
B10
B12
6
60

Figure 2.15. Controls for fig 2.13: 5XASW did not simulate translation of reporters expressed in either isolated SNs or SNs paired with non-target motor neuron L11. **(A and B)** Low magnification images indicating perfused region (black box), non-perfused region (white box), removed SN soma (dashed circle) and direction of local perfusion (blue arrow). **(A-B panels 2 and 3)** Merged DIC, green and red images of boxed regions showing sites of synaptic contact before UV photoconversion. **(A-B panels 4-7)** Pseudocolored confocal images of green dendra signal after photoconversion and before (pre) and after (post) local perfusion. **(A-B panels 8-11)** Confocal images of red dendra signal after photoconversion and before (pre) and after (post) local perfusion. **(A-B panels 12 and 13)** RNA staining at the end of experiments revealed equivalent RNA intensity in both perfused and non-perfused sites Note that no significant morphological changes occurred during the stimulation, as indicated by the lack of change in the red dendra signal. Scale bars: 50μm.

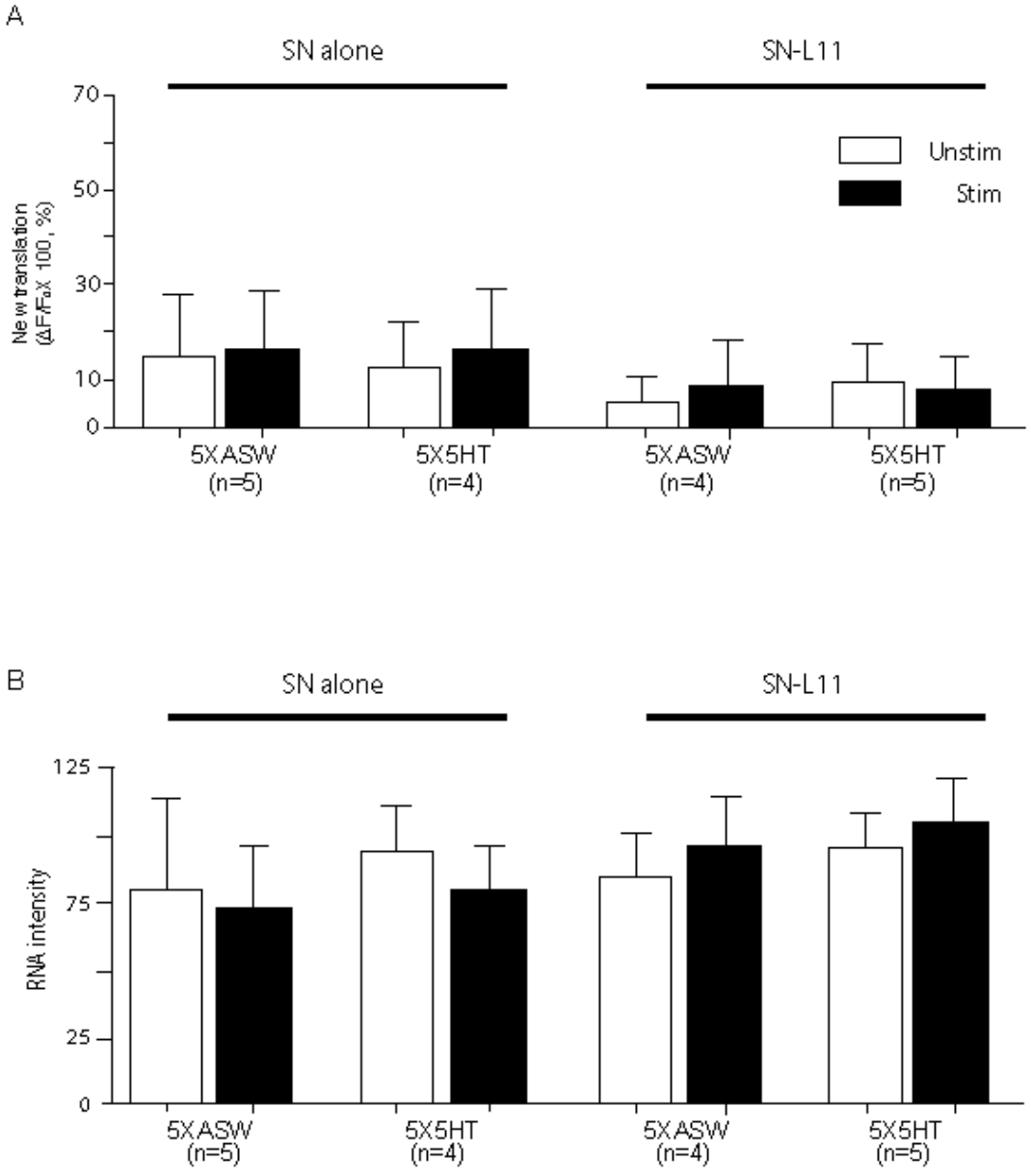

Figure 2.16. Quantification of new translation and RNA intensity in local stimulation experiments included in Fig. 2.13 and fig 2.15.
(A) Group data of new translation. **(B)** RNA staining intensity (Wilcoxon-Mann-Whitney test).

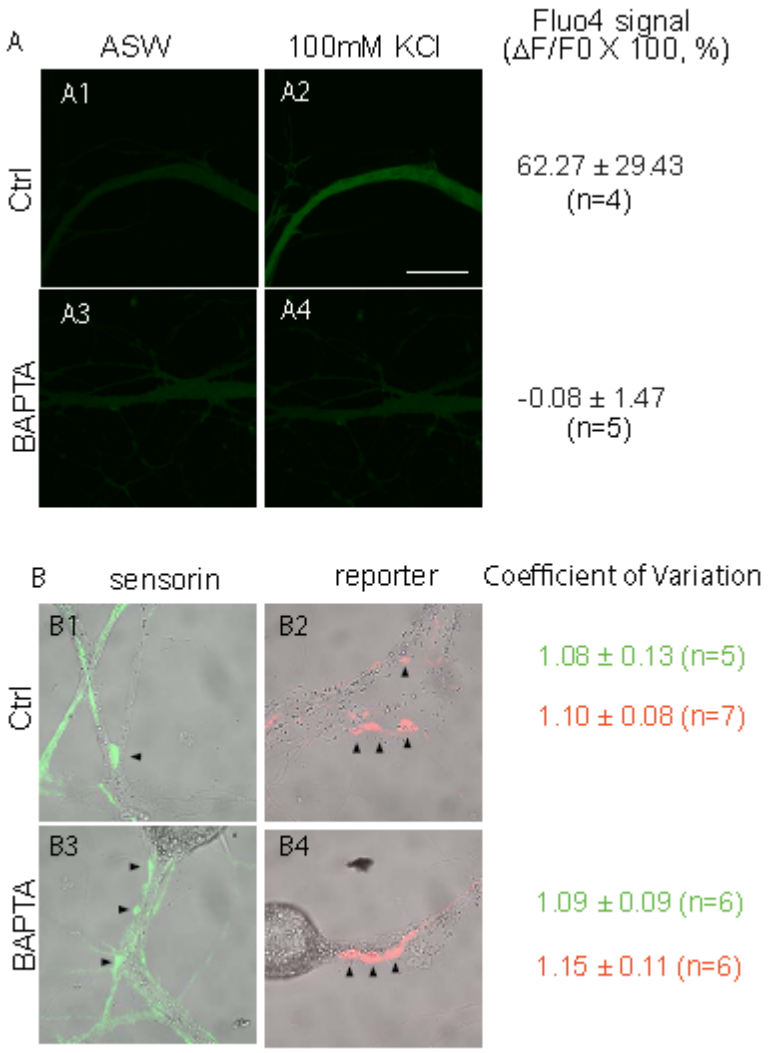
A
ASW
100mM KCl
Fluo4 signal
(ΔF/F0 X 100, %)
A1
A2
A3
A4
Ctrl
BAPTA
62.27 ± 29.43
(n=4)
-0.08 ± 1.47
(n=5)
B
sensorin
reporter
Coefficient of Variation
B1
B2
B3
B4
Ctrl
BAPTA
1.08 ± 0.13 (n=5)
1.10 ± 0.08 (n=7)
1.09 ± 0.09 (n=6)
1.15 ± 0.11 (n=6)

Figure 2.17. Acute injection of BAPTA completely blocks depolarization-induced elevations in intracellular calcium in MNs but did not affect either endogenous sensorin or reporter mRNA concentration at SN-MN synapses.
(A) SNs were cocultured with LFS MNs. On DIV5, 50mM BAPTA (A3 and A4) or vehicle (1.5M K-acetate, 0.5M KCl, 0.01M HEPEs (pH 7.2), A1, A2) were injected into cytoplasm of LFS motor neurons together with Fluo4 (5 mM). Confocal images were acquired when cultures were in ASW (A1, A3) or 100mM KCl (added to the bath to depolarize the cells, A2, A4). The increase in Fluo4 signal was quantified as $\Delta F/F$ X100, %. **(B)** In parallel experiments, cultures were fixed 1hr after BAPTA/vehicle injection, and processed for FISH to detect endogenous sensorin (green) and reporter mRNA (red) clustering. In control cultures, MNs were injected with vehicle (B1, B2); in experimental cultures, MNs were injected with BAPTA (B3, B4). BAPTA injection did not alter the concentration of either reporter mRNA or endogenous sensorin mRNA at synapses, as quantified by measuring the coefficient of variation (Lyles et al. 2006 and unpublished data). Scale bars: 50μm.

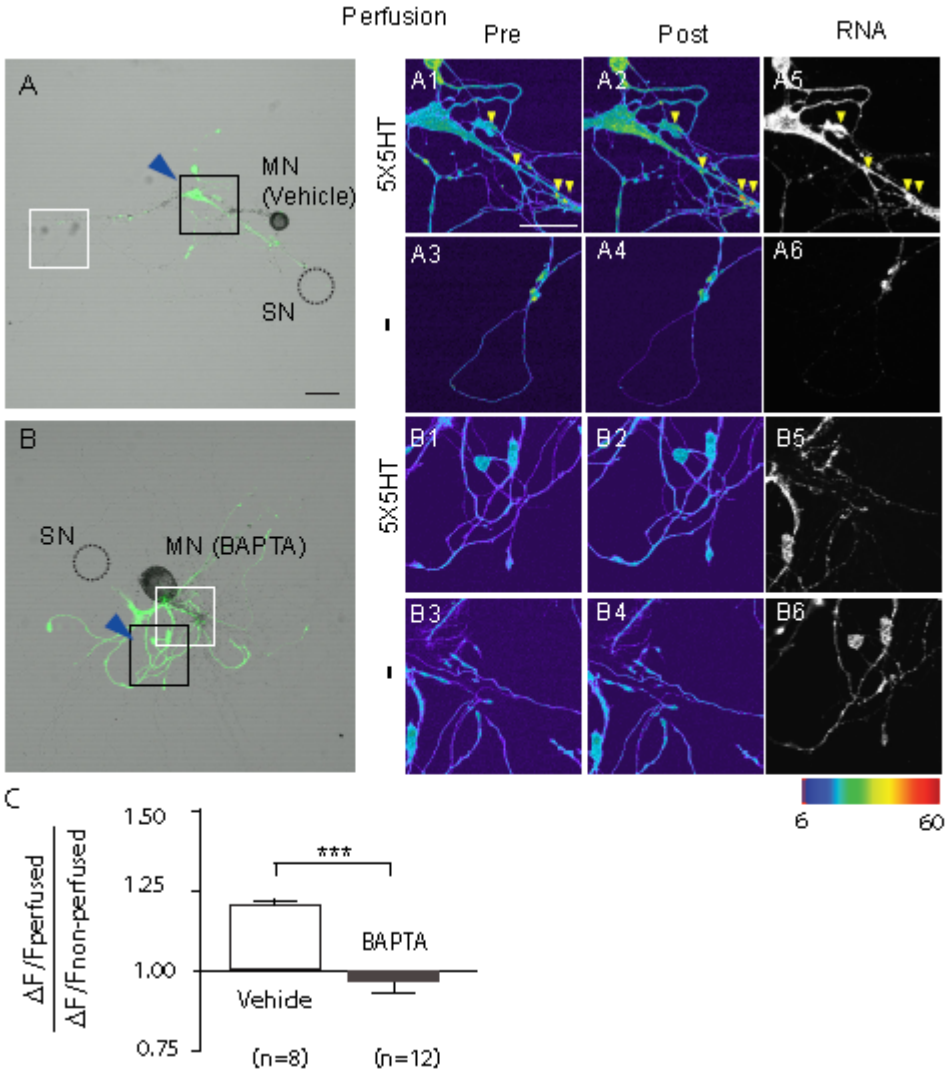
Perfusion
Pre
Post
RNA
A
MN
(Vehicle)
SN
B
SN
MN (BAPTA)
5X5HT
-
5X5HT
-
A1
A2
A5
A3
A4
A6
B1
B2
B5
B3
B4
B6
6
60
C
ΔF/Fperfused
ΔF/Fnon-perfused
1.50
1.25
1.00
0.75
***
BAPTA
Vehide
(n=8)
(n=12)

Figure 2.18. Calcium signaling in motor neuron is required for 5HT-induced translation of reporter in sensory neuron.
Sensorin translational reporter was expressed in *Aplysia* sensory neurons (SNs) culturedwith motor neurons (MNs). The SN soma was removed, either vehicle (1.5 M K+ acetate, 0.5M KCl, 0.01 M HEPES pH 7.2, **A**) or BAPTA (50mM, **B**) was microinjected into the MN, and dendra was photoconverted from green to red by UV illumination. Perfusion electrodes were used to locally apply compounds to subsets of synapses formed between SN and MN. **(A, B)** Low magnification image of dendra-reporter expressing SN in SN-MN coculture. Dashed circle indicates removed soma; blue arrowheads indicate direction of perfusion flow; black squares denote regions imaged before and after local perfusion; white squares denote imaged non-perfused regions. **(A and B panels 1-4)** Pseudocolored images of green dendra signal after photoconversion and before (pre) and after (post) local perfusion. **(A and B panels 5 and 6)** FISH for reporter mRNA. See fig 2.16 for images of pre-UV and photoconverted dendra signal. Scale bar: 50μm; *D,* Quantification of translation as ratio of ΔF/F at perfused compared to non-perfused sites reveals that BAPTA injection into the MN blocks 5HT-induced translation in the SN (***$p<0.0005$, t-test).

REFERENCE

1. C. M. Alberini, *J Exp Biol* 202, 2887 (1999).

2. E. R. Kandel, *Science* 294, 1030 (2001).

3. P. L. Greer, M. E. Greenberg, *Neuron* 59, 846 (2008).

4. P. V. Nguyen, T. Abel, E. R. Kandel, *Science* 265, 1104 (1994).

5. K. C. Martin *et al.*, *Cell* 91, 927 (1997).

6. U. Frey, R. G. Morris, *Nature* 385, 533 (1997).

7. A. Casadio *et al.*, *Cell* 99, 221 (1999).

8. K. C. Martin, *Curr Opin Neurobiol* 14, 305 (2004).

9. M. A. Sutton, E. M. Schuman, *Cell* 127, 49 (2006).

10. A. Govindarajan, R. J. Kelleher, S. Tonegawa, *Nat Rev Neurosci* 7, 575 (2006).

11. O. Steward, W. B. Levy, *J Neurosci* 2, 284 (1982).

12. L. E. Ostroff, J. C. Fiala, B. Allwardt, K. M. Harris, *Neuron* 35, 535 (2002).

13. S. J. Tang *et al.*, *Proc Natl Acad Sci U S A* 99, 467 (2002).

14. J. Eberwine, B. Belt, J. E. Kacharmina, K. Miyashiro, *Neurochem Res* 27, 1065 (2002).

15. R. Moccia *et al.*, *J Neurosci* 23, 9409 (2003).

16. J. Zhong, T. Zhang, L. M. Bloch, *BMC Neurosci* 7, 17 (2006).

17. M. M. Poon, S. H. Choi, C. A. Jamieson, D. H. Geschwind, K. C. Martin, *J Neurosci* 26, 13390 (2006).

18. T. Suzuki, Q. B. Tian, J. Kuromitsu, T. Kawai, S. Endo, *Neurosci Res* 57, 61 (2007).

19. H. Kang, E. M. Schuman, *Science* 273, 1402 (1996).

20. K. M. Huber, J. C. Roder, M. F. Bear, *J Neurophysiol* 86, 321 (2001).

21. G. Aakalu, W. B. Smith, N. Nguyen, C. Jiang, E. M. Schuman, *Neuron* 30, 489 (2001).

22. C. Job, J. Eberwine, *Nat Rev Neurosci* 2, 889 (2001).

23. W. Ju *et al.*, *Nat Neurosci* 7, 244 (2004).

24. K. F. Raab-Graham, P. C. Haddick, Y. N. Jan, L. Y. Jan, *Science* 314, 144 (2006).

25. V. F. Castellucci, S. Schacher, *Prog Brain Res* 86, 105 (1990).

26. S. L. Mackey *et al.*, *Proc Natl Acad Sci U S A* 84, 8730 (1987).

27. V. Lyles, Y. Zhao, K. C. Martin, *Neuron* 49, 349 (2006).

28. D. L. Glanzman, E. R. Kandel, S. Schacher, *Neuron* 3, 441 (1989).

29. J. F. Brunet, E. Shapiro, S. A. Foster, E. R. Kandel, Y. Iino, *Science* 252, 856 (1991).

30. J. Y. Hu, F. Wu, S. Schacher, *J Neurosci* 26, 1026 (2006).

31. N. G. Gurskaya *et al.*, *Nat Biotechnol* 24, 461 (2006).

32. K. Liu, J. Y. Hu, D. Wang, S. Schacher, *J Neurobiol* 56, 275 (2003).

33. Z. Guan *et al.*, *Cell* 111, 483 (2002).

34. L. Santarelli, P. Montarolo, S. Schacher, *J Neurobiol* 31, 297 (1996).

35. D. Cai, S. Chen, D. L. Glanzman, *Curr Biol* 18, 920 (2008).

CHAPTER THREE

IDENTIFICATION OF A CIS-ACTING ELEMENT THAT LOCALIZES mRNA TO SYNAPSES

(Meer et al., PNAS 2012)

INTRODUCTION

mRNA localization and regulated translation provide a means of spatially restricting gene expression within distinct subcellular compartments. In the brain, local protein synthesis is critical to the development and experience-driven refinement of neural circuits, playing roles in axon guidance, synaptogenesis, and synaptic plasticity (1, 2).A large but select population of transcripts localizes to axons and dendrites(3-8), indicating that local translation subserves diverse cell biological functions. Where studied, the localization of mRNAs to axons or dendrites has been shown to depend on cis-acting localization elements (LEs) usually found in the 3' UTR, although occasionally present in the coding sequence or 5'UTR(1, 2, 9). These *cis*-acting mRNA LEs recruit specific trans-acting RNA binding proteins, and the resulting messenger ribonucleoproteins (mRNPs) are packaged into RNA transport granules that interact with molecular motors to be delivered to their final subcellular destination(10-12).

In situ hybridization studies in neurons indicate that localized mRNAs in neurons are targeted to distinct subcellular compartments and domains within neuronal processes. For example, MAP2 mRNA concentrates within proximal dendrites, while CaMKIIα mRNA extends to distal dendrites(13). mRNA localization also appears to be dynamically regulated during development and with activity. In mature neurons, β-actin mRNA localizes to dendrites, and its concentration to distal dendrites is stimulated by depolarization(14). Stimuli that activate NMDA or TrkB receptors drive specific BDNF mRNA isoforms into distal dendrites of hippocampal neurons(15). High frequency

stimulation of perforant path projections to the dentate gyrus has been shown to direct localization of the mRNA encoding the immediate-early gene Arc selectively and specifically to activated dendritic lamina(16), and to drive localization of pre-existing CaMKIIα mRNA into synaptosome fractions(17). Together, these findings indicate that specific transcripts undergo constitutive as well as developmental- and activity-dependent localization to distinct subcellular compartments.

Although a handful of *cis*-acting RNA localization elements, ranging in size from five to several hundred nucleotides have been shown to mediate constitutive localization of specific mRNAs into distal processes of neurons(18), little is known about cis-acting elements that target mRNAs to more restricted subcellular compartments, such as synapses, or that mediate activity-dependent redistribution of mRNAs within neuronal processes. To identify such *cis*-acting LEs, we generated and expressed chimeric reporters to study the localization of the mRNA encoding the Aplysia sensory neuron (SN) specific peptide transmitter, sensorin(19). Release of sensorin from the sensory neuron is required for both synapse formation and long-term facilitation(19, 20). The localization of sensorin mRNA is regulated by synapse formation, such that it is diffusely localized in neurites of isolated SNs (which do not form synapses), but concentrates at synapses in SNs paired with target motor neurons (MNs,(19). Synapse formation does not alter the localization of other neuritically localized mRNAs, including those encoding α-tubulin and β-thymosin(4), suggesting that sequences within the sensorin mRNA specify its synaptic localization. Dissection of the mechanisms underlying sensorin mRNA localization thus provides not only a means of identifying *cis*-acting LEs involved in the

export of mRNA from the soma to distal neuronal processes and in the localization of mRNA specifically to synapses, but also LEs that dynamically mediate changes in mRNA localization in response to synapse formation.

We previously demonstrated that the full-length 5' and 3'UTRs of sensorin are sufficient for synaptic localization of reporter mRNAs, and for stimulus-induced translational regulation of the reporter at synapses(21). While the 3'UTR was sufficient for localization of reporter mRNA to distal neurites, the 5'UTR was required for synaptic localization of the reporter(21). To define the minimal LE for synaptic targeting, we have now characterized a series of deletion and point mutations in the 5'UTR, focusing on stem-loop structures. Our studies identify a 66-nucleotide-long stem-loop *cis*-element in 5'UTR, just upstream of the translational start site that functions as asynaptic LE (sLE).

RESULTS

To define the RNA sequences that mediate localization of sensorin mRNA to neurites and to synapses, we fused the 5' UTR, coding sequence and/or the 3' UTR of sensorin to the coding sequence of fluorescent protein dendra2 (Fig 3.1A). We microinjected each construct into cultured Aplysia SNs, fixed the cultures 48 hrs later and processed them for fluorescence in situ hybridization (FISH) with antisense dendra2 riboprobes to detect reporter mRNA. To differentiate between sequences mediating neuritic localization and sequences mediating synaptic localization, we performed experiments in isolated SNs, which do not form chemical synapses(19, 22), and in SNs forming glutamatergic synapses with target MNs.

As shown in Fig 3.1B, when no sensorin sequences were included, dendra2 reporter mRNA was restricted to the soma and proximal neurites of isolated SNs. Addition of either the 5'UTR or the coding sequence of sensorin to dendra2 did not alter this pattern of distribution. In contrast, the sensorin 3'UTR distributed dendra2 reporter mRNA into distal neurites, and addition of 5' UTR increased the distal distribution. To quantify the localization, we measured fluorescence pixel intensity along neurites length and measured the percent of FISH signal in the proximal, middle and distal third of the neurites. As shown in Fig 3.1C, in the absence of any sensorin sequence, or with the sensorin 5'UTR or coding sequence alone, little reporter RNA was present in the distal third (9±1%, 12±1%, and 14±4% respectively). In contrast, addition of the 3' UTR significantly increased the FISH signal in the distal third (to 26±3%), and when both 5'

and 3’ UTRs were included, the percent of reporter RNA in the distal third rose to 45±3%. By comparison, FISH for endogenous sensorin mRNA in parallel sets of cultures revealed that 34±2% of signal was present in the distal third (Fig 3.1C and Fig 3.3). Note that the mean pixel intensity in the cell body did not differ significantly between reporter constructs (Fig 3.3), indicating that differences in distal localization were not due to changes in expression levels. Collectively, our results show that the sensorin 3’UTR is sufficient to promote mRNA localization from the soma into distal processes. The sensorin 5’UTR does not promote distal localization on its own, but enhances distal localization of 3’UTR-containing reporters.

We next asked which sequences were required for synaptic localization by expressing the reporters shown in Fig 3.1A in SNs that were paired with MNs. As shown in Fig 3.2A, while the reporter with the 3’UTR of sensorin localized to distal sensory neurites, it did not concentrate at synapses. In contrast, the reporter with both the 5’ and the 3’ UTR of sensorin not only localized to distal neurites, but also concentrated at SN-MN synapses. We quantified this redistribution by comparing the coefficient of variation (CV) of the FISH signal in isolated SNs and in SN-MN cocultures (Fig. 3.2B). As previously reported for endogenous sensorin mRNA(19), we found that the CV was significantly greater when the 5’3’ UTR reporter construct was expressed in SN-MN cocultures than in isolated SNs (0.46±0.04 in SN vs. 1.07±0.09 in SN-MN, $p<0.001$, unpaired Student’s t-test), whereas the CV of 3’UTR reporter was not significantly different in cocultures as compared to isolated SNs (0.46±0.04 in SN vs. 0.51±0.04 in SN-MN). The CV of cytoplasmic diffusible dendra2 reporter proteins from the same

neurites did not differ between SN and SN-MN, showing that the different CV of reporter mRNA was not due to local volumetric variation (5'3'UTR reporter protein: 0.53±0.05 in SN vs. 0.52±0.03 in SN-MN; 3'UTR-reporter protein: 0.41±0.02 in SN vs. 0.56±0.03 in SN-MN).

To confirm that the sites of reporter mRNA concentration represented synapses, we expressed the pre-synaptic marker Vesicle-Associated Membrane Protein (VAMP)-mCherry in the SN and labeled the postsynaptic MN with Alexa-fluor 647 (Fig. 3.2C). We defined synapses as SN varicosities of >2 micron diameter containing a concentration of VAMP-mCherry and contacting the Alexa-fluor (blue) labeled MN. To measure synaptic localization, we quantified the percent of VAMP-mCherry positive varicosities adjacent to MNs that contained clusters of reporter mRNA. We limited our data analysis to neurons in which reporter mRNA was abundant in adjacent neurites (mean fluorescent RNA in situ intensity above 40 in an 8 bit image). As shown in Fig 3.2D, 87±3% of synapses colocalized with 5'3'UTR reporter mRNA concentration while only 38 ±7% also contained 3'UTR reporter mRNA concentration (see also (21), Fig 3.3). Together, these data indicate that the dynamic redistribution of sensorin mRNA from neuritic shafts to synapses upon synapse formation is mediated by signals in the 5'UTR.

Studies of mRNA localization in other cell types have revealed that LEs often consist of stem-loop structures(1, 18, 23). To define the minimal sequences within the sensorin 5'UTR that mediate localization to synapses, we focused on stem-loop secondary structures predicted by structural motif discovery programs. Twenty stem-loop structures were predicted, present within four distinct regions of the 5'UTR (Fig 3.4A

and Table 1(23-25). We deleted each region from the 5'3'UTR dendra reporter to generate reporters with intact 3'UTR and 5'UTRs lacking one of the four regions predicted to contain local stem-loop structures (ΔR1-R4, Fig 3.4B).

We expressed these reporters together with VAMP-mCherry in SNs paired with MNs and quantified synaptic localization. As shown in Fig 3.4C and D, ΔR1 and ΔR3 retained synaptic localization comparable to the intact 5'3'UTR reporter (81±2% for ΔR1 and 80±9% for ΔR3, compared to 87±3% for intact 5'UTR). The synaptic localization of ΔR2 was not as high as that of the intact 5'3'UTR reporter or endogenous sensorin mRNA, but was significantly greater than a 3'UTR-dendra reporter lacking the 5'UTR (68±7% compared to 38±7%). In contrast, the synaptic localization of ΔR4 mRNA was completely abolished, and did not differ significantly from that of the 3'UTR reporter (33±6% compared to 38±7%). RNA FISH intensity in the soma for each mutant was used as an indicator for overall RNA expression level. There was no correlation between RNA FISH intensity and synaptic localization, indicating that synaptic localization of mRNA did not depend on mRNA expression level (Fig 3.3).

To test whether R4was sufficient for localizing distally localized reporter mRNA to synapses, we inserted R4 (iR4, 66 nts) into the dendra reporter, downstream of the RSV promoter and upstream of the translation initiation site (iR4, Fig 3.3E). This reporter showed synaptic localization that was not significantly different from endogenous sensorin mRNA (Fig 3.3F, 70±7% and 83±3% respectively), indicating that the 66 nt R4 sequence is sufficient for localizing RNA to synapses (Fig 3.3F). By comparison, insertion of a sequence including R1, 2 and part of 3 (iR1-3) or R2 (iR2) was not

sufficient to mediate synaptic mRNA localization (iR1-3: 37±9% and iR2: 35±10%, Fig 3.3E and F). Since R4 was necessary and sufficient for synaptic RNA localization, we term it a synaptic LE (sLE).

We next set out to further define the sLE. Closer inspection of the primary sequence of this structure revealed a 24 nt-long sequence that contains two repeated 7mers (5'-CAGTCTTGAAACAGAAACAGTCTT-3', with two "CAGTCTT"s at the ends, and two "GAAACAG"s in the center, Fig 3.8A). Repeated hexamers or heptamers have been identified in LEs in various RNAs, often sites of recognition by RNA binding proteins. We thus set out to test whether this 24 nt tandem repeat element constituted the minimal synaptic LE. When we deleted either the entire 24 nt double-7mer-repeating sequence from 5'3'UTR-dendra reporter (ΔR5), just one set of the two heptamers(ΔR6), or 10-nt of the center repeat (ΔR7)the synaptic concentration of the reporter mRNA was strongly reduced (Fig 3.8A and B, 34±6%, 52±9% and 53±11%, respectively). The fact that loss of a single repeat reduced localization suggested to us that synaptic RNA targeting depended on the secondary structure rather than the primary sequence of the sLE.

To specifically test the role of secondary structure in mediating synaptic RNA localization, we generated and analyzed two additional reporters in which we introduced 1) eight mutations to "collapse" the two internal loops into a long stem (Fig 4.8C and D, "Zipper"); and 2) nine mutations to maintain the predicted secondary structure while disrupting the primary sequence of the tandem repeats (Fig 3.8C and D, "RTR" for Remove Tandem Repeats"). The synaptic localization of the Zipper mutant was

completely abolished (Fig 3.8E, 34±7% of VAMP-mCherry sites containing reporter RNA). In contrast, the synaptic localization of the RTR mutant was intact (Fig 3.8E, 84±8% of VAMP-mCherry sites containing reporter RNA). Moreover, insertion of the RTR 66 nt sequence into the dendra2 reporter, downstream of the RSV promoter and upstream of the translation initiation site (iR4-RTR) was sufficient to mediate synaptic localization of reporter RNA, while insertion of the Zipper 66 nt sequence (iR4-Zipper) was not (iR4-RTR: 70±4%, iR4-Zipper: 20±3%, Fig 3.8F and G). Together, these data are consistent with a critical role for the secondary structure of the sLE in mediating synaptic RNA localization.

Since the half-life of a RNA could affect the ability of that transcript to concentrate at synapses, we measured the stability of a subset of constructs by expressing them in isolated sensory neurons, severing the soma and then fixing the remaining neurites at 0 or 48hrs after soma removal. FISH was performed and mean pixel intensity measured. Our data show that all reporter RNAs were stable over a 48hr period (Fig 3.9).

To further analyze the secondary structure of the sLE, we employed selective 2'-hydroxyl acylation analyzed by primer extension (SHAPE, (26, 27). SHAPE takes advantage of the difference in reactivity between base-paired and unpaired nucleotides to the electrophile N-methylisatoic anhydride (NMIA). Modification of unpaired RNA at the 2' hydroxyl group with NMIA blocks primer extension by reverse transcriptase, which can be detected by sequencing gels with single nucleotide resolution.

We used SHAPE to test the structure of two sequences that localize to the synapse, R4 and RTR, and one sequence that does not, Zipper (Fig. 3.10). Consistent with algorithm-based prediction, Zipper collapses the two loops into a long stem while maintaining the tandem repeat elements. In contrast, the reactivity of RTR is remarkably similar to the wildtype sequence R4. Incorporation of the SHAPE data (ΔG_s) into a secondary structure prediction program(28) decreased the minimal free energy (ΔG) of R4 from -7.2 to -23.1, of RTR from -7.7 to -21.3, and of Zipper from -20.5 to -74.1kcal/mol (Fig 3.10). Chemical analysis by SHAPE thus supports the predicted in silicosecondary structure of the identified synaptic LE.

DISCUSSION

Our studies identify the first, to our knowledge, cis-acting LE that mediates localization of mRNA to neuronal synapses. Our data support a multi-step mRNA localization mechanism within neurons, in which specific cis-acting LEs mediate localization from the soma to the neuronal process, while other cis-acting LEs mediate further targeting to synapses(29). This type of multi-step mechanism for localization to distinct subcellular compartments has previously been reported for myelin basic protein mRNA localization in oligodendrocytes(29)and protein kinase Mzeta in neurons (30).While our data demonstrate that the 5'UTR is necessary for synaptic localization, they do not, however, rule out the possibility that synaptic localization involves combined actions of the 5' and 3' UTRs.

Bioinformatic analyses of the 5' UTR of sensorin does not reveal homology at the primary sequence level with any known localization elements. Although it is possible that the identified 66 nt sequence is unique, we believe that it is more likely that the conservation is at the level of secondary structure or three dimensional structure since mutations that maintain secondary structure localize reporter RNA to synapses despite disrupting the primary sequence (Fig 3.8A-C). As RNA secondary structure alignment programs are developed and optimized(31, 32), it will be interesting to use the R4 stem-loop structure to search for similar structures in other mRNAs, and to then determine whether these mRNAs are synaptically localized.

The large size of cultured Aplysia sensory-motor neurons facilitates the study of mRNA subcellular localization in neurons. The ability to compare mRNA localization in neurons that do and do not form chemical synapses provides a means of detecting dynamic changes in mRNA localization that occur upon synapse formation. Together, this level of spatial resolution and control over stimulation (synapse formation) permits determination of where and when mRNAs localize in neurons. As such, our studies extend studies in mammalian neurons that have described cis-acting LEs for mRNA localization and/or dynamic changes in mRNA localization, where analysis has been restricted to the level of localization to proximal and distal dendrites, rather than to specific compartments within the dendrite (e.g., (16, 33).

Our data show that mRNAs are remarkably stable within isolated neuronal processes. As shown in Fig S4we do not detect any decrease in FISH signal for endogenous sensorin or for any of the reporter RNAs in neurites that have been severed from their cell bodies after 48 hrs. Although it has been proposed that localized mRNAs are transported in structures in which they are protected from degradation(10), to ourknowledge these are the first studies to specifically monitor RNA stability in isolated neuronal processes,

Our discovery of a cis-acting RNA sLE is a first step towards dissecting the mechanisms whereby RNAs localize to distinct subcellular compartments within neurons. It opens the door to identifying the specific RNA binding proteins, cytoskeletal elements, molecular motors and transport structures that function to regulate gene expression with exquisite spatial and temporal control within neural synapses and circuits.

EXPERIMENTAL PROCEDURES

Reporter Constructs:

pNEX-dendra2, sensorin 3'UTR pNEX-dendra2, sensorin 5'UTR pNEX dendra2, sensorin 5'3'UTR-dendra2 and mCherry-VAMP constructs were generated as described in(21).

Aplysia neuronal cultures, microinjection, electrophysiology, stimulations:

Aplysia SN-MN cultures were prepared as described in(34). Reporter plasmids were microinjected into SNs 24-36 hours after plating. Synaptic connectivity was assayed by measuring EPSP amplitude between SN and target MN, as described in(21).

Live cell imaging:

Confocal images were acquired on a Zeiss Pascal scanning laser microscope (Zeiss, Germany). Green dendra2 protein was excited with a 488nm Argon laser (at 2.5mW). To detect VAMP-mCherry positive SN varicosities in contact with Alexa-fluor 647 labeled MNs, pNEX vectors encoding VAMP-mCherry were microinjected into SNs 24-36 hrs after plating and the MN was microinjected with Dextran, Alexa Fluor 647 (Invitrogen, Eugene, OR) 60 minutes prior to imaging on DIV 4. Neuronal morphology was traced from DIC images using Neurolucida trace software (MBF Bioscience, Vermont).

Fluorescence in situ hybridization (FISH):

Cells were fixed with 4%PFA/30% sucrose in PBS and processed for FISH as previously described(21). Sense riboprobe did not produce any background signal;

antisense riboprobe did not produce signal in MNs (which do not express sensorin, (21)). Since dendra2 protein fluorescence does not persist following processing of samples for FISH, we manually aligned RNA images to live cell images based on the morphology of SN and MN. We limited our data analysis to neurons in which reporter mRNA was abundant (e.g. mean fluorescent RNA in situ intensity above 40 in an 8 bit image) in adjacent shafts.

Statistical analysis

GraphPad Prism software (La Jolla, CA) was used for all statistical analysis as specified in figure legends. Kruskal-Wallis test followed by Dunnett's multiple comparison tests were used when data distribution did not follow Gaussian distribution.SHAPE analysis

SHAPE was used to determine paired and unpaired regions within predicted secondary structures(26, 27). Details are provided in Supplemental information.

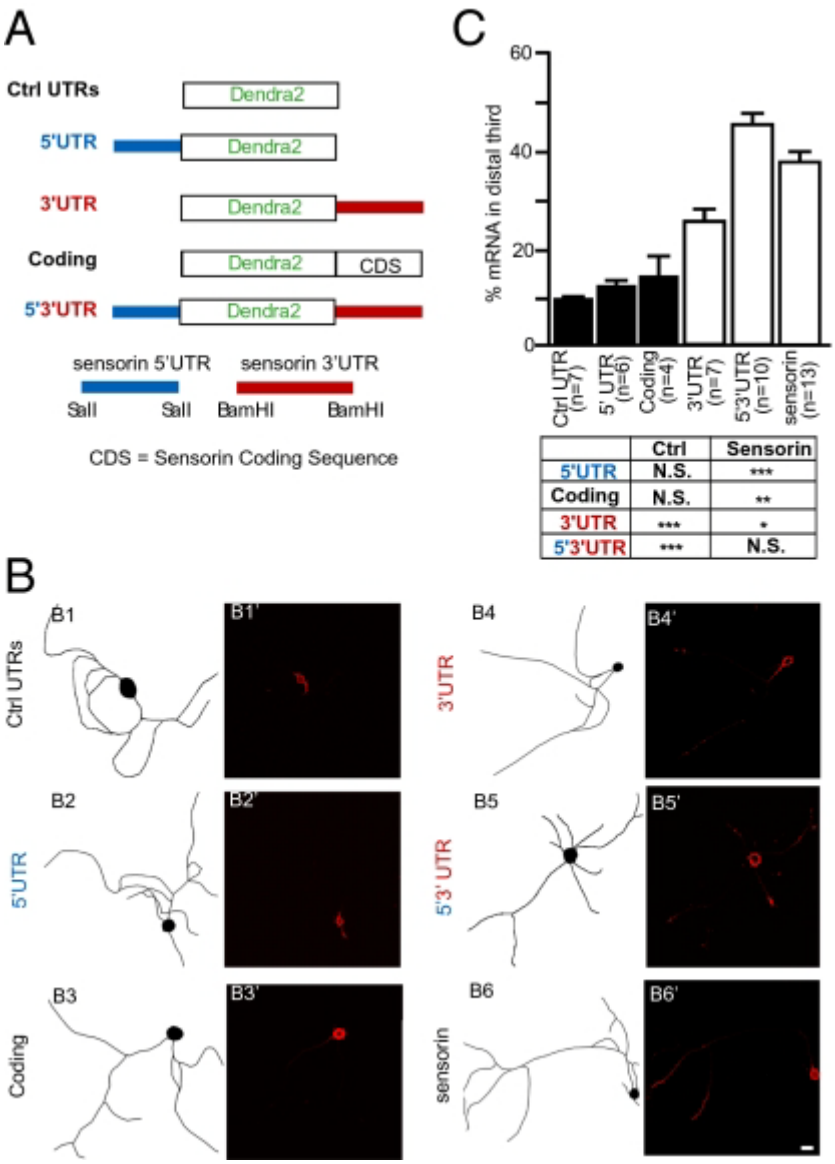
A
Ctrl UTRs
Dendra2
5'UTR
Dendra2
3'UTR
Dendra2
Coding
Dendra2
CDS
5'3'UTR
Dendra2
sensorin 5'UTR
sensorin 3'UTR
SalI
SalI
BamHI
BamHI
CDS = Sensorin Coding Sequence
C
% mRNA in distal third
60
40
20
0
Ctrl UTR (n=7)
5' UTR (n=6)
Coding (n=4)
3'UTR (n=7)
5'3'UTR (n=10)
sensorin (n=13)
Ctrl
Sensorin
5'UTR
N.S.
***
Coding
N.S.
**
3'UTR
***
*
5'3'UTR
***
N.S.
B
B1
B1'
B2
B2'
B3
B3'
B4
B4'
B5
B5'
B6
B6'
Ctrl UTRs
5'UTR
Coding
3'UTR
5'3' UTR
sensorin

Fig. 3.1. The 3'UTR of sensorin is sufficient to target reporter mRNA into distal neurites.

pNEX vectors encoding translational reporters were microinjected into isolated Aplysia sensory neurons (SNs) in culture (DIV2). Neurons were fixed (DIV4) and processed for fluorescence in situ hybridization (FISH) with dendra antisense riboprobes. A, Cartoons of reporter constructs in pNEX3 expression vector. B, Representative images of reporter (dendra2) mRNA FISH in isolated SNs. B1-6, neurolucida tracing of each SN; B1'-6', FISH (detected with dendra antisense riboprobes for B1'-5', and with sensorin antisense riboprobes for B6'). The FISH signal only extends to distal neurites when the 3'UTR of sensorin is present; distal localization is enhanced by 5'UTR. Scale bar, 100μm; C, Quantification of the distribution of reporter mRNA within sensory neurites.Neurites were linearized and divided into proximal, middle and distal segments. The percent of total FISH signal in distal segments is shown (see also Figure S1. ***$p<0.0001$, Kruskal-Wallis one-way analysis of variance followed by Dunnett's multiple comparison test.

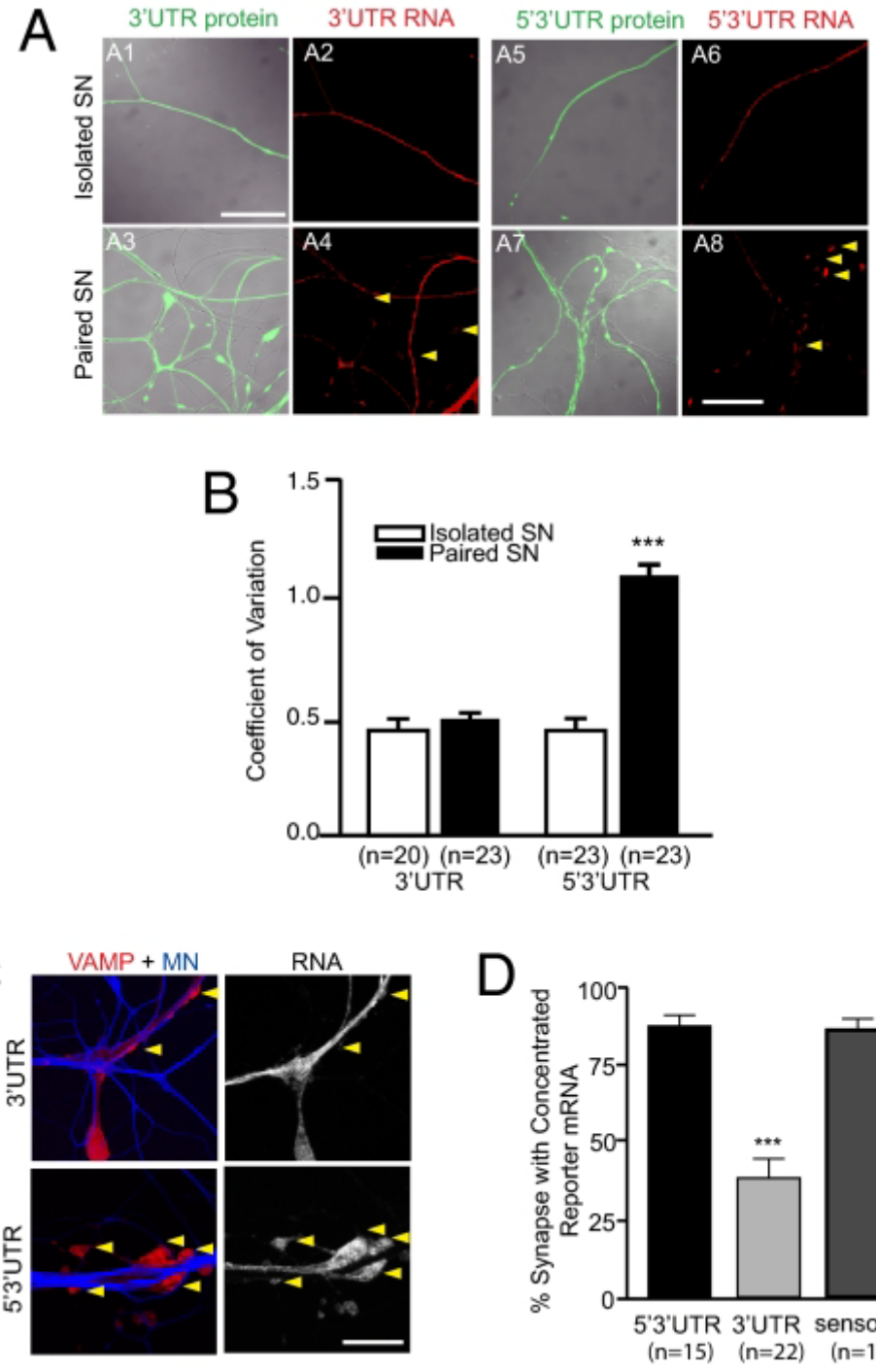
A
3'UTR protein
3'UTR RNA
5'3'UTR protein
5'3'UTR RNA
A1
A2
A5
A6
Isolated SN
A3
A4
A7
A8
Paired SN
B
1.5
1.0
0.5
0.0
Isolated SN
Paired SN
***
Coefficient of Variation
(n=20) (n=23) (n=23) (n=23)
3'UTR
5'3'UTR
C
VAMP + MN
RNA
3'UTR
5'3'UTR
D
100
75
50
25
0
***
% Synapse with Concentrated Reporter mRNA
5'3'UTR 3'UTR sensorin
(n=15) (n=22) (n=14)

Fig. 3.2. 5'UTR of sensorin is required for localizing reporter mRNA to synapses. Expression vectors encoding dendra2 reporters with either the 3'UTR or both the 5' and 3' UTRs (5'3'UTR) of sensorin were microinjected into Aplysia sensory neurons (SN, DIV2) cultured in isolation (isolated SN) or with motor neurons (MNs). Neurons were fixed (DIV4) and processed for fluorescence in situ hybridization (FISH) using dendra2 antisense riboprobes. A, Representative photomicrographs of dendra reporter protein (green, A1, 3, 5, 7) and mRNA (red, A2, 4, 6, 8) distribution in isolated and paired SNs. Scale bar, 50μm. B, Quantification of the change in distribution of reporter mRNA by measuring the coefficient of variation (CV, standard deviation/mean) of the FISH signal. ***$p<0.0001$, unpaired Student's t-test.C,The 5'3'UTR reporter or the 3'UTR reporter was co-expressed with the presynaptic marker VAMP-mCherry in Aplysia SNs paired with target MNs on DIV2. On DIV4, the MN was injected with the volume filling dye Alexa-fluor 647 (blue), and images of VAMP-mCherry and blue Alexa-fluorwere acquired, followed by fixation and FISH with dendra antisense riboprobes.Left panels, merged VAMP/MN images of a co-culture with SN over-expressing 5'3'UTR or 3'UTRreporter and VAMP-mCherry (VAMP-mCherry in red, MN in blue); right panels, FISH signal for reporter mRNA. Scale bar,100μm.D, Quantification of the percent of synapses (VAMP-mCherry clusters adjacent to MN) containing reporter mRNA (error bars = SEM). ***$p< 0.0001$, One-way ANOVA followed by Dunnett's multiple comparison test.(See also (21), Figure 3.5).

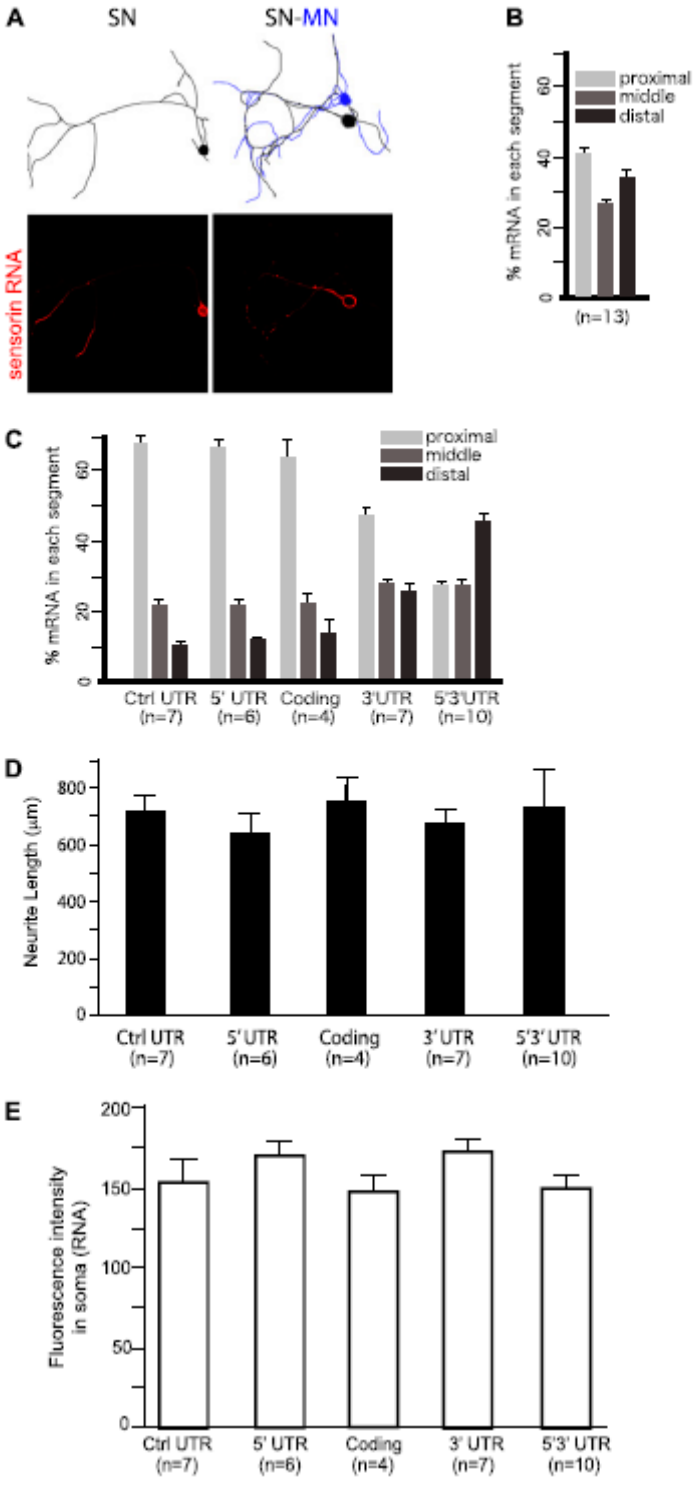
A
SN
SN-MN
sensorin RNA
B
% mRNA in each segment
proximal
middle
distal
(n=13)
C
% mRNA in each segment
proximal
middle
distal
Ctrl UTR (n=7)
5' UTR (n=6)
Coding (n=4)
3'UTR (n=7)
5'3'UTR (n=10)
D
Neurite Length (μm)
Ctrl UTR (n=7)
5'UTR (n=6)
Coding (n=4)
3'UTR (n=7)
5'3'UTR (n=10)
E
Fluorescence intensity in soma (RNA)
Ctrl UTR (n=7)
5' UTR (n=6)
Coding (n=4)
3' UTR (n=7)
5'3' UTR (n=10)

Fig. 3.3, related to figures 3.1 and 3.2. A, Localization of endogenous sensorin mRNA in isolated sensory neurons (SNs) and SNs co-cultured with target motor neuron (MN). Top panel, neuronal morphology traced from DIC images of cultured SNs and MNs (DIV 4). Black, SN, Blue, MN; bottom panel, fluorescent in situ hybridization (FISH) of endogenous sensorin mRNA. Note that sensorin mRNA is diffusely localized in distal neurites of isolated SNs but concentrated at varicosities in SNs co-cultured with target (LFS) MNs. Relevant to figs. 3.1 and 3.2. B, Quantification of sensorin mRNA localization in isolated SNs quantified as percent of mRNA FISH intensity in proximal, middle, and distal neurites. C,Quantification of reporter mRNAs FISH intensity in the proximal, middle and distal neurites in isolated sensory neurons (DIV 4, this data completes the data presented in Fig 1; see Fig 3.2D for quantification of synaptic localization of sensorin mRNA). D, The average length of sensory neurites is similar across groups analyzed. This indicates that expression of the various reporters does not alter neuritic growth.E, The mean intensity of FISH signal in the soma is similar across groups analyzed. This indicates that the various reporters are expressed at relatively similar levels.

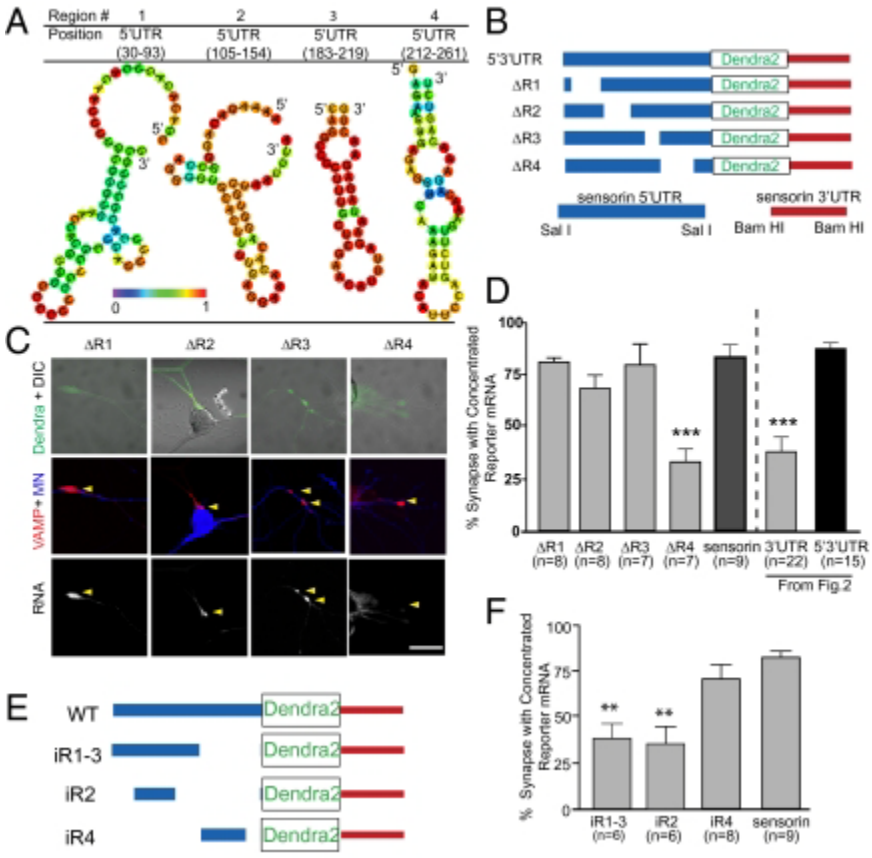

Fig. 3.4. A region directly upstream of the sensorin translation start site, in the 5'UTR,is necessary and sufficient for synaptic localization of the reporter mRNA. A, Representative graphic depictions of potential stem loop structures in 5'UTR of sensorin predicted by RNAfold(35), color scale denotes base pair probabilities; B, Cartoon representation of deletions made to the reporter construct. C, Representative images of deletion constructs ΔR1-R4 expressed in SNs synaptically connected with MNs. Top panel, photomicrograph of Dendra protein (SN, green) merged with DIC image; middle panel, synapses marked as VAMP-mCherry clusters (red) contacting the MN (blue, Alexa 647); bottom panel, FISH images showing clustering of reporter mRNA. D, Quantification of synaptic localization of reporter mRNAs as the percent of synapses (VAMP-mCherry clusters adjacent to MN) containing reporter mRNA.E, Cartoon of insertion constructs (iR1-4) in which the designated regions of the sensorin 5'UTR were inserted into a control pNEX 5'UTR to test their ability to localize the reporter mRNA to synapses. The mutants were co-expressed in SNs paired with target MNs at DIV2 and neurons were fixed on DIV4 and processed for FISH. F, Percent of synapses (VAMP-mCherry clusters adjacent to MN) containing reporter mRNA.

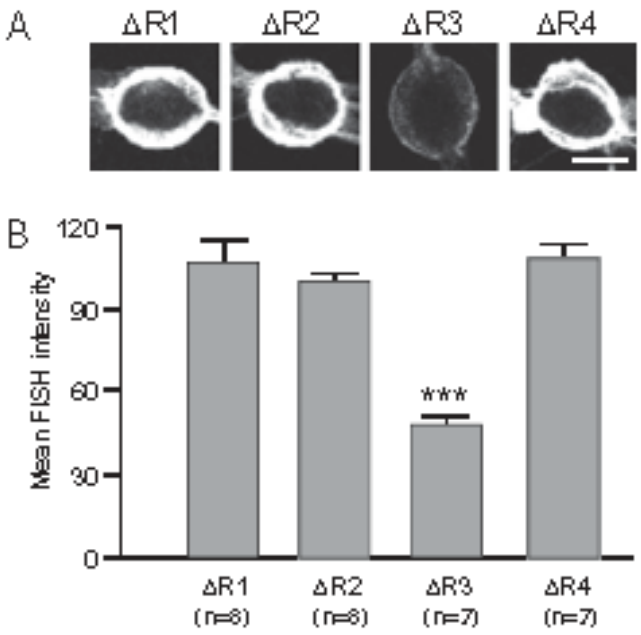

Fig. 3.5, Expression level of deletion mutants, related to fig 3.4. A, Confocal images of somatic FISH signals for ΔR1-4 in SN-MN cultures; B, quantification of fluorescence intensity of dendra2 FISH intensity. Only ΔR3 shows decreased RNA concentration, yet this construct retained synaptic localization.

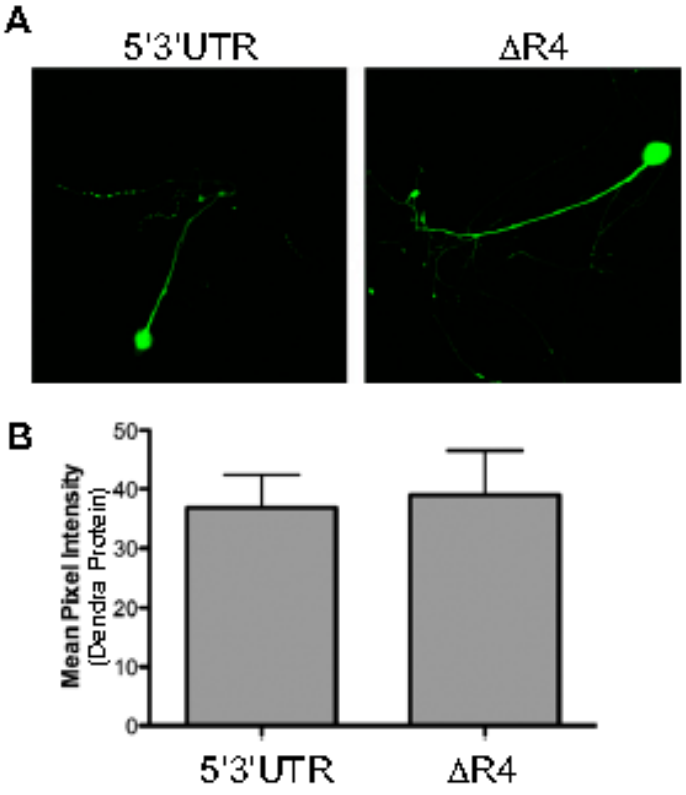

Fig. 3.6. Deletion of the synaptic localization element does not alter dendra2 protein concentration, related to Fig. 3.4. (A) Representative confocal images of dendra2 protein (green) in sensory neurons (paired with motor neurons) expressing the 5′3′ UTR reporter or the ΔR4 reporter. (B) Quantification of mean pixel fluorescence intensity of dendra2 protein; Student t test, ns.

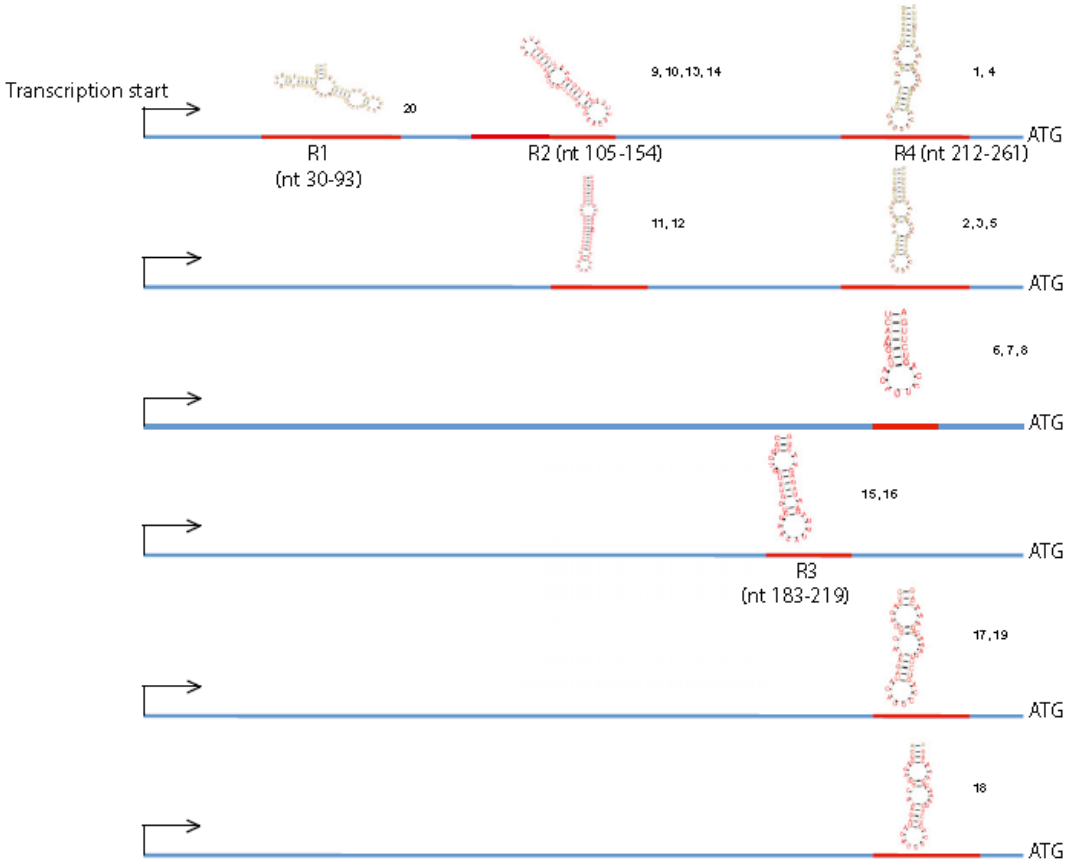

Fig. 3.7. Secondary structures predicted using RNApromo (1) and their corresponding regions within the sensorin 5′ UTR. RNApromo was used in the initial screen for secondary structure(s) within the 5′ UTR. Relevant to Figs 3.3 and 3.4. A total f 20 candidate secondary structures were predicted using RNApromo software, numbered 1 through 20. The structures that were located in the same region (red line) and that shared similar secondary structures were clustered together, and a representative structure is displayed (e.g., structures with probability color code variation). After further secondary structure analysis with RNAfold (2), R1–4 were chosen for the initial deletion screening analysis; the numbers in parentheses denote the specific positions of R1–4 within the 5′ UTR of sensorin.

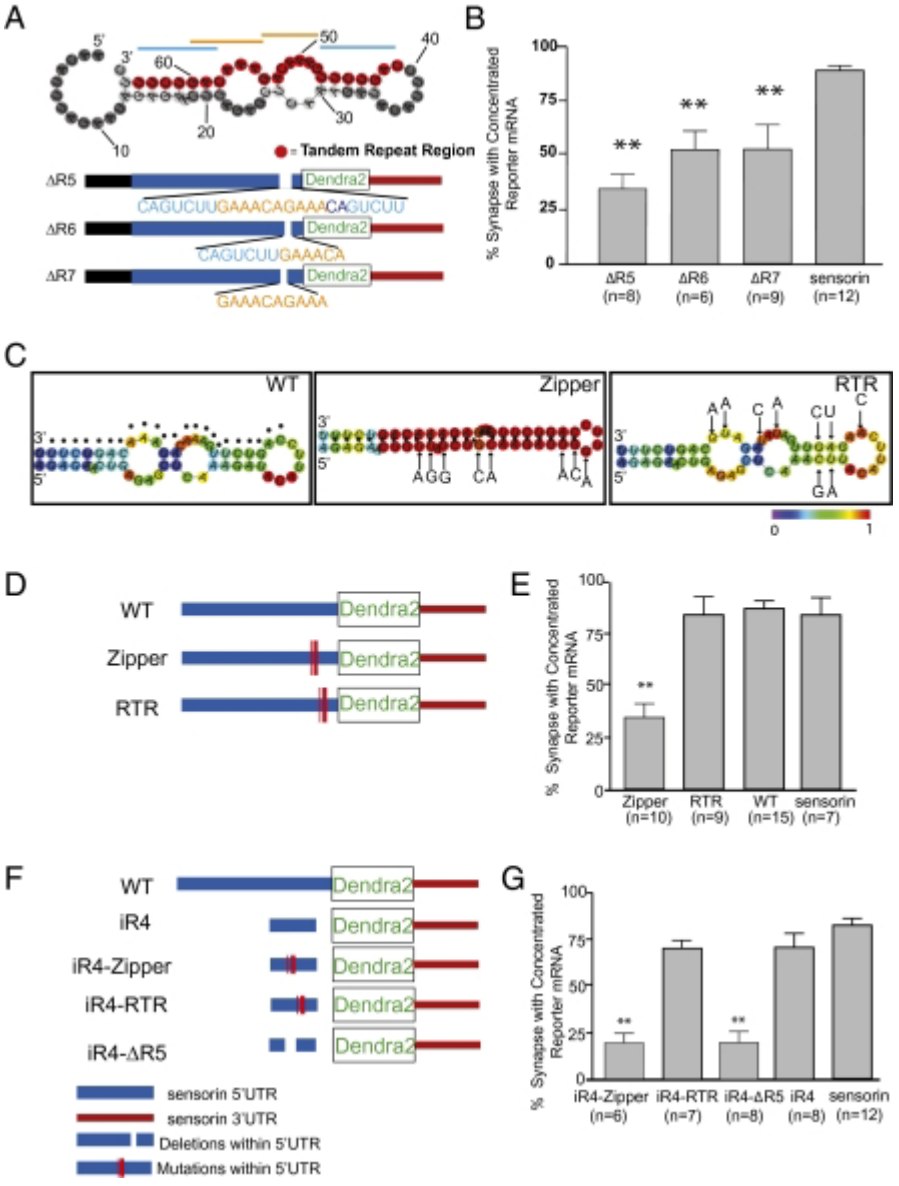
A
5'
3'
60
50
40
30
20
10
= Tandem Repeat Region
ΔR5
Dendra2
CAGUCUUGAAACAGAAACAGUCUU
ΔR6
Dendra2
CAGUCUUGAAACA
ΔR7
Dendra2
GAAACAGAAA
B
% Synapse with Concentrated Reporter mRNA
100
75
50
25
0
**
**
**
ΔR5 (n=8)
ΔR6 (n=6)
ΔR7 (n=9)
sensorin (n=12)
C
WT
Zipper
RTR
3'
5'
AGG
CA
AC
A
AA
C
A
CU
C
GA
0
1
D
WT
Zipper
RTR
Dendra2
E
% Synapse with Concentrated Reporter mRNA
100
75
50
25
0
**
Zipper (n=10)
RTR (n=9)
WT (n=15)
sensorin (n=7)
F
WT
iR4
iR4-Zipper
iR4-RTR
iR4-ΔR5
Dendra2
sensorin 5'UTR
sensorin 3'UTR
Deletions within 5'UTR
Mutations within 5'UTR
G
% Synapse with Concentrated Reporter mRNA
100
75
50
25
0
**
**
iR4-Zipper (n=6)
iR4-RTR (n=7)
iR4-ΔR5 (n=8)
iR4 (n=8)
sensorin (n=12)

Fig. 3.8. A 66 ntstem-loop structure localizes reporter mRNA to synapses. A, Predicted secondary structure of the region corresponding to R4 (RNAfold, (35); highlighted in red is the 24-nt primary sequence containing a double-tandem 7mer-repeat (indicated with blue/orange lines). Mutants were generated in which the entire 24-nt (ΔR5), the first 13-nt set of repeat elements (ΔR6) or 10 -nt of the center repeat (ΔR7) were deleted from the 5'3'UTR reporter construct. B, Mutants were co-expressed with VAMP-mCherry in SNs paired with target MNs and the percent of synapses containing reporter RNA was measured. ** $p<0.01$, one-way ANOVA followed by Dunnett's multiple comparison test compared to 3'UTR reporter or endogenous sensorin. See also Table S1 and Figures S2 and S3. *C*, Predicted secondary structures (RNAfold,(35)) of WT (dots denote tandem repeat region described in Fig 3.4); zipper construct, 8 point mutations were introduced to collapse the predicted secondary structure without disrupting the tandem repeat sequence; RTR construct, 9 mutations were introduced to disrupt the primary sequence of the tandem repeat region, while retaining predicted secondary structure. D, Cartoon showing the location within the sensorin 5'UTR of the mutations in the zipper and RTR constructs. The mutants were co-expressed in SNs paired with target MNs at DIV2 and neurons were fixed on DIV4 and processed for FISH. E, Percent of synapses (VAMP-mCherry clusters adjacent to MN) containing reporter mRNA.F, Cartoon of mutant insertion reporter constructs, including WT iR4 (66 nt), iR4-RTR (iR4 with mutations shown in RTR in C), iR4-Zipper (iR4 with mutations shown in zipper in C), or iR4-ΔR5 (iR4 lacking the 24 nt repeat element). The mutants were co-expressed in SNs paired with target MNs at DIV2 and neurons were fixed on DIV4 and processed for FISH. G, Percent of synapses (VAMP-mCherry clusters adjacent to MN) containing reporter mRNA. **$p<0.001$, One way ANOVA followed by Dunnett's multiple comparison test.

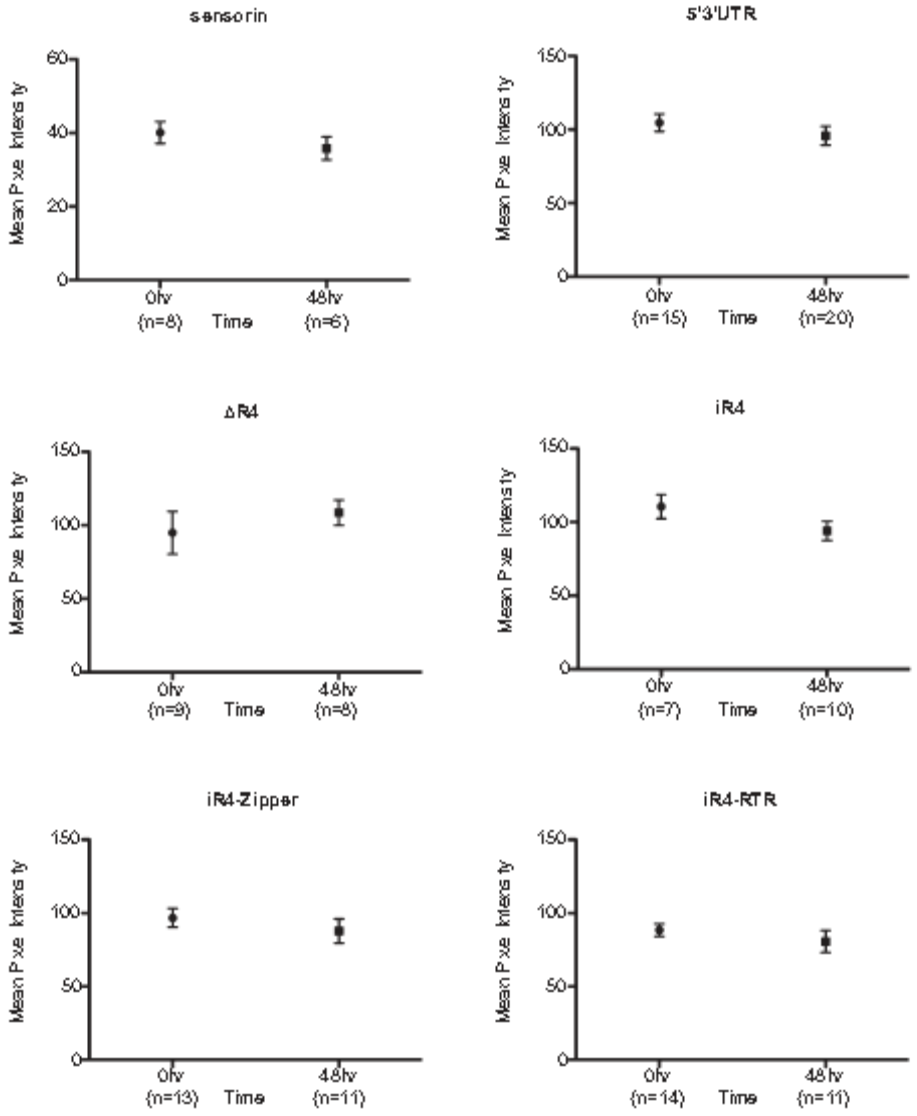

Fig. 3.9. Endogenous sensorin and reporter RNAs are stable in isolated neurites. The stability of endogenous sensorin and select reporter RNAs was measured by injecting isolated sensory neurons (DIV 1) with pNEX vectors encoding sensorin reporters. Cell bodies were mechanically removed 48 h later, and neuritis were fixed at either 0 or 48 h after soma removal and processed for FISH. Images were analyzed to determine the mean pixel intensity for each cell. The concentration of endogenous sensorin and of all reporter RNAs did not decrease significantly between 0 and 48 h. Student t test. n, number of cells analyzed.

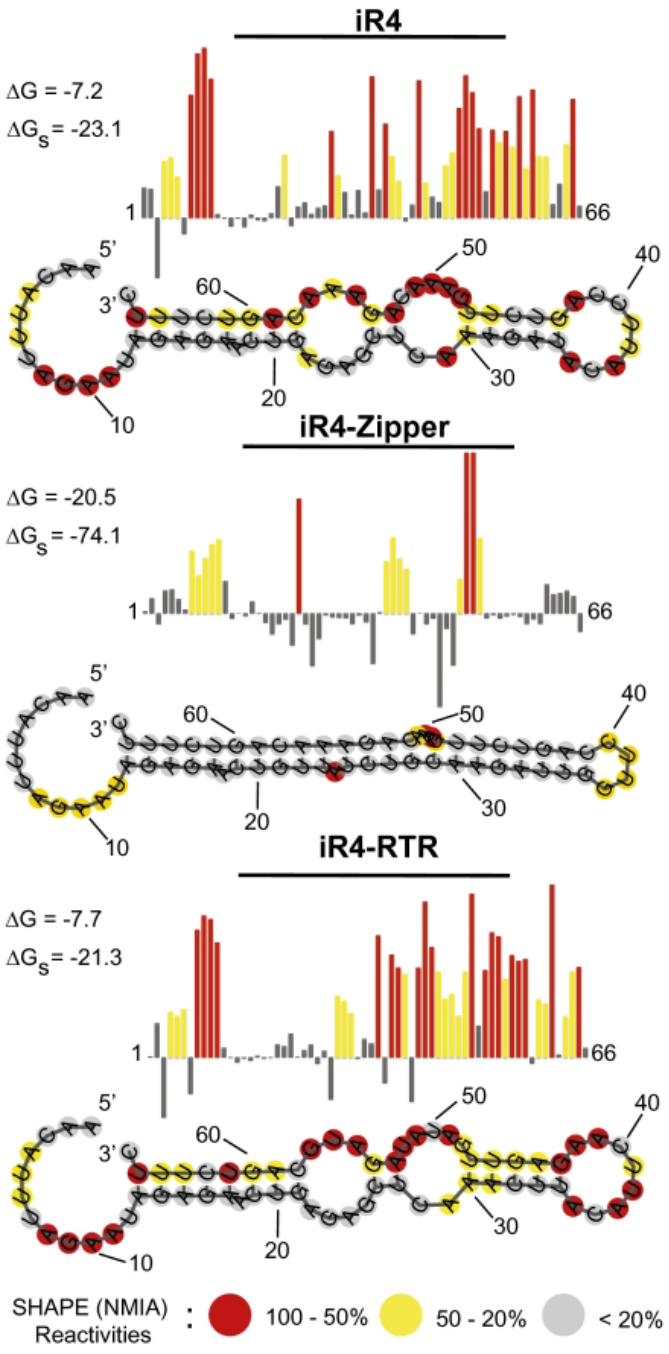
iR4
ΔG = -7.2
ΔGs = -23.1
1
66
5'
3'
10
20
30
40
50
60
iR4-Zipper
ΔG = -20.5
ΔGs = -74.1
iR4-RTR
ΔG = -7.7
ΔGs = -21.3
SHAPE (NMIA) Reactivities
100 - 50%
50 - 20%
< 20%

Fig. 3.10. SHAPE analysis of the 66-nt element and mutants. Above, SHAPEreactivities, determined from the sequencing gels in Fig S5. Residues with intensities between 0% and 20%, 20% and 50% and 50% and 100% are labeled gray, yellow and red, respectively. Bars show the amounts of modification at each position relative to the most highly modified nucleotide. Numbers denote nucleotide position. Below, SHAPE modification intensities mapped onto the predicted secondary structures; structures were generated using RNAfold(35). Residues with intensities between 0% and 20%, 20% and 50% and 50% and 100% are shown in gray, yellow and red, respectively. Both ΔG and ΔG_s (predicted with SHAPE Data) were generated using RNAstructure(28). Numbers denote nucleotide position.

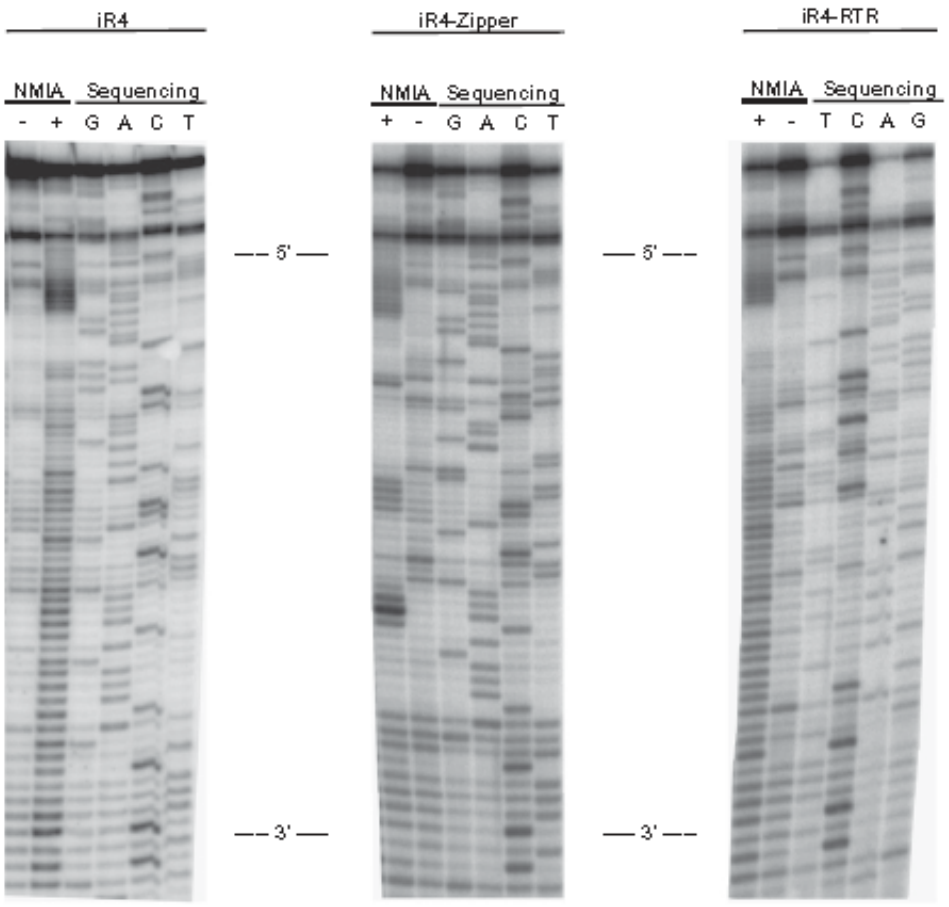

Fig. 3.11. SHAPE polyacrylamide gels. Sequencing polyacrylamide gels for SHAPE (1) analysis of the RNA (from 5′ to 3′, as denoted). The lanes marked sequencing are lanes in which ddNTPs were added to the reverse transcription to cause chain termination and are exactly 1 nt longer than the corresponding NMIA lanes. NMIA lanes (+) and (-) correspond to incubation with 130 mM NMIA for 45 min at 37°C and a control with NMIA omitted. Unbased paired segments are visible as regions of increased NMIA modification in the (+) lane compared with the (-) lane.

REFERENCES

1. Martin KC, EphrussiA (2009) mRNA Localization: Gene Expression in the Spatial Dimension. *Cell* 136:719–730.

2. Holt CE, Bullock SL (2009) Subcellular mRNA Localization in Animal Cells and Why It Matters. *Science* 326:1212–1216.

3. Eberwine J, Belt B, Kacharmina JE, Miyashiro K (2002) Analysis of subcellularly localized mRNAs using in situ hybridization, mRNA amplification, and expression profiling. *Neurochem Res* 27:1065–1077.

4. Moccia R et al. (2003) An unbiased cDNA library prepared from isolated Aplysia sensory neuron processes is enriched for cytoskeletal and translational mRNAs. *J Neurosci* 23:9409–9417.

5. Poon MM, Choi S-H, Jamieson CAM, Geschwind DH, Martin KC (2006) Identification of process-localized mRNAs from cultured rodent hippocampal neurons. *Journal of Neuroscience* 26:13390–13399.

6. Suzuki T, Tian QB, Kuromitsu J, Kawai T, Endo S (2007) Characterization of mRNA species that are associated with postsynaptic density fraction by gene chip microarray analysis. *Neurosci Res* 57:61–85.

7. Zivraj KH et al. (2010) Subcellular profiling reveals distinct and developmentally regulated repertoire of growth cone mRNAs. *Journal of Neuroscience* 30:15464–

15478.

8. Zhong J, Zhang T, Bloch L (2006) Dendritic mRNAs encode diversified functionalities in hippocampal pyramidal neurons. *BMC Neurosci* 7:17.

9. Subramanian M et al. (2011) G-quadruplex RNA structure as a signal for neurite mRNA targeting. *EMBO Rep* 12:697–704.

10. Kiebler MA, Bassell GJ (2006) Neuronal RNA granules: movers and makers. *Neuron* 51:685–690.

11. Hirokawa N (2006) mRNA transport in dendrites: RNA granules, motors, and tracks. *Journal of Neuroscience* 26:7139–7142.

12. Krichevsky AM, Kosik KS (2001) Neuronal RNA granules: a link between RNA localization and stimulation-dependent translation. *Neuron* 32:683–696.

13. Steward O, Wallace CS (1995) mRNA distribution within dendrites: relationship to afferent innervation. *J Neurobiol* 26:447–449.

14. Tiruchinapalli DM et al. (2003) Activity-dependent trafficking and dynamic localization of zipcode binding protein 1 and beta-actin mRNA in dendrites and spines of hippocampal neurons. *Journal of Neuroscience* 23:3251–3261.

15. Tongiorgi E, Righi M, CattaneoA (1997) Activity-dependent dendritic targeting of BDNF and TrkB mRNAs in hippocampal neurons. *J Neurosci* 17:9492–9505.

16. Steward O, Worley PF (2001) Selective targeting of newly synthesized Arc mRNA to active synapses requires NMDA receptor activation. *Neuron* 30:227–240.

17. Havik B, Rokke H, Bardsen K, Davanger S, Bramham CR (2003) Bursts of high-frequency stimulation trigger rapid delivery of pre-existing alpha-CaMKII mRNA to synapses: a mechanism in dendritic protein synthesis during long-term potentiation in adult awake rats. *Eur J Neurosci* 17:2679–2689.

18. Doyle M, Kiebler MA (2011) Mechanisms of dendritic mRNA transport and its role in synaptic tagging. *EMBO J* 30:3540–3552.

19. Lyles V, Zhao Y, Martin KC (2006) Synapse formation and mRNA localization in cultured Aplysia neurons. *Neuron* 49:349–356.

20. Hu JY, Glickman L, Wu F, Schacher S (2004) Serotonin regulates the secretion and autocrine action of a neuropeptide to activate MAPK required for long-term facilitation in Aplysia. *Neuron* 43:373–385.

21. Wang DO et al. (2009) Synapse- and stimulus-specific local translation during long-term neuronal plasticity. *Science* 324:1536–1540.

22. Glanzman DL, Kandel ER, Schacher S (1989) Identified target motor neuron regulates neurite outgrowth and synapse formation of aplysia sensory neurons in vitro. *Neuron* 3:441–450.

23. Rabani M, Kertesz M, Segal E (2008) Computational prediction of RNA structural

motifs involved in posttranscriptional regulatory processes. *ProcNatlAcadSci USA* 105:14885–14890.

24. Hamilton RS, Davis I (2011) Identifying and searching for conserved RNA localisation signals. *Methods MolBiol* 714:447–466.

25. Zuker M (2003) Mfold web server for nucleic acid folding and hybridization prediction. *Nucleic Acids Res* 31:3406–3415.

26. Merino EJ, Wilkinson KA, Coughlan JL, Weeks KM (2005) RNA structure analysis at single nucleotide resolution by selective 2'-hydroxyl acylation and primer extension (SHAPE). *J Am ChemSoc* 127:4223–4231.

27. Wilkinson KA, Merino EJ, Weeks KM (2006) Selective 2'-hydroxyl acylation analyzed by primer extension (SHAPE): quantitative RNA structure analysis at single nucleotide resolution. *Nat Protoc* 1:1610–1616.

28. Deigan KE, Li TW, Mathews DH, Weeks KM (2009) Accurate SHAPE-directed RNA structure determination. *ProcNatlAcadSci USA* 106:97–102.

29. Ainger K et al. (1997) Transport and localization elements in myelin basic protein mRNA. *J Cell Biol* 138:1077–1087.

30. Muslimov IA et al. (2004) Dendritic transport and localization of protein kinase Mzeta mRNA: implications for molecular memory consolidation. *The Journal of biological chemistry* 279:52613–52622.

31. Hamada M, Sato K, Asai K (2011) Improving the accuracy of predicting secondary structure for aligned RNA sequences. *Nucleic Acids Res* 39:393–402.

32. Taly J-F et al. (2011) Using the T-Coffee package to build multiple sequence alignments of protein, RNA, DNA sequences and 3D structures. *Nat Protoc* 6:1669–1682.

33. Muslimov IA, Iacoangeli A, Brosius J, Tiedge H (2006) Spatial codes in dendritic BC1 RNA. *J Cell Biol* 175:427–439.

34. Zhao Y, Wang DO, Martin KC (2009) Preparation of Aplysia sensory-motor neuronal cell cultures. *J Vis Exp*.

35. Gruber AR, Lorenz R, Bernhart SH, Neubock R, Hofacker IL (2008) The Vienna RNA websuite. *Nucleic Acids Res* 36:W70–4.

CHAPTER FOUR

NETRIN/DCC DEPENDENT LOCALIZED TRANSLATION MEDIATES SPATIAL REGULATION OF GENE EXPRESSION DURING SYNAPSE FORMATION

INTRODUCTION

mRNA localization and regulated translation provide a mechanism for spatially restricting gene expression in asymmetric cells. In neurons, this process allows subcellular compartments such as growth cones and synapses to undergo localized changes in protein composition in response to stimuli, and has been shown to be critical to axon guidance, synapse formation, synaptic plasticity and regeneration following axonal injury (Sutton and Schuman, 2006; Willis and Twiss, 2006; Jung et al., 2012). Studies of local translation have revealed that a large number of transcripts localize to subcellular compartments, subserving a wide and diverse range of cellular functions (Moccia et al., 2003; Poon et al., 2006; Eberwine et al., 2002; Cajigas et al., 2012).

In this study, we asked whether the spatial restriction of gene expression is mediated primarily at the level of mRNA targeting or translational regulation. Studies showing highly specific patterns of subcellular mRNA localization in asymmetric cells have suggested that mRNA targeting mediates protein localization (Lecuyer et al., 2007). Similarly, studies of activity-dependent localization of *Arc* mRNA in hippocampal dentate granule cell dendrites following perforant pathway stimulation have suggested that mRNA targeting locally regulates gene expression during synapse-specific forms of neuronal plasticity (Steward et al., 1998). On the other hand, studies of synaptic tagging during neuronal plasticity have suggested that the products of gene expression are targeted throughout the neuron, and can be captured at any synapse with subsequent subthreshold stimulation (Martin et al., 1997; Casadio et al., 1999; Fonseca et al., 2004).

These findings are more consistent with cell-wide distribution of transcripts, with regulated translation controlling local gene expression. These studies suggest two models for spatially regulating gene expression within neurons during synapse formation: one in which mRNAs and other components of the translational machinery are targeted specifically to sites of synaptic contact, and the other in which mRNAs and other components of the translational machinery are distributed throughout the neuronal arbor but are only translated at synapses.

We set out to directly determine whether spatial regulation of gene expression during synapse formation was mediated primarily by RNA localization or by local translation using the *Aplysia* sensory neuron (SN)-motor neuron (MN) culture system. Specifically, we cultured a single bifurcated SN with a target (L7) MN, with which it formed glutamatergic synapses, and a nontarget (L11) MN, with which it fasciculated but did not form chemical synapses (Glanzman et al., 1989). We then asked whether and how synaptogenic stimuli regulate RNA and protein localization and concentration by analyzing the distribution of ribosomal RNA (rRNA), messenger RNA (mRNA), RNA binding proteins and translation factors. We find that rRNA, mRNA, ribosomal proteins and translation factors are delivered throughout the sensory neuron, to both synaptic and non-synaptic sites, but that translation is significantly enriched at sites of synaptic contact. These results indicate that the spatial regulation of gene expression in neurons is mediated at the level of translation rather than at the level of RNA localization. In investigating the nature of the synaptic signals that stimulate translation during synapse formation, we find that netrin1, a chemotropic factor known to induce synaptogenesis in

C. elegans (Colon-Ramos et al., 2007) and to stimulate translation in growth cones during axon guidance (Campbell and Holt, 2001), is sufficient to promote translation of localized mRNAs at nonsynaptic sites. Our findings are thus consistent with neurons delivering transcripts and translational machinery throughout the neuron, but with a synaptically restricted netrin1-dependent signal triggering localized translation at synapses.

RESULTS

Ribosomal RNA targets equally well to SN branches contacting target and nontarget MNs

To examine the localization of the most abundant cellular RNA, rRNA, we performed fluorescent in situ hybridization (FISH) for 18S and 28S rRNA. As shown in Fig 4.2A and B, we detected 18S in distal neurites of isolated cultured sensory neurons after 1 to 4 days *in vitro* (DIV). SN-MN cultures are actively growing and forming new synapses between 1-3 DIV, but have largely stabilized by 4DIV. Unlike sensorin mRNA, which we have shown accumulates preferentially in the distal third of isolated sensory neurons (Wang et al., 2009), consistent with an active mRNA transport process, there was no distal accumulation of rRNA. Instead, rRNA concentration decreased with distance (Fig 4.2B), consistent with a passive rather than an active transport mechanism.

We then performed a set of experiments in which we cultured a bifurcated SN with a target L7 MN, with which it formed glutamatergic synapses, and non-target L11 MNs, with which it fasciculated but did not form chemical synapses (Fig 4.1A). We fixed the cultures at 3 DIV, and performed FISH for 18S (Fig 4.1B-D) and 28S rRNA (Fig 4.2C and E). Quantification of rRNA in the proximal sensory neuron branches did not reveal any significant difference in concentration in the branch contacting the L7 target motor neuron and the branch contacting the L11 nontarget motor neuron (Fig 4.1C and D, Fig 4.2D and E*)*. We also examined the distribution of ribosomes by expressing the *Aplysia* ribosomal protein S6 tagged with the fluorescent tag dendra2 in bifurcated SNs

contacting both target L7 and nontarget L11 MNs. As shown in Fig 4.2F-H, S6-dendra2 targeted equally to SN branches contacting target or nontarget MNs. Together, these data indicate that ribosomes are delivered throughout the SN, and are not targeted specifically from the soma to branches receiving synaptogenic signals.

Sensorin mRNA targets equally well to SN branches contacting target and nontarget MNs

As a candidate mRNA, we examined the transcript encoding the sensory-cell specific neuropeptide sensorin, which not only localizes to distal sensory neurites, but also concentrates at synapses (Lyles et al., 2006). We have previously shown that neuritic and synaptic localization are mediated by distinct mechanisms (Wang et al., 2009; Meer et al., 2012), and that sensorin mRNA undergoes localized translation at synapses during serotonin-mediated long-term facilitation (LTF, Wang et al., 2009). FISH for sensorin mRNA revealed that the sensorin transcript localized equally to both distal (Fig 4.1D-F) and proximal (Fig 4.2I-K) branches of bifurcated sensory neurons contacting L7 or L11 MNs. The pattern of sensorin mRNA in distal branches was distinct, with diffuse distribution of sensorin mRNA in branches contacting a nontarget motor neurons and punctate concentrations of sensorin RNA at sensory neuron synapses onto target motor neurons (see Fig 4.2L for quantification of coefficient of variation). However, the same amount of RNA was present in both sensory neuron branches.

RNA binding protein Aplysia Staufen targets equally well to SN branches

contacting target and nontarget MNs

We next studied the localization of the RNA binding protein Staufen in sensory neurons contacting target and nontarget motor neurons by expressing *Aplysia* Staufen tagged with the fluorescent protein dendra2 in bifurcated sensory neurons. We chose to focus on Staufen because of its previously described role in transporting transcripts into dendrites of mammalian cells (Kiebler et al., 1999; Tang et al., 2001). As shown in Fig 4.3, we found that Staufen-dendra2 was transported equally well to branches contacting target and nontarget motor neurons.

Translation is significantly enriched in SN branches contacting target MNs

Together, our experiments using FISH to analyze rRNAs and sensorin mRNA, and overexpression to analyze S6 ribosomal protein and Staufen, argue that ribosomes, mRNAs and RNA binding proteins are transported throughout the neuron, without any preferential targeting from the soma to branches receiving synaptic signals. We thus next asked whether translation was spatially regulated. To do this, we performed immunocytochemistry with anti-sensorin antibodies in sensory-motor cocultures (3DIV). As shown in Figures 4.4F and G, sensorin protein was present at much higher concentrations in sensory neuron branches contacting target motor neurons than in branches contacting nontarget motor neurons. These data suggest that sensorin expression is spatially regulated at the level of translational regulation rather than mRNA targeting.

To directly measure local translation (as opposed to somatic translation followed by protein transport into the neurite), we conducted live imaging experiments using a

sensorin translational reporter that consists of the 5' and 3' UTRs of sensorin fused to the photoconvertible fluorescent protein dendra2 (Wang et al., 2009). We expressed this reporter in bifurcated sensory neurons contacting L7 and L11 MNs and removed the SN cell body so that we could specifically monitor translation in neuronal processes. We photoconverted dendra2 in the branches from green to red, and used live cell imaging to detect the appearance of newly translated, green dendra2 signal, which we have previously demonstrated represent new translation (Wang et al., 2009). As shown in Figure 4.4A-D, we detected a significantly greater increase in green signal in SN processes contacting the L7 target MN than in the SN processes contacting the L11nontarget MN. Together, these experiments indicate that although sensorin mRNA is delivered throughout the sensory neuron, it is preferentially translated at sites of synaptic contact.

To determine whether this effect was specific to sensorin mRNA, or whether it applied more generally to global translation, we analyzed the localization of the translation eukaryotic initiation factor4E (eIF4E) and the 4E binding protein (4EBP) in bifurcated sensory neurons contacting L7 and L11 motor neurons. As shown in Figures 4.4E-G and Figures 4.5, both eIF4E and 4EBP proteins distributed equally in branches contacting target and nontarget motor neurons. However, when we used phosphospecific antibodies that recognize the activated forms of eIF4E (peIF4E) and 4EBP (p4EBP), we detected significantly higher concentrations in branches making synaptic contact with L7 motor neurons. These findings indicate that translational machinery is distributed throughout the neuron, but is preferentially activated at sites receiving a synaptogenic

signal. Since phosphorylation of eIF4E and 4EBP activates global translation, our results indicate that translational regulation, rather than mRNA targeting, broadly controls the local proteome.

Netrin-1 promotes translation in SN branches contacting target and nontarget MNs.

Our previous study using translational reporters to visualize local translation of sensorin mRNA during long-term facilitation of *Aplysia* SN-MN synapses (Wang et al., 2009) revealed that serotonin regulated translation specifically at stimulated synapses, and that this regulation required a calcium-dependent trans-synaptic signal from the MN to the SN (Wang et al., 2009). Our current finding that sensorin protein was enriched at synaptic as compared to non-synaptic sites (Figures 4.4F and G) are also consistent with a role for a synaptically localized translational regulation mechanism.

We considered the possibility that the guidance factor netrin-1 might serve as such a signal. Netrin-1 has been shown to promote translation in neuronal growth cones (Cambell and Holt, 2001), and Flanagan and colleagues recently reported that components of the translational machinery, including ribosomal subunits and translation factors, are tethered at the plasma membrane in neuronal dendrites by binding to the cytoplasmic tail of the netrin receptor Delected in Colorectal Cancer (DCC, Tcherkezian et al., 2010). Netrin-1 binding was shown to trigger the release of bound translational components, and to thereby promote localized, netrin-1 dependent protein synthesis. Together, these findings suggested that release of netrin-1 from either SN or MN during synapse formation triggers translation at sites of synaptic but not non-synaptic contacts.

We tested the possibility that netrin-1 regulates the synthesis of localized transcripts by incubating *Aplysia* sensory-motor neuronal cultures with recombinant Fchuman netrin-1. As shown in Fig 4.6A- C, bath application of netrin1 (250 ng/ml) for 24 hrs increased sensorin immunoreactivity in SN branches contacting the L11 nontarget motor neuron, such that there was no longer any branch-specificity of sensorin protein concentration.

To further examine the effect of netrin-1 on sensorin expression, we cultured SNs with target LFS MNs in the presence or absence of netrin-1, and compared sensorin immunoreactivity. As shown in Fig 4.6D and E, incubation with netrin-1 significantly increased sensorin immunoreactivity. To differentiate between stimulated local translation and stimulated somatic translation followed by transport into the branches, we cultured bifurcated SN-LFS, removed the SN cell body, incubated with netrin-1 and processed the cultures 24 hrs later for sensorin immunoreactivity (Fig 4.8A-C). These experiments revealed that netrin1 increased sensorin concentration equally well in branches contacting both L7 and L11 MNs, consistent with local stimulation of translation. Netrin-1 also increased peIF4E immunoreactivity in SN-LFS cultures in which the SN soma had been removed (Fig 4.8C). The netrin-1 induced increase in sensorin immunoreactivity in intact SN-LFS cocultures was similar to that observed with five spaced applications of serotonin (5HT), which produces long-term facilitation (LTF) of SN-MN synapses and which has been shown to promote sensorin translation (Fig 4.6E, Hu et al 2006., Wang et al., 2009). Moreover, netrin-1 induced translation in intact or soma-lacking sensory neurons was blocked by preincubation with the protein synthesis

inhibitor anisomycin (10μM for 24hr), indicating that the increased immunoreactivity did indeed result from increased translation (Fig 4.6E and Fig 4.8C).

We considered the possibility that netrin-1 might transform non-synaptic sites to synapses, and that the increase in translation occurred as a result of the conversion to non-synaptic to synaptic sites. However, incubation of SN-L11 cocultures with netrin-1 did not result in the formation of synapse as shown by the absence of an excitatory postsynaptic potential (EPSP) in the L11 MN after SN stimulation (data not shown). We did find, however, that incubation with netrin-1 significantly increased EPSP amplitude between SN and LFS target MNs (Fig 4.6F and G). The increase in EPSP amplitude was similar to that seen during LTF induced by 5 spaced applications of 5HT (data not shown). LTF induced by 5 applications of 5HT has also been shown to involve significant increases in the number of SN varicosities (sites of synaptic connections) in SN-MN cultures (Glanzman et al., 1990). We thus measured the effect of netrin-1 on varicosity numbers, and, as shown in Fig 4.4H, found that it significantly increased the number of SN synaptic varicosities in SN-LFS MN cultures. Together, these findings suggest that the local translation induced by netrin-1 increases synaptic strength and synapse number.

Netrin-1 binds to presynaptic DCC receptors to promote translation

To explore the mechanisms by which netrin-1 regulates translation, we first asked whether it did so by binding to DCC. To test this, we incubated cultured neurons with recombinant netrin-1 in the presence of monoclonal anti-DCC antibodies that have

previously been shown to block netrin binding to the DCC receptor (Bennett et al., 1997; Braisted et al., 2000; Manitt et al., 2009). We first showed that a 24 hr incubation of isolated SNs with netrin-1 triggered a significant increase in sensorin immunoreactivity, but that incubation of isolated SNs with anti-DCC (in the absence of netrin-1) did not change sensorin immunoreactivity (Fig 4.7A and B). While anti-DCC antibodies had no effect on the basal concentration of sensorin in isolated SNs, they significantly decreased basal sensorin immunoreactivity in SN-MN cocultures (Fig 4.7C and D). Taken together, these findings are consistent with netrin-1 being endogenously released from the postsynaptic MN and binding to DCC on the SN to promote presynaptic translation of sensorin.

We next explored the function of netrin-1/DCC signaling during synapse formation. Towards this end, we cultured a SN for 24 h, then added a MN in the presence or absence of vehicle (ASW), control IgG (non-immune mouse IgG), or function-blocking anti-DCC antibodies, and measured EPSP amplitude 24 hrs later. As shown in Fig 4.7B, EPSP amplitude was significantly lower in cultures incubated with anti-DCC antibodies than in control cultures. This was accompanied by a decrease in sensorin immunoreactivity in the cultures incubated with anti-DCC antibodies (Fig 4.7C and D). To determine whether netrin-1/DCC also regulated synapse maintenance and/or stability, we cultured SN-MN neurons for two days, added anti-DCC antibodies, and then measured EPSP amplitude 24 hrs later. As shown in Fig 4.7F, this also triggered a significant decrease in EPSP amplitude (Fig 4.7H) and sensorin immunoreactivity (Fig 4.7G), consistent with netrin-1/DCC signaling contributing to synapse stability/maintenance.

DISCUSSION

This study was aimed at determining the relative importance of mRNA targeting and locally regulated translation in spatially restricting gene expression in neurons. Using a simple system consisting of a single, birfurcated *Aplysia* SN contacting a nontarget L11 MN, with which it did not form chemical synapses, and a target L7 MN, with which it formed glutamatergic synapses, we asked whether and how synaptogenic signals regulate RNA localization and/or local translation. The results of our experiments reveal that RNAs and translational machinery are delivered throughout the neuron, but that translation is spatially restricted to sites of synaptic contact. Our results further indicate that the guidance factor netrin1 promotes translation at synapses, and are most consistent with a model in which synapse formation leads to release of netrin-1 from the MN, which in turn triggers presynaptic DCC to promote translation in the presynaptic compartment.

Local regulation of translation, rather than RNA targeting, mediates spatial regulation of gene expression during synapse formation

Studies of mRNA localization in asymmetric cells have revealed that a large number of transcripts localize to specific subcellular compartments. For example, high throughput FISH analyses of over 3,000 transcripts in *Drosophila* embryos revealed that over 70% of mRNAs were expressed in highly specific subcellular patterns (Lecuyer et al., 2007). These findings suggest that targeted localization of mRNA spatially regulates gene expression, and thereby define discrete subcellular compartments in *Aplysia* neurons.

We have previously identified hundreds of mRNAs in the neurites of *Aplysia* SNs (Moccia et al., 2003), and studies of localized mRNAs in mammalian hippocampal neurons have indicated that hundreds (Eberwine et al., 2001; Poon et al., 2006) to thousands of transcripts (Cajigas et al., 2012) localize to dendrites. A handful of these mRNAs have been shown to undergo regulated localization to specific subcellular loci within the neuronal process. For example, in *Aplysia* sensory neurons, sensorin mRNA concentrates at synapses upon pairing with a target motor neuron, and in mammalian dentate granule neurons, arc mRNA has been reported to concentrate at stimulated synapses following induction of long-term potentiation of the perforant pathway (Steward et al., 1998). These studies suggest that directed mRNA targeting functions to alter the local proteome.

In contrast, our studies of RNA localization and regulated translation during synapse formation indicate that the local proteome is regulated primarily at the level of translation rather than mRNA targeting. Thus, transcripts, ribosomes and translational machinery are delivered throughout the neuron, but translation is selectively activated in response to local stimuli such as synapse formation. This mechanism of gene regulation poses considerable advantages to the wiring and activity-dependent rewiring of the nervous system because it renders every subcellular compartment, from dendrites and axons to synapses and growth cones, capable of locally changing their proteome, and hence their structure and function, in response to local stimuli. As such, it maximizes the plasticity of each subcellular compartment within the brain.

Netrin-1 serves as a local cue to spatially regulate translation within neurons

We focused on a role for netrin-1 as the retrograde signal driving translation in the sensory neuron because it has been shown to promote translation in axonal growth cones (Cambell and Holt, 2001) and because Flanagan and colleagues have reported that the netrin receptor DCC serves as a transmembrane translation regulation complex in dendrites and axons (Tcherkezian et al., 2010). The finding that anti-DCC antibodies decrease sensorin immunoreactivity in SNs paired with MNs, but not in isolated SNs, is consistent with netrin-1 being released from the motor neuron and binding to DCC on the adjacent presynaptic sensory neuron to promote translation of sensorin at synapses. Netrin-1 binding to DCC may promote translation by releasing translational machinery from binding DCC cytoplasmic domains within the presynaptic terminal, as proposed by Flanagan and colleagues (2010). Alternatively, netrin1-induced translation may be downstream of PI3 kinase and/or MAPK pathways, both of which are activated by netrin1 binding to DCC (Li et al., 2004; Round and Stein, 2007). How netrin is released from the motor neuron, and whether and how this release is regulated, remain open questions. We also previously reported that serotonin-induced translation of sensorin in sensory neurons required a calcium-dependent retrograde signal from the motor neuron (Wang et al., 2009). This raises the possibility that netrin1 release from the motor neuron is a calcium-dependent process, triggered for example by spontaneous release of glutamate from the presynaptic sensory neuron during synapse formation and/or during synaptic plasticity (Eliot et al., 1994; Villareal et al., 2007; Jin et al., 2012, although see also Sutton et al., 2005, which indicates that spontaneous release serves to suppress local

translation in hippocampal neurons).

While we use recombinant human netrin-1 and function blocking antibodies against human DCC, we are confident that these reagents reflect the endogenous functions of netrin and DCC in *Aplysia.* As shown in Fig 4.9 and 4.10, we have cloned *Aplysia* netrin, and find that it is 47% identical and 60% similar to human netrin-1 (by comparison, *C. elegans* netrin is 44% identical and 59% similar to human netrin-1). We have also cloned *Aplysia* DCC, and find that it is 31% identical and 47% similar to human DCC (by comparison, *C. elegans* DCC is 18% identical and 31% similar to human DCC). Moreover, the function-blocking antibody recognizes the extracellular domain, which is the most highly conserved region of the protein (extracellular domain of *Aplysia* DCC is 39% identical and 55% similar to human DCC).

We also note that netrin-1/DCC signaling is likely one of multiple pathways that regulate translation in neurons, and that translation is not regulated in a digital on/off manner, but rather in a graded manner. This explains, for example, why there is some sensorin translation in SN neurites contacting nontarget L11 (Figs 4.4B and C), and why sensorin protein is expressed in isolated sensory neurons that have been incubated with anti-DCC antibodies (Figs 4.7A and B). Additionally, our results raise the possibility that netrin-1 not only regulates local translation, but that it plays additional roles in triggering synapse formation. As such, netrin-1, in conjunction with additional signals, may serve as a synapse specificity factor. Our previously published report that synapse formation alters the localization of sensorin mRNA such that it concentrates at synapses (Lyles et al., 2006; Meer et al., 2012), and that serotonin-regulated translation of a sensorin-based

translational reporter was restricted to sites of synaptic contact, suggested that the activity-dependent localization of mRNA played a critical role in the regulation of its expression. Our current finding that netrin-1 increases translation at synaptic and nonsynaptic sites indicates that the precise subcellular localization of the mRNA is secondary to the localization of the netrin1 signal. Thus, sensorin mRNA does not have to be in the synaptic milieu *per se* to be translated, but rather has to localize to a site in which netrin-DCC signaling can occur. We also note that we previously found that there was a significant increase in the concentration of sensorin mRNA in SN branches contacting target as compared to nontarget MNs in more mature (5 DIV) cocultures (Lyles et al., 2006). This suggests that while there is not directed targeting of sensorin mRNA from soma to process during synapse formation, there may be preferential stabilization, over time, of sensorin mRNA at sites of synaptic contact.

Local translation contributes substantially to the local proteome

Our study also sheds light on the relative contributions of local translation and somatic translation to the local proteome. Thus, we can compare the amount of netrin induced translation of the sensorin reporter in SN-LFS cocultures with and without the soma (Fig S4D). Although one cannot directly compare the total concentration of sensorin in intact SN and isolated SN neurites, the data do indicate that netrin is able to induce an equivalent increase in SN neurites in the presence or absence of a SN soma. This suggests that local translation contributes substantially to stimulus-induced changes in the local proteome.

Taken together, our findings show that a signaling pathway involved in axon guidance also regulates synapse formation by spatially restricting neuronal gene expression. Decentralizing the control of gene expression to individual subcellular compartments in this manner enriches the adaptability and plasticity of the nervous system by enabling each compartment to change its proteome in response to local cues.

EXPERIMENTAL PROCEDURES

Aplysia Cell Culture

Animals were obtained from 80—100 gram Aplysia (Alacrity, Redondo Beach, CA) for sensory-LFS motor neuron or from the abdominal ganglion of juvenile Aplysia (1-4 g, National Aplysia Resource, University of Miami,FL) for L7 and L11 motor neurons. Sensory-Motor neuron cocultures and medium were prepared from Aplysia as previously described (Montarolo et al., 1986). Bifurcated sensory-motor neuron cocultures were prepared as described by Martin el al., 1997(b). A detailed culture method is available at http://www.biolchem.ucla.edu/labs/martinlab/ or as described in Zhao et al., 2009. Briefly, Bifurcated sensory neurons from 80-100g Aplysia were placed on poly-L-Lysine coated glass bottom dish with L7 and L11 motor neurons which were gotten from abdominal ganglia of 1-4g juveniles Aplysia. LFS motor neurons were also from 80-100g Aplysia. Cultures were maintained for 3 days at 18℃ before performing experiments.

Microinjection and Electrophysiology

For most experiments for FISH and ICC, 5mM Fluorescent dye Alexa647 (bifurcated sensory neuron) or Alexa546 (L7 motor neuron) as a volume control was microinjected with a Picospritzer (World Precision Instrument, Sarasota, FL) on Day3 before confocal imaging. To microinject dye or plasmid into sensory neuron, a sharp glass electrode was connected to a picospritzer (World Precision Instrument, Sarasota, FL) and 10psi pressure was applied. All plasmids or dyes were filtered with Spin-X

centrifuge tube filter (0.22μm cellulose acetate, Corning Incorporated, NY). Aplysia ribosomal S6 protein and Aplysia Staufen-Dendra2 constructs in pNEX3 with fluorescent dye Alexa 647 as a volume control were microinjected into SNs the day after culture preparations. To count the number of RNA granules, 200ng/μl Staufen-Dendra2 in pNEX3 vector with Alexa647 and, to measure new translation, 200ng/μl reporter protein Dendra2 fused with sensorin 5'3' UTR in pNEX3 vector were microinjected on Day1. After 48hr expression, Photoconversion of reporter protein Dendra2 was performed as a described by Wang et al., 2009 and slightly modified. To photoconvert Dendra2 green signal to red, we used X-cite series120Q excitation light (a 120-watt lamp) and delivered UV for two times for 5sec with 10sec interval. Neurons were left for 24hr and detected new green signals at basal state in both contacting sensory neuron neurites. To measure changes of varicosities in sensory-motor neuron co-culture, VAMP (synaptobrevin)-mCherry RFP in pNEX3 vector was used in sensory-LFS motor neuron for 48hr expression and counted varicosities before/after 250ng/ml netrin-1 in L15 medium

In relevant experiments, 5HT-creatinine (10μM; Sigma), anisomycin (10μM; Calbiochem), Netrin-1 (250ng/ml; Enzo Life Science), anti-DCC (250ng/ml, Calbiochem) and anti-mouse IgG (250ng/ml, Calbiochem) was delivered to the neurons. ASW (artificial sea water; NaCl 27.89g, CaCl2H2O 1.62g, KCl 0.738g, MgCl2 6H2O 11.18g, HEPES 2.38g in 1L nanopure water) was used as delivery vehicle in all experiments.

EPSP amplitude was measured as described by Zhao et al., 2003. Briefly, the LFS motor neurons were impaled with sharp glass electrode of 10~15 MΩ resistance with 2M

potassium acetate, and LFS motor neurons were initially hyperpolarized with additional current as necessary to -80mV and Sensory neurons -50mV. EPSPs were evoked by intracellular stimulation of sensory neuron (1-3 nA for 5ms) with a Grass S88 stimulator. EPSPs were recorded and measured with Axoscope 8.2 and pClamp8 software (Axon Instruments, Union City, CA). To investigate netrin-1 effects during synapse formation, pre-EPSPs were measured on Day3 before netrin-1(250ng/ml in L15 media) treatment and then after 24hr, post-EPSPs were measured. Artificial Sea Water (ASW) or ASW containing anti-mouse IgG (250ng/ml) was used as a control treatment. In experiment in which netrin-1 effects on synapse formation was tested with anti-DCC (250ng/ml in L15 media) treatment for neutralizing DCC receptor on Day2 and measured EPSP amplitude on Day3.

Live Cell Imaging and Quantification

For data analysis, Flourescent Dye Alexa 647 was used as a volume control and injected to Sensory neuron and also into L7 motor neuron to differentiate encroached L7 motor neuron neurites in sensory neuron neurites contacting L11 motor neuron. Images were transferred to slidebook4.2 and mean pixel intensity were measured for FISH and ICC samples. All images were analyzed with a volume control Alexa dye.

Fluorescence In Situ Hybridization (FISH) and Immunocytochemistry (ICC) in Cultured Aplysia neurons

FISH was performed and slightly modified as described by Lyles et al., 2006 and Martin et al., 1997. Briefly, cultured neurons were fixed with 4%PFA / 30% sucrose for 30min at room temperature. For FISH, after fixation, we used 40ng/ml concentrations of riboprobe for 18S rRNA or sensorin RNA as previous described protocol and then neurons were immediately imaged after FISH.

ICC was performed as described in Martin et al., 1997. Primary Antibodies included custom made chicken anti-sensorin antibodies (generated against peptide CATRSKNNVPRRFPRARYRVGYMF by Aves Labs, Inc., Tigard, OR), Anti-phospho eIF4E(Cell signaling,1:100), Anti-eIF4E, Anti-phopspho 4EBP, Anti-4EBPin 10% Goat serum in PBS were incubated at 4℃ for 18-24hr after confocal imaging for some experiment with Alexa 647 and followed previous protocols

Multiple Alignments of Aplysia Netrin-1 and DCC

Identical (black) and similar (gray) amino acid residues are marked by using software (GeneDoc)

Statistical Analysis

All results are presented as a mean ±SEM. Prism GraphPad was used to perform all statistical analysis.

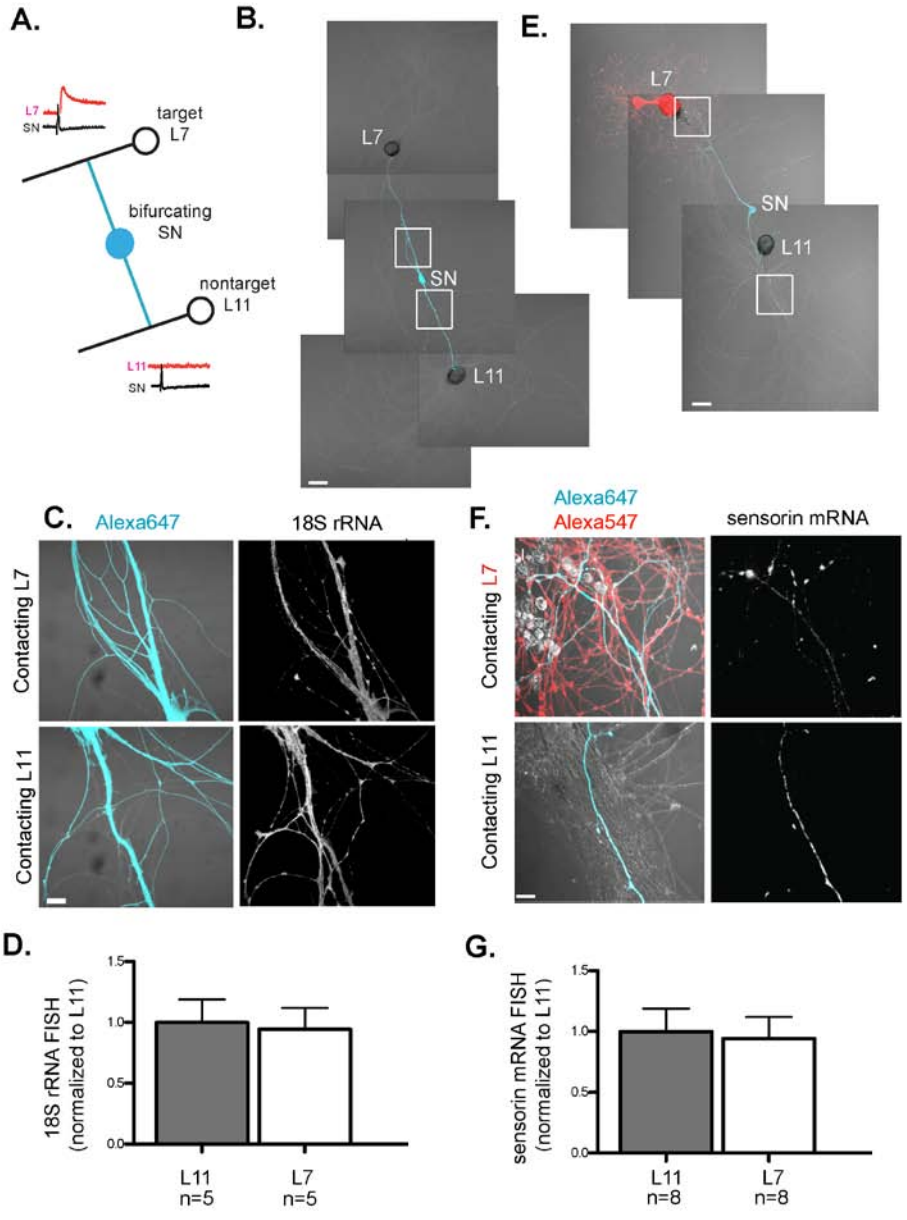
A.
B.
E.
L7
SN
target
L7
bifurcating
SN
nontarget
L11
L11
SN
L7
SN
L11
L7
SN
L11
C.
Alexa647
18S rRNA
Contacting L7
Contacting L11
F.
Alexa647
Alexa547
sensorin mRNA
Contacting L7
Contacting L11
D.
18S rRNA FISH
(normalized to L11)
1.5
1.0
0.5
0.0
L11
n=5
L7
n=5
G.
sensorin mRNA FISH
(normalized to L11)
1.5
1.0
0.5
0.0
L11
n=8
L7
n=8

Figure 4.1. rRNA and sensorin mRNA target equally well to SN branches contacting target and non-target MNs.
A bifurcated SN was cultured with an L7 target MN and a L11 non-target MN (cartoon in A; photomicrographs in B and E) for 3 days. Alexa647 (cyan) was microinjected into the SN before imaging (B and E) and Alexa546 (red) was injected into the L7 target MN (E) to differentiate between SN, target and non-target MN neurites. Cultures were processed for Fluorescent In Situ Hybridization (FISH) for 18S rRNA (C) in proximal sensory neuron neurites and for sensorin mRNA (F) in distal neurites contacting L7 and L11 MNs. Areas outlined with white squares in (B) and (E) were imaged at high magnification in (C) and (F); left panels show merged images of DIC and Alexa fluorescence, and right panels show FISH signals. The Alexa fluor served as a volume control to analyze FISH RNA intensity. Group data indicates that both 18S rRNA (D) and sensorin mRNA (G) are evenly distributed in neurites contacting L7 target and L11 non-target MNs. Error bars represent SEM. ns = nonsignificant. Scale bar in (B) and (E) = 100μm; in (C) and (F) =10 μm.

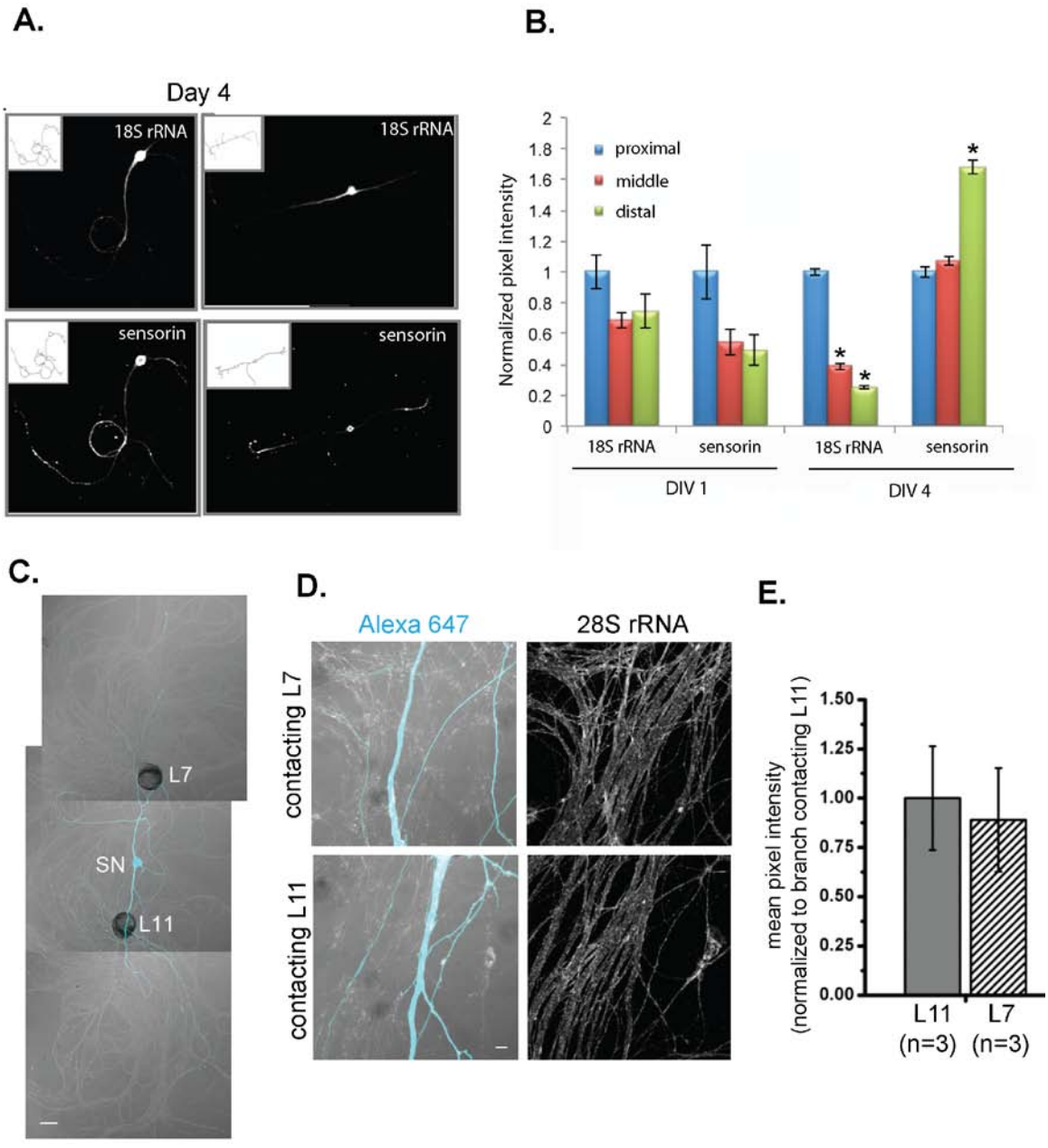
A.
Day 4
18S rRNA
18S rRNA
sensorin
sensorin
B.
Normalized pixel intensity
proximal
middle
distal
18S rRNA
sensorin
18S rRNA
sensorin
DIV 1
DIV 4
C.
L7
SN
L11
D.
Alexa 647
28S rRNA
contacting L7
contacting L11
E.
mean pixel intensity
(normalized to branch contacting L11)
L11
(n=3)
L7
(n=3)

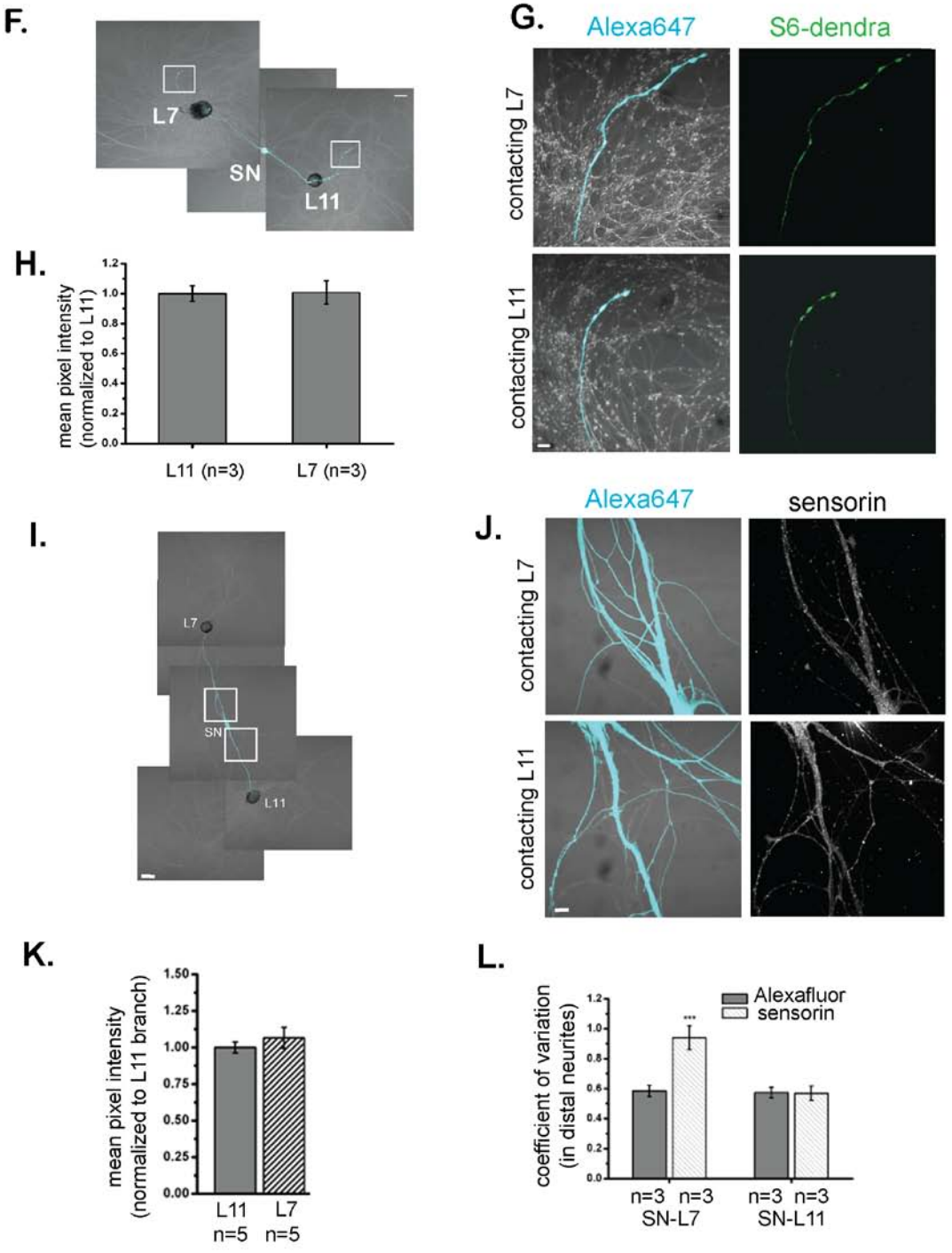
F.
L7
SN
L11
G.
Alexa647
S6-dendra
contacting L7
contacting L11
H.
mean pixel intensity
(normalized to L11)
1.2
1.0
0.8
0.6
0.4
0.2
0.0
L11 (n=3)
L7 (n=3)
I.
L7
SN
L11
J.
Alexa647
sensorin
contacting L7
contacting L11
K.
mean pixel intensity
(normalized to L11 branch)
1.50
1.25
1.00
0.75
0.50
0.25
0.00
L11
n=5
L7
n=5
L.
coefficient of variation
(in distal neurites)
Alexafluor
sensorin
***
1.2
1.0
0.8
0.6
0.4
0.2
0.0
n=3 n=3
SN-L7
n=3 n=3
SN-L11

Figure 4.2 (accompanies Figure 4.1). RNAs target equally well to SN neurites contacting L7 target MNs and L11 non-target MNs.
To examine the distribution of rRNA over time, isolated SNs were cultured, fixed at 1, 2 and 4 DIV, and processed for FISH for 18S rRNA and sensorin mRNA (A). Representative images at DIV1 and DIV4 are shown in (B). Neurites were linearized, mean pixel intensity along the neurite was quantified, the neurite was divided into Proximal (P), Middle (M) and Distal (D) thirds, and the relative amount of pixel intensity in each segment was quantified. While sensorin mRNA concentrates in the distal third of the neurite over time, 18S rRNA concentration decreases with the length of the neurite. In (C), a bifurcated SN was cultured with L7 target MN and L11 non-target MN for 3 days. Alexa647 (cyan) was microinjected into the SN before imaging to visualize SN neurites. Cultures were processed for Fluorescent In Situ Hybridization (FISH) for 28S rRNA (D) in proximal sensory neuron neurites contacting L7 and L11 MNs. Areas outlined with white squares in (C) were imaged at high magnification in (D); left panels show merged images of DIC and Alexa fluorescence, and right panels show FISH signals. The Alexa fluor served as a volume control to analyze FISH RNA intensity. Group data (E) indicates that both 28S rRNA is evenly distributed in neurites contacting L7 target and L11 non-target MNs. To further examine RNA localization, we microinjected the ribosomal S6 protein tagged with dendra into a bifurcated SN contacting a target L7 MN and a nontarget L11 MN (F). Representative high magnification images of areas denoted by white squares in (F), with merged DIC and Alexa fluor in the left panels and S6-dendra signal (green) shown in G. Group data (H) show that equal amounts of S6-dendra localize to SN neurites contacting L7 target MNs and L11 non-target MNs. Complementing images of sensorin FISH in distal neurites in Fig 4.1E and F, (I-K) show FISH signals for sensorin mRNA in proximal branches of bifurcated SN contacting target L7 and non-target L11 MNs (J), revealing equal targeting to both branches (K). Also complementing Fig 1E, (L) shows the coefficient of variation for sensorin immunoreactivity in SN neurites contacting target L7 and non-target L11 MNs. Error bars represents ±SEM. Scale bar in (A) = 100μm; in B = 10 μm.

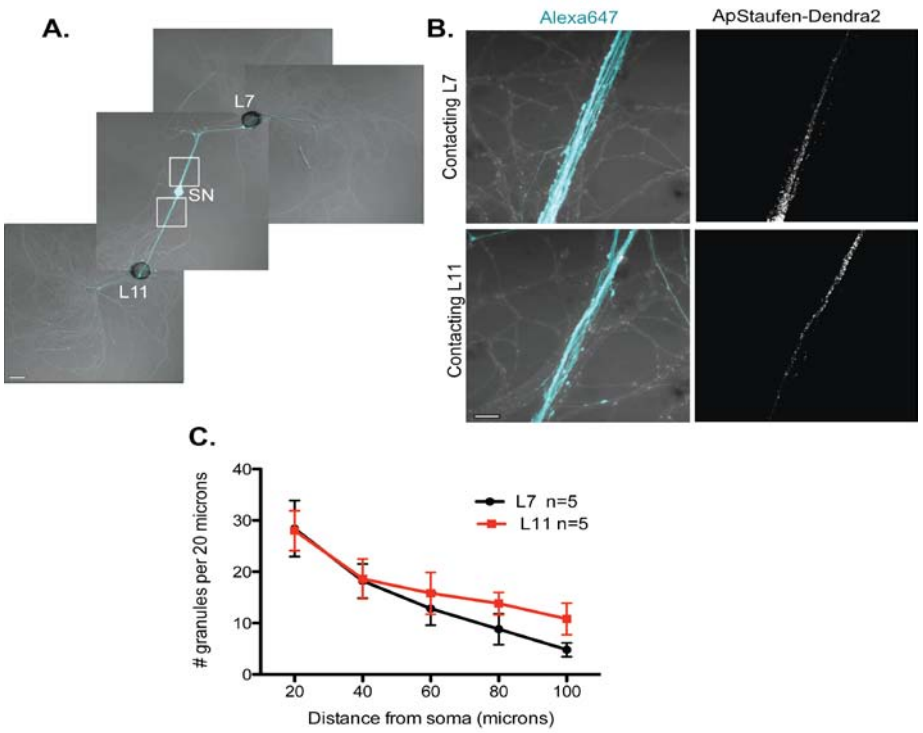

Figure 4.3. The RNA binding protein *Aplysia* Staufen targets equally well to SN neurites contacting L7 target and L11 nontarget MNs.
(A) Dendra2-tagged *Aplysia* Staufen was microinjected together with Alexa fluor 647 (cyan) into a cultured bifurcated SN contacting an L7 target MN and an L11 non-target MN at 1DIV. Staufen granules in SN neurites were imaged 48 hrs later. Representative high magnification images of areas denoted by white squares in (A) are shown in (B). Left panels show merged DIC/Alexa fluor images, and right panels show Staufen dendra2 images. (C) Group data reveals that the number of Staufen granules per 20um was the same in neurites contacting target L7 MNs (black, closed circle) and non-target L11 MNs (red, square). Error bars represent SEM. Scale bar in (A) = 100μm; in B = 20μm.

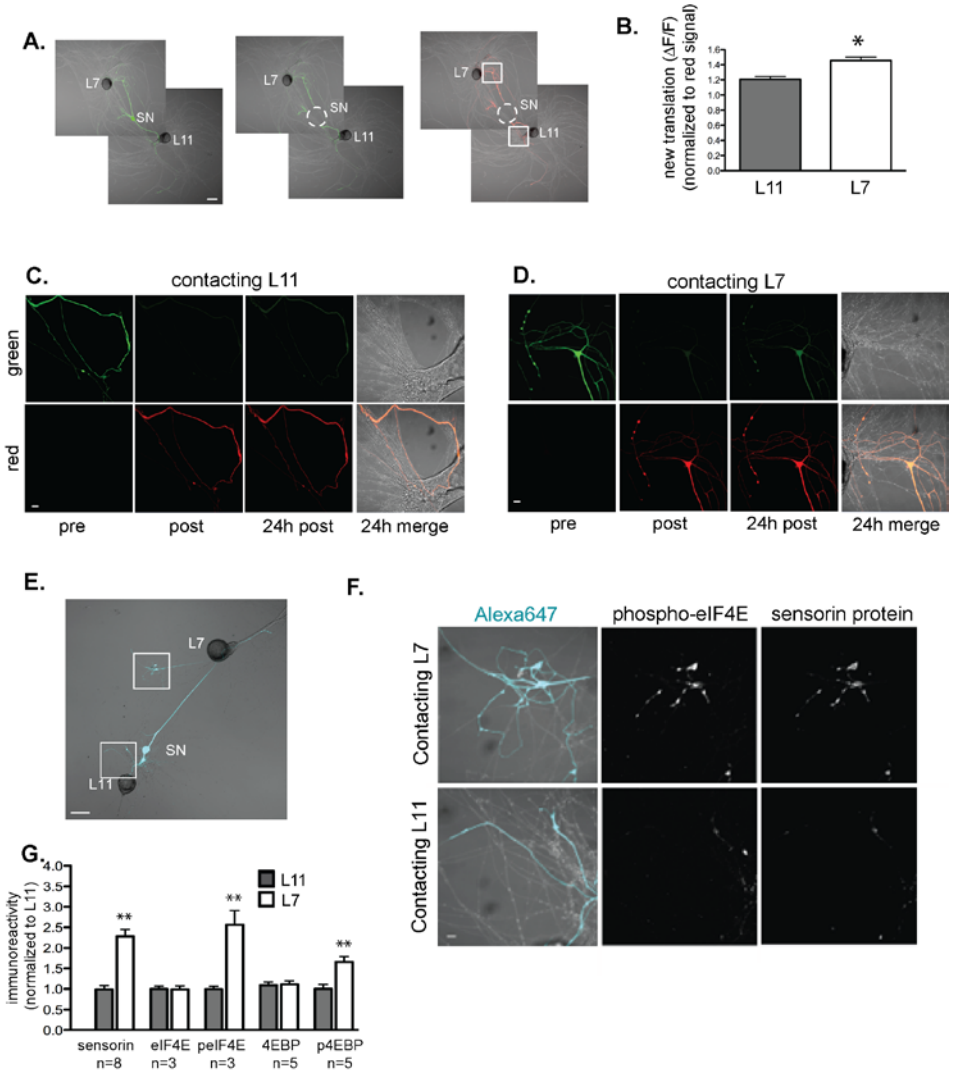
A.
L7
SN
L11
B.
new translation (ΔF/F)
(normalized to red signal)
L11
L7
C.
contacting L11
green
red
pre
post
24h post
24h merge
D.
contacting L7
pre
post
24h post
24h merge
E.
L7
SN
L11
F.
Alexa647
phospho-eIF4E
sensorin protein
Contacting L7
Contacting L11
G.
immunoreactivity
(normalized to L11)
L11
L7
sensorin n=8
eIF4E n=3
peIF4E n=3
4EBP n=5
p4EBP n=5

Figure 4.4. Local translation is greater in SN neurites contacting L7 target MNs than in neurites contacting L11 non-target MNs.
(A) To directly image local translation, we expressed a translational reporter consisting of sensorin mRNA fused to the photoconvertible fluorescent protein Dendra2 (see experimental procedures), removed the SN soma (dotted circle in middle panel of A), and 12-18 hrs later photoconverted the Dendra2 signal from green to red (right panel of A). Shown in (C, neurite contacting L11) and (D, neurite contacting L7) are high magnification images of regions marked by white squares in (A), including images before photoconversion (pre), right after PC (post), 24 hrs later (24h post). The top panels show the green channel, and the bottom show the red channel (which was used as volume control for quantification of the green signal). Increased green signal represents newly translated reporter. Group data (B) show that there is significantly more translation, measured as $\Delta F/F$, in neurites contacting L7 target MNs than in neurites contacting L11 nontarget MNs. (E) A bifurcated SN was cultured with an L7 target MN and L11 nontarget MN for 3 days. Alexa647 was microinjected into SNs, and served as a volume filling control for analysis of immunocytochemistry (ICC). To monitor local translation, we performed ICC for phosphorylated eIF4E (phospho-eIF4E), phosphorylated 4EBP and sensorin protein. Representative high magnification images of areas denoted by white squares in (E) are shown in (F), with merged DIC/Alexa fluor in the left panel, phosphoeIF4E ICC in the middle panel, and sensorin ICC in the right panel. Group data in (G) reveal that phospho-eIF4E, phospho-4EBP and sensorin protein concentrations are significantly greater in neurites contacting L7 target MNs than in neurites contacting L11 non-target MNs. As shown in Fig S3, total eIF4E and total 4EBP protein were distributed equally well in neurites contacting L7 target and L11 non-target MNs. Error bars represent SEM. ***$p < 0.001$ and **$p < 0.05$, unpaired t-test. Scale bars in (A) and (E) =100μm; in (C), (D) and (F) = 10 μm.

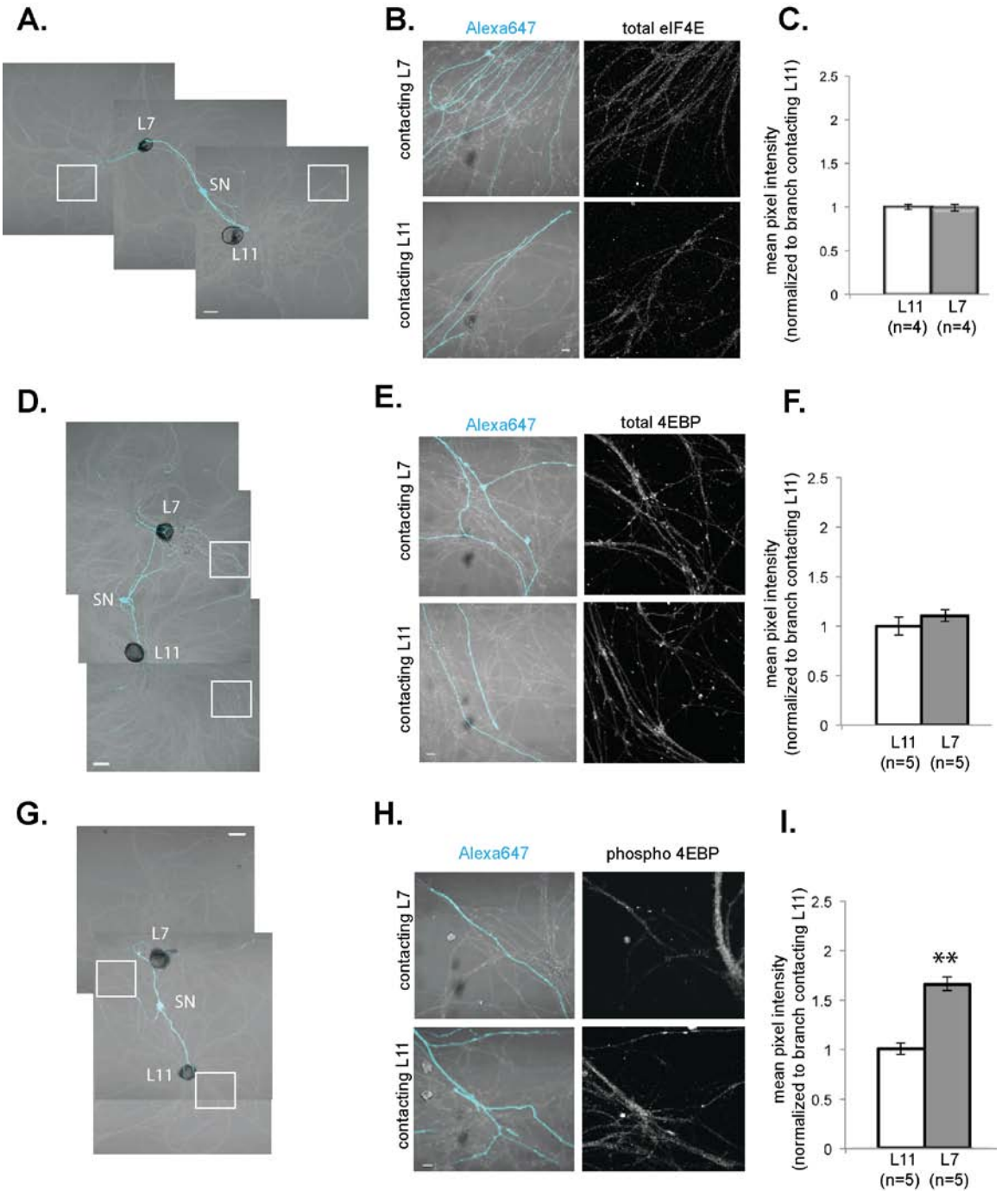
A.
L7
SN
L11
B.
Alexa647
total eIF4E
contacting L7
contacting L11
C.
mean pixel intensity
(normalized to branch contacting L11)
2.5
2
1.5
1
0.5
0
L11
(n=4)
L7
(n=4)
D.
L7
SN
L11
E.
Alexa647
total 4EBP
contacting L7
contacting L11
F.
mean pixel intensity
(normalized to branch contacting L11)
2.5
2
1.5
1
0.5
0
L11
(n=5)
L7
(n=5)
G.
L7
SN
L11
H.
Alexa647
phospho 4EBP
contacting L7
contacting L11
I.
mean pixel intensity
(normalized to branch contacting L11)
**
2.5
2
1.5
1
0.5
0
L11
(n=5)
L7
(n=5)

Figure 4.5. Translation is significantly increased in SN neurites contacting L7 target MNs.

Complementing Figure 4.4B and C, bifurcated SNs cultured with target L7 MNs and nontarget L11 MNs (A, D and G) were fixed at DIV3, and processed for immunocytochemistry with anti-eIF4E (B and C), anti-4EBP (E and F) or anti-phospho-4EBP (H and I) antibodies. Quantification of group data shows that total eIF4E (C) and total 4EBP (F) target equally well to SN branches contacting L7 target and L11 nontarget MNs, but that phopho-4EBP (I) is enriches in branches contacting L7 target MNs. Error bars represents ±SEM. **$p < 0.001$, unpaired student's t-test. Scale bars in (A, D and G) = 100μm; in (B, E and H) = 10 μm.

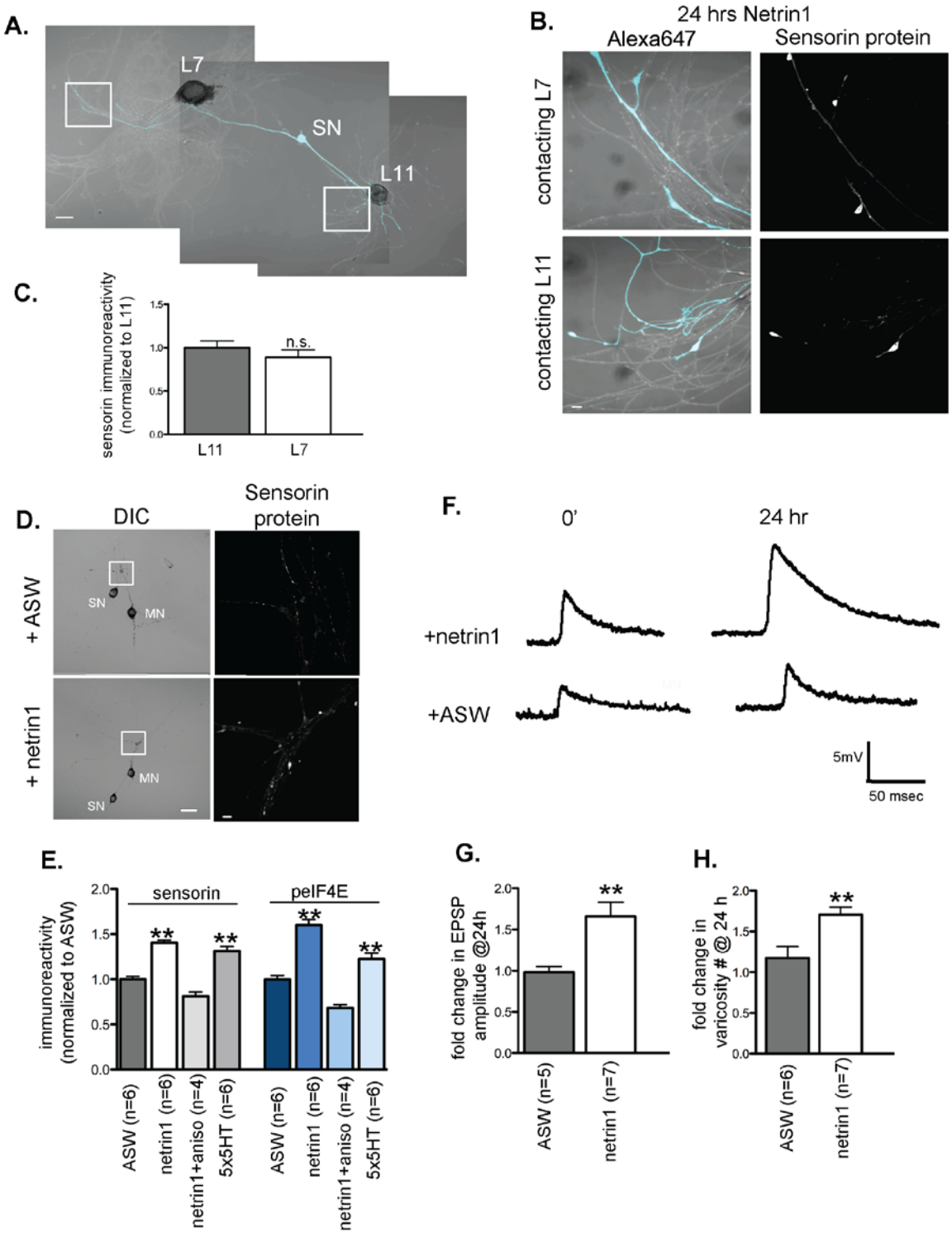
A.
L7
SN
L11
B.
24 hrs Netrin1
Alexa647
Sensorin protein
contacting L7
contacting L11
C.
sensorin immunoreactivity (normalized to L11)
n.s.
L11
L7
D.
DIC
Sensorin protein
+ ASW
+ netrin1
SN
MN
F.
0'
24 hr
+netrin1
+ASW
5mV
50 msec
E.
immunoreactivity (normalized to ASW)
sensorin
peIF4E
ASW (n=6)
netrin1 (n=6)
netrin1+aniso (n=4)
5x5HT (n=6)
G.
fold change in EPSP amplitude @24h
ASW (n=5)
netrin1 (n=7)
H.
fold change in varicosity # @ 24 h
ASW (n=6)
netrin1 (n=7)

Figure 4.6. Netrin-1 increases protein synthesis in SNs and strength of SN-target MN synapses.
(A) A bifurcated sensory neuron was cultured with an L7 target MN and a L11 non-target MN for 3 days. Alexa647 was microinjected into SNs, and served as a volume filling control for analysis of immunocytochemistry (ICC). Cultures were incubated with 250ng/ml netrin-1 for 24hrs. Representative high magnification images of areas marked by white squares in (A) are shown in (B), with merged DIC/Alexa fluor in the left panels, and sensorin ICC in the right panels. Group data (C) reveal that the concentration of sensorin in netrin1-treated SNs is the same in neurites contacting L7 target MNs andL11 non-target MNs. We compared sensorin and phospho-eIF4E immunoreactivity in SN-LFS target MN cultures (D) in the presence and absence of 250ng/ml netrin-1 (24 hrs). Representative high magnification images of areas denoted by white squares in left panels of (D) stained with anti-sensorin antibodies are shown in right panels of (D). Group data (E) reveal that netrin1 triggers an increase in sensorin and phospho-eIF4E immunoreactivity that is equivalent to the increase observed 24 hrs after 5 spaced applications of 5HT (which produce long-term facilitation) and that is blocked by the protein synthesis inhibitor anisomycin (10 μM). Netrin-1 also increased synaptic strength: representative traces of EPSPs evoked in LFS MNs after stimulation of SN, at time 0 and 24 hrs after incubation with vehicle (artificial seawater, ASW) or netrin-1 are shown in (F); histogram of group data is shown in (G). Histogram in (H) shows fold change in the number of varicosities between SN and LFS MN after 24 hrs of incubation with vehicle (ASW) and netrin-1. Error bars represent SEM. **$p < 0.001$, students unpaired ttest for (G) and (H); ANOVA and Newman-Keul's multiple comparison test for (E). Scale bars in (A) and (D) = 100μm; in (B), (E) = 10 μm.

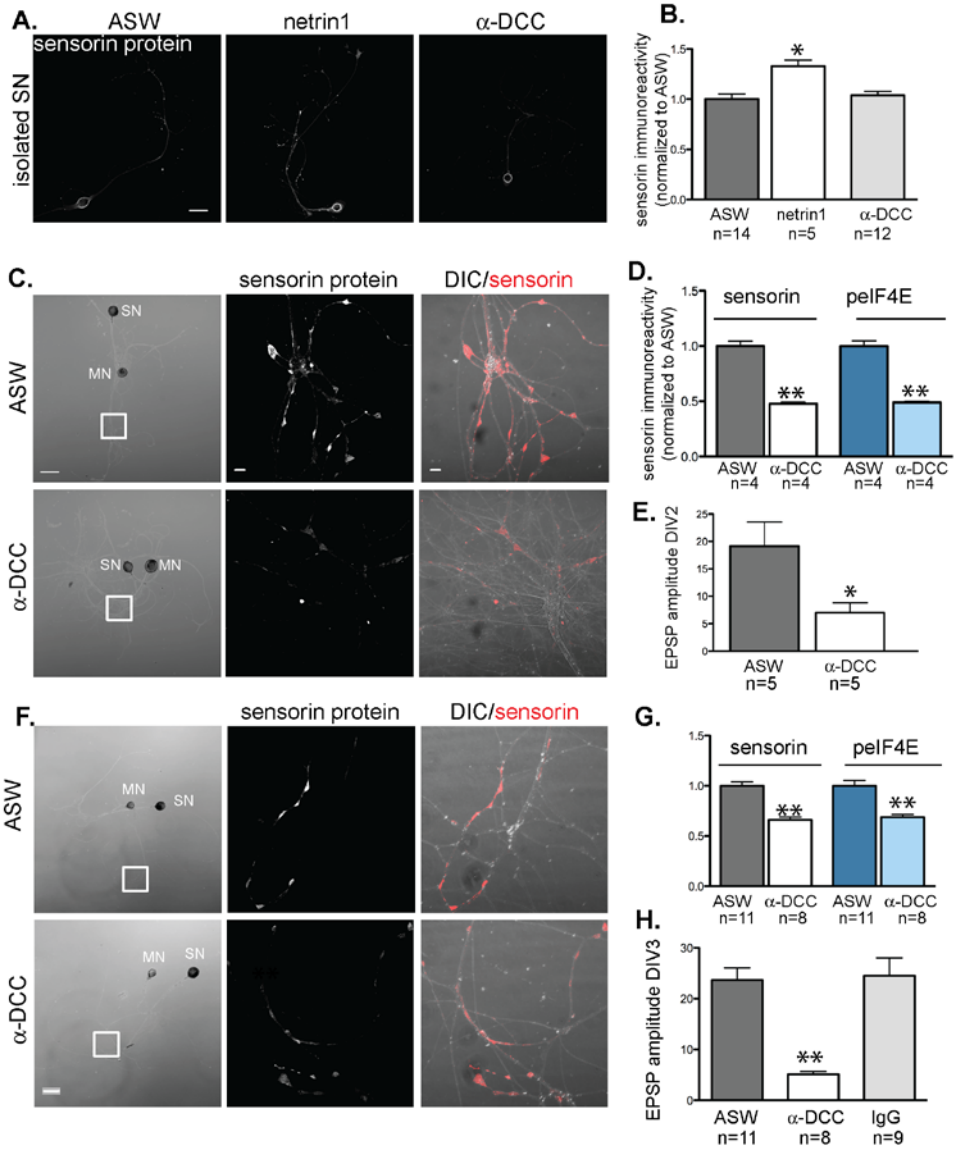
A.
ASW
netrin1
α-DCC
sensorin protein
isolated SN
B.
sensorin immunoreactivity (normalized to ASW)
ASW n=14
netrin1 n=5
α-DCC n=12
C.
sensorin protein
DIC/sensorin
ASW
α-DCC
SN
MN
D.
sensorin
peIF4E
sensorin immunoreactivity (normalized to ASW)
ASW n=4
α-DCC n=4
E.
EPSP amplitude DIV2
ASW n=5
α-DCC n=5
F.
G.
ASW n=11
α-DCC n=8
H.
EPSP amplitude DIV3
IgG n=9

Figure 4.7. Netrin binds DCC to promote SN translation and to increase strength of SN-MN synapses.
(A) and (B): Immunocytochemistry (ICC) of isolated SNs (3DIV) reveals an increase in sensorin immunoreactivity with netrin-1 incubation (250ng/ml for 24 hrs), but no change from baseline following 24 hrs of incubation with function blocking anti-DCC antibodies (250ng/ml). Representative images are shown in (A); group data in (B). To test the effect of function-blocking anti-DCC antibodies on sensorin and phospho-eIF4E (peIF4E) immunoreactivity and synapse formation in SN-LFS target MN cocultures, we cultured isolated SNs for a day, added anti-DCC (250ng/ml) and 6 hrs later paired the SN with a target LFS MN. EPSP amplitude was recorded the next day, and cultures were fixed for ICC. Representative cultures are shown in (C). High magnification images of areas denoted by white squares in left DIC images are shown in middle (sensorin ICC) and right (merged DIC and sensorin, red) panels. Group data (D) show that anti-DCC significantly decreases sensorin and peIF4E immunoreactivity, suggesting that netrin is released from the MN to drive translation in the SN. SN-LFS MN pairs incubated with anti-DCC antibodies also showed significantly smaller EPSP amplitudes than control cultures (E). To query the function of netrin-DCC signaling in mature, established SN-LFS MN synapses, we cultured SN-LFS MNs for two days, added anti-DCC antibodies (250ng/ml) for 24 hrs, and then measured EPSP amplitude and fixed the cultures for ICC. Representative cultures are shown in (F). High magnification images of areas denoted by white squares in left-most panels (F) are shown in middle (sensorin immunoreactivity) and right (merged DIC and sensorin, red) panels. Group data show that anti-DCC antibodies significantly decreased sensorin and peIF4E immunoreactivity (G) and EPSP amplitude between SN-LFS MNs (H). Control cultures were incubated with anti-mouse IgG antibodies (250ng/ml), which did not affect EPSP amplitude (H). Error bars represent SEM. *$p < 0.05$, **$p < 0.001$, unpaired student's t-test. Scale bars in (A) and in left panel of (C) and (F) = 100μm; in middle and right panels of (C) and (F) = 10 μm.

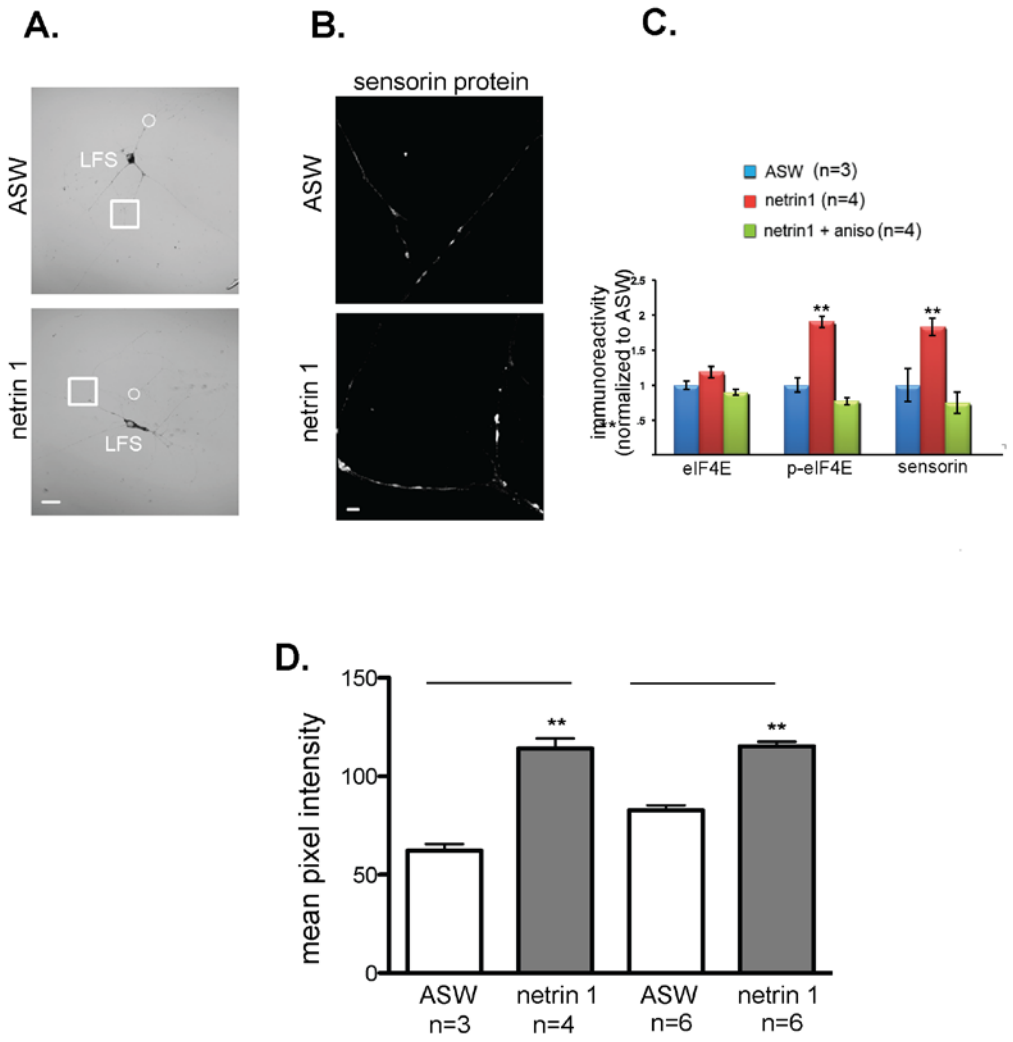

Figure 4.8. Netrin-1 increases local translation.
SNs were cultured with LFS MNs for 2 days (A), the SN soma was removed, and the cultures were then incubated with vehicle (ASW) and netrin-1 (250 mg/ml) for 24 hrs, then fixed and processed for immunoreactivity with anti-eIF4E, anti-p-eIF4E antibodies and anti-sensorin antibodies. Representative cultures are shown in (A). Representative high magnification images of areas denoted by white squares in (A) are shown in (B), with merged DIC and Alexa fluor (blue) on left, and sensorin immunoreactivity on right. Group data (C) show that total eIF4E immunoreactivity is not altered by netrin, but that both p-eIF4E and sensorin immunoreactivities are significantly increased by netrin. Netrin-induced immunoreactivity was measured in intact SN-LFS MN cocultures (see Figure 4D and E) and in SNs paired with LFS MNs in which the SN cell body has been removed (D). These results show that netrin-1 induces equivalent increases in sensorin immunoreactivity in soma-containing and soma-less SNs. Error bars represents ±SEM. **$p < 0.001$, unpaired student's t-test. Scale bars in (A) = 100μm; in (B) = 10 μm.

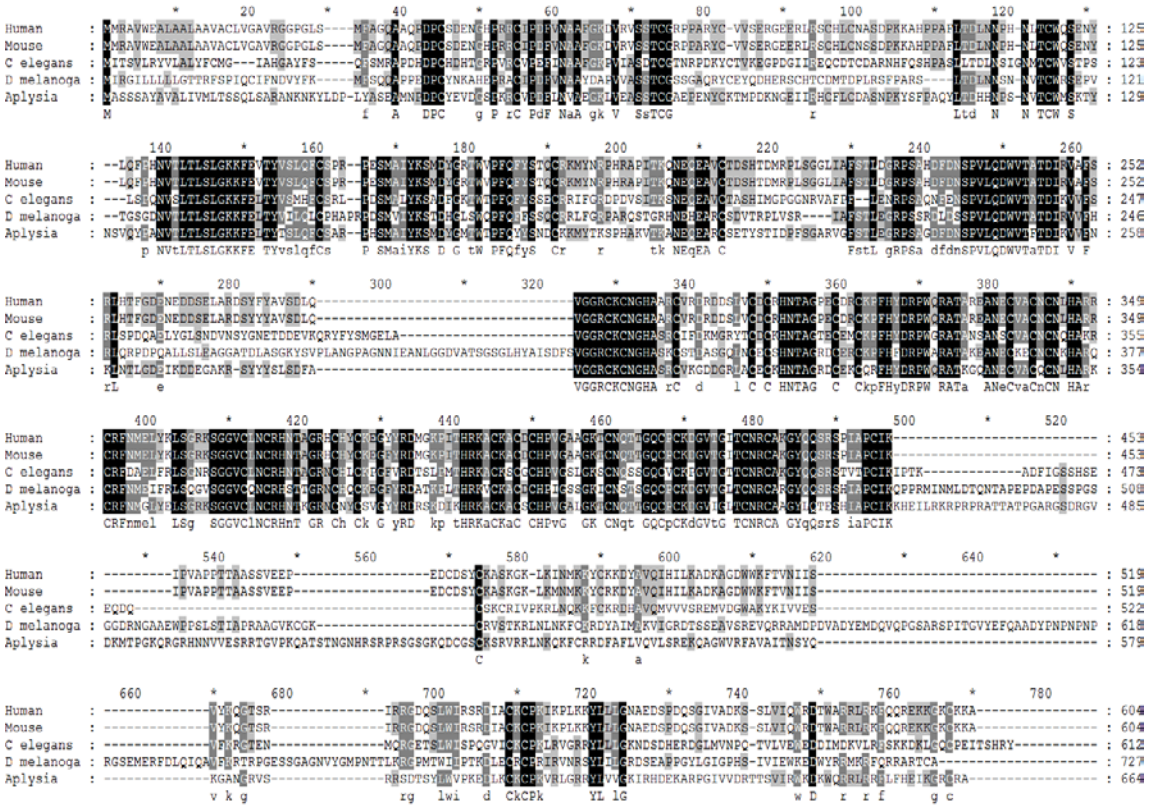

Figure 4.9. *Aplysia* Netrin-1 alignment
It shows an alignment of *Aplysia* netrin-1 with human, mouse, *C. elegans* and *D. melanogaster* netrins.

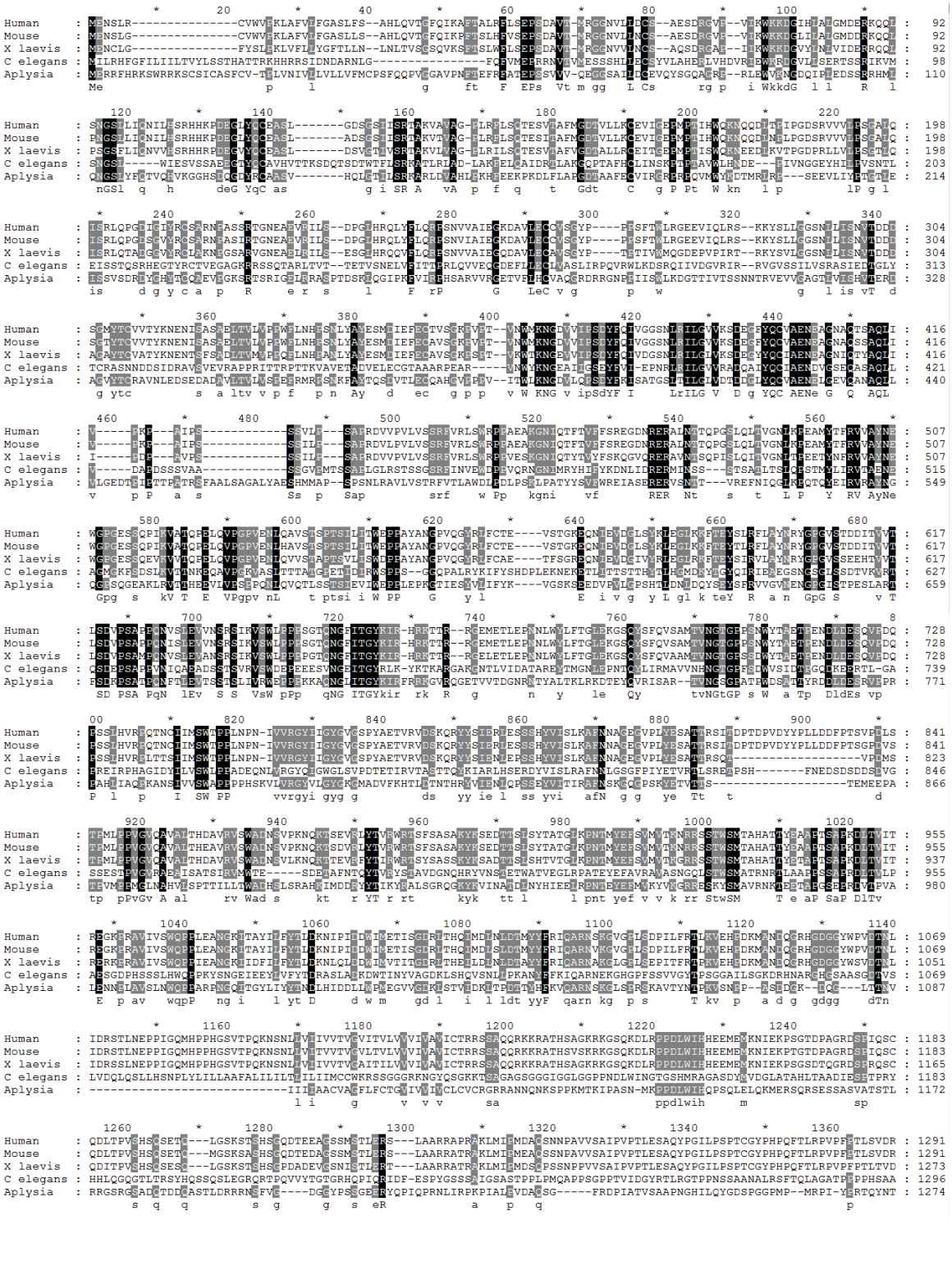

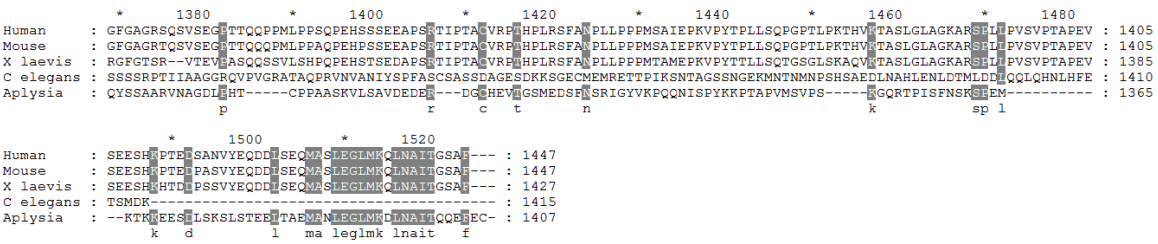

Figure 4.10. *Aplysia* DCC.receptor alignment
Alignment of *Aplysia* DCC with human, mouse, *X. laevis,* and *C. elegans* DCC.

REFERENCES

Bennett, K.L., Bradshaw, J., Youngman, T., Rodgers, J., Greenfield, B., Aruffo, A., and Linsley, P.S. (1997). Deleted in colorectal carcinoma (DCC) binds heparin via its fifth fibronectin type III domain. J Biol Chem *272*, 26940-46.

Braisted, J.E., Catalano, S.M., Stimac, R., Kennedy, T.E., Tessier-Lavigne, M., Shatz, C.J., and O'Leary, D.D. (2000). Netrin-1 promotes thalamic axon growth and is required for proper development of the thalamocortical projection. J Neurosci *20*, 5792-5801.

Cajigas, I.J., Tushev, G., Will, T.J., tom Dieck, S., Fuerst, N., and Schuman, E.M. (2012). The local transcriptome in the synaptic neuropil revealed by deep sequencing and high-resolution imaging. Neuron *74*, 453-466.

Campbell, D.S., and Holt, C.E. (2001). Chemotropic responses of retinal growth cones mediated by rapid local protein synthesis and degradation. Neuron *32*, 1013-026.

Casadio, A., Martin, K.C., Giustetto, M., Zhu, H., Chen, M., Bartsch, D., Bailey, C.H., and Kandel, E.R. (1999). A transient, neuron-wide form of CREB-mediated long-term facilitation can be stabilized at specific synapses by local protein synthesis. Cell *99*, 221-237.

Colón-Ramos, D.A., Margeta, M.A., and Shen, K. (2007). Glia promote local synaptogenesis through UNC-6 (netrin) signaling in C. elegans. Science *318*, 103-06.

Eberwine, J., Belt, B., Kacharmina, J.E., and Miyashiro, K. (2002). Analysis of subcellularly localized mRNAs using in situ hybridization, mRNA amplification, and expression profiling. Neurochem Res *27*, 1065-077.

Eliot, L.S., Kandel, E.R., and Hawkins, R.D. (1994). Modulation of spontaneous transmitter release during depression and posttetanic potentiation of Aplysia sensorymotor neuron synapses isolated in culture. J Neurosci *14*, 3280-292.

Fonseca, R., Nägerl, U.V., Morris, R.G., and Bonhoeffer, T. (2004). Competing for memory: hippocampal LTP under regimes of reduced protein synthesis. Neuron *44*, 1011-020.

Glanzman, D.L., Kandel, E.R., and Schacher, S. (1989). Identified target motor neuron regulates neurite outgrowth and synapse formation of aplysia sensory neurons in vitro. Neuron *3*, 441-450.

Glanzman, D.L., Kandel, E.R., and Schacher, S. (1990). Target-dependent structural changes accompanying long-term synaptic facilitation in Aplysia neurons. Science *249*, 799-802.

Ho, V.M., Lee, J.A., and Martin, K.C. (2011). The cell biology of synaptic plasticity. Science *334*, 623-28.

Jin, I., Puthanveettil, S., Udo, H., Karl, K., Kandel, E.R., and Hawkins, R.D. (2012). Spontaneous transmitter release is critical for the induction of long-term and intermediate-term facilitation in Aplysia. Proc Natl Acad Sci U S A *109*, 9131-36.

Jin, I., Udo, H., Rayman, J.B., Puthanveettil, S., Kandel, E.R., and Hawkins, R.D. (2012). Spontaneous transmitter release recruits postsynaptic mechanisms of long-term and intermediate-term facilitation in Aplysia. Proc Natl Acad Sci U S A *109*, 9137-142.

Jung, H., Yoon, B.C., and Holt, C.E. (2012). Axonal mRNA localization and local protein

synthesis in nervous system assembly, maintenance and repair. Nat Rev Neurosci *13*, 308-324.

Kiebler, M.A., Hemraj, I., Verkade, P., Köhrmann, M., Fortes, P., Marión, R.M., Ortín, J., and Dotti, C.G. (1999). The mammalian staufen protein localizes to the somatodendritic domain of cultured hippocampal neurons: implications for its involvement in mRNA transport. J Neurosci *19*, 288-297.

Lécuyer, E., Yoshida, H., Parthasarathy, N., Alm, C., Babak, T., Cerovina, T., Hughes, T.R., Tomancak, P., and Krause, H.M. (2007). Global analysis of mRNA localization reveals a prominent role in organizing cellular architecture and function. Cell *131*, 174-187.

Li, W., Lee, J., Vikis, H.G., Lee, S.H., Liu, G., Aurandt, J., Shen, T.L., Fearon, E.R., Guan, J.L., et al. (2004). Activation of FAK and Src are receptor-proximal events required for netrin signaling. Nat Neurosci *7*, 1213-221.

Lyles, V., Zhao, Y., and Martin, K.C. (2006). Synapse formation and mRNA localization in cultured Aplysia neurons. Neuron *49*, 349-356.

Manitt, C., Nikolakopoulou, A.M., Almario, D.R., Nguyen, S.A., and Cohen-Cory, S. (2009). Netrin participates in the development of retinotectal synaptic connectivity by modulating axon arborization and synapse formation in the developing brain. J Neurosci *29*, 11065-077.

Martin, K.C., and Ephrussi, A. (2009). mRNA localization: gene expression in the spatial dimension. Cell *136*, 719-730.

Martin, K.C., and Kosik, K.S. (2002). Synaptic tagging -- who's it? Nat Rev Neurosci *3*,

813-820.

Martin, K.C., Casadio, A., Zhu, H., Yaping, E., Rose, J.C., Chen, M., Bailey, C.H., and Kandel, E.R. (1997). Synapse-specific, long-term facilitation of aplysia sensory to motor synapses: a function for local protein synthesis in memory storage. Cell *91*, 927-938.

Meer, E.J., Wang, D.O., Kim, S., Barr, I., Guo, F., and Martin, K.C. (2012). Identification of a cis-acting element that localizes mRNA to synapses. Proc Natl Acad Sci U S A *109*, 4639-644.

Moccia, R., Chen, D., Lyles, V., Kapuya, E., E, Y., Kalachikov, S., Spahn, C.M., Frank, J., Kandel, E.R., et al. (2003). An unbiased cDNA library prepared from isolated Aplysia sensory neuron processes is enriched for cytoskeletal and translational mRNAs. J Neurosci *23*, 9409-417.

Poon, M.M., Choi, S.H., Jamieson, C.A., Geschwind, D.H., and Martin, K.C. (2006). Identification of process-localized mRNAs from cultured rodent hippocampal neurons. J Neurosci *26*, 13390-99.

Round, J., and Stein, E. (2007). Netrin signaling leading to directed growth cone steering. Curr Opin Neurobiol *17*, 15-21.

Steward, O., Wallace, C.S., Lyford, G.L., and Worley, P.F. (1998). Synaptic activation causes the mRNA for the IEG Arc to localize selectively near activated postsynaptic sites on dendrites. Neuron *21*, 741-751.

Sutton, M.A., and Schuman, E.M. (2006). Dendritic protein synthesis, synaptic plasticity, and memory. Cell *127*, 49-58.

Sutton, M.A., Ito, H.T., Cressy, P., Kempf, C., Woo, J.C., and Schuman, E.M. (2006). Miniature neurotransmission stabilizes synaptic function via tonic suppression of local dendritic protein synthesis. Cell *125*, 785-799.

Tang, S.J., Meulemans, D., Vazquez, L., Colaco, N., and Schuman, E. (2001). A role for a rat homolog of staufen in the transport of RNA to neuronal dendrites. Neuron *32*, 463-475.

Tcherkezian, J., Brittis, P.A., Thomas, F., Roux, P.P., and Flanagan, J.G. (2010). Transmembrane receptor DCC associates with protein synthesis machinery and regulates translation. Cell *141*, 632-644.

Villareal, G., Li, Q., Cai, D., and Glanzman, D.L. (2007). The role of rapid, local, postsynaptic protein synthesis in learning-related synaptic facilitation in aplysia. Curr Biol *17*, 2073-080.

Wang, D.O., Kim, S.M., Zhao, Y., Hwang, H., Miura, S.K., Sossin, W.S., and Martin, K.C. (2009). Synapse- and stimulus-specific local translation during long-term neuronal plasticity. Science *324*, 1536-540.

Wang, D.O., Martin, K.C., and Zukin, R.S. (2010). Spatially restricting gene expression by local translation at synapses. Trends Neurosci *33*, 173-182.

Willis, D.E., and Twiss, J.L. (2006). The evolving roles of axonally synthesized proteins in regeneration. Curr Opin Neurobiol *16*, 111-18.

Zhao, Y., Wang, D.O., and Martin, K.C. (2009). Preparation of Aplysia sensory-motor neuronal cell cultures. J Vis Exp 28, e1355

CHAPTER FIVE

CONCLUSIONS

IMPLICATIONS OF SPATIALLY REGULATED GENE EXPRESSION IN NEURONS

CONCLUSION

In this dissertation, I investigated the relative importance of mRNA targeting versus regulated translation in spatially restricting gene expression in neurons during synapse formation. In collaboration with Dan Ohtan Wang and Elliot Meer, I also used live-cell imaging to show local translation occurs at synapses in response to extracellular stimuli that induce transcription-dependent, learning-related synaptic plasticity (Wang et al., 2009) and identified the cis-acting localization elements that targets sensorin mRNA to synapses (Meer et al., 2012).

Local regulation of translation, rather than RNA targeting, mediates spatial regulation of gene expression during synapse formation

The human brain contains approximately 300 billion neurons, each of which makes an average of 1,000 synapses. Each of these synapses can undergo activity-dependent chages in structure and function; the persistence of these chages requires new gene expression. Previous studies have described a common and essential role of mRNA localization and a regulated translation in this process (Eberwine et al., 2002; Martin and Zukin, 2006; Dictenberg et al., 2008). While these studies have revealed a role for local translation in regulating the synaptic proteome, they have not addressed the question of how stimulus-induced local translation is integrated with stimulus-induced changes in RNA synthesis in the nucleus. My thesis work is aimed at investigating this question.

Towards this end, I first asked whether we can visualize local translation to understand regulation of gene expression during long-term synaptic plasticity in *Aplysia* sensory-motor neuron culture system. My collaborative work with postdoc fellow Dan Ohtan Wang showed that translation is regulated in a synapse and stimulus specific manner during long-term synaptic plasticity. Also, with fellow graduate student Elliot Meer in the Martin lab, we identified a 66-nt-long stem loop in the sensorin 5'UTR that is necessary for synaptic localization of the mRNA.

Next, I addressed how synaptogenic signals spatially regulate gene expression during synapse formation. I used a simple nervous system consisting of a single, birfurcated *Aplysia* SN contacting a nontarget L11 MN, with which it did not form chemical synapses, and a target L7 MN, with which it formed glutamatergic synapses (Glanzman et al., 1989). The results of my experiments reveal that RNAs and translational machinery are delivered throughout the neuron, but that translation is spatially restricted to sites of synaptic contact during synapse formation.

Having demonstrated a role for local translation during synapse formation and learning-related plasticity, my results further indicate that the guidance factor netrin-1 promotes translation at synapses, and are most consistent with a model in which synapse formation leads to release of netrin-1 from the target MNs, which upon binding presynaptic DCC receptors acts to promote translation in the presynaptic compartment (cartoon below).

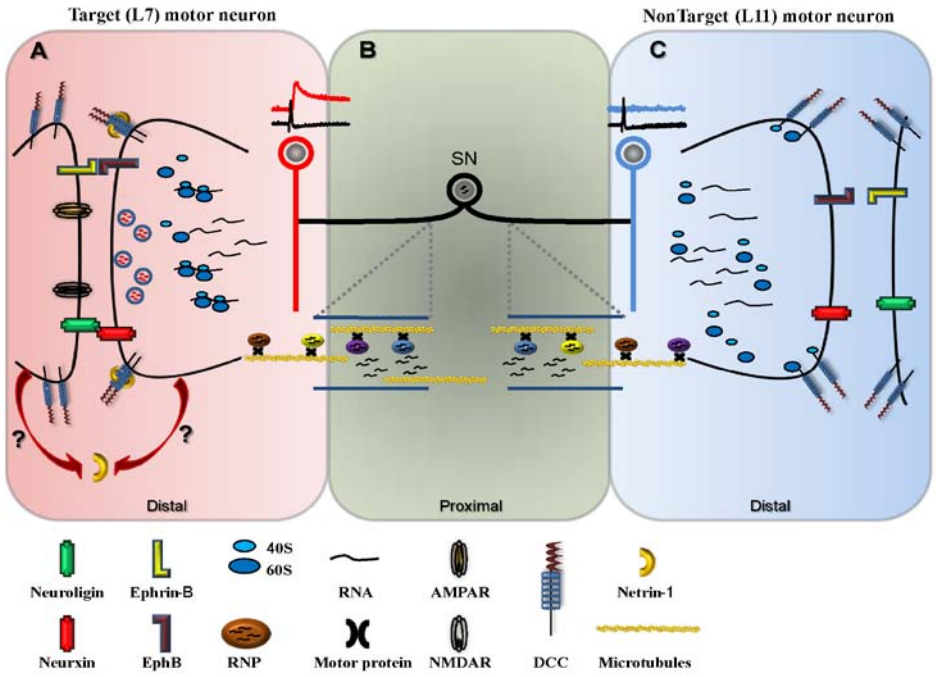

Studies in a variety of model systems have shown that the intracellular localization of a subpopulation of mRNAs serves as an essential mechanism for spatially regulating gene expression in the development and function of many polarized cells. Moreover, mRNA localization is dynamically regulated by extracellular stimuli. For example, in fibroblasts, β-actin mRNA is rapidly redistributed to the leading edge of starved cells by serum stimulation (Latham et al., 1994). In developing neurons, β-actin mRNA localizes to both the developing growth cone in axons and filopodial protrusion in dendrites, unlike γ-actin mRNAs, which are restricted to the cell body (Bassell et al., 1998). In axons, neutrophic factors BDNF and netrin-1 induces accumulation of β-actin mRNA in the growth cone as well as the asymmetrical distribution of β-actin mRNPs to the side of the growth cone near the source of BDNF and netrin-1 (Yao et al., 2006; Leung et al., 2006). The asymmetrical distribution and subsequent translation of β-actin mRNA within a

single growth cone are required for BDNF- and netrin-1-induced growth turning. Thus, physiologically relevant extracellular stimuli function to redistribute localized mRNAs and thereby to spatially regulate their translation.

Previous studies in the Martin lab identified hundreds of mRNA that localized to *Aplysia* sensory neuron processes (Moccia et al., 2003). Further studies revealed that the mRNA encoding the sensory neuron specific neuropeptide sensorin is diffusely localized in sensory neurites that do not form synapses, but concentrates at synapses upon pairing with a target motor neuron (Lyles et al., 2006). This finding led to the hypothesis that the synaptic targeting of distally localized sensorin mRNA depended on an extracellular stimulus from the target motor neuron

In different organisms and various cell types, the localization of mRNA in subcellular compartments of cells mediates multiple processes. The active transport and asymmetric distributions of mRNAs depends on intrinsic mRNA targeting elements known as localization element or zipcode sequences, initially described for β–actin mRNA (Kislauskis et al., 1994). These *cis*-acting elements are frequently located within 3'UTR of a localized mRNA and, less frequently within the 5'UTR and coding sequences. These *cis*-acting elements recruit specific trans-acting RNA binding protein to form ribonucleoproteins (RNPs), which then assemble into RNA transport granules. Numerous studies have demonstrated that localized mRNAs are transported by motor proteins along cytoskeletal elements to their final destinations in the cell. For example, the recruitment of multiple Myo4p myosin motor protein to the localization element increases the efficiency of ASH1 mRNA transport in yeast (Chung et al., 2010). The RNA-binding

protein FMRP has been shown to correlate with dendritic mRNA transportation, and to bind to kinesin light chain (KLC) as well as to the dynein-interacting protein BicD protein (Dictenberg et al., 2008; Bianco et al., 2010). Also, FMRP with distinct miRNAs, including miR125b and miR132 suppresses translation of NMDA-R mRNAs (Edbauer et al., 2010)

How is distally localized sensorin mRNA targeted to synapses during synapse formation? Our studies of sensorin mRNA localization indicate that there are at least two distinct localization elements, one in the 3'UTR that mediates localization from soma to process, and another in the 5'UTR that mediates synaptic localization (Meer et al., 2012). The identification of a 66nt-long *cis*-acting synaptic mRNA localization elements of sensorin mRNA give us one possibility that *cis*-acting element will allow us to use affinity-purification approach to identify trans-acting factors that are involved in synaptic mRNA targeting and potentially in translational repression and translational regulation.

Although I found that RNAs are evenly distributed throughout the neuron at 3 DIV, the Martin lab previously reported that there was significantly more sensorin mRNA in SN branches contacting target as compared to nontarget MNs in more mature (5 DIV) cocultures (Lyles et al., 2006). This suggests that while there is not directed targeting of sensorin mRNA from soma to process during synapse formation, there may be preferential stabilization, over time, of sensorin mRNA at sites of synaptic contact. This in turn raises questions about the mechanism underlying mRNA stability and degradation.

Roles of Netrin-1 to spatially regulate translation in the brain

Growing axons contain a subpopulation of localized mRNAs and translational machinery, providing the growth cone with spatially and functionally restricted from the cell body (Lin and Holt, 2008). In Xenopus retinal ganglion cells, the application of netrin-1 rapidly activates translation initiation factors and increases the local protein synthesis of β-actin (Leung et al., 2006).

My results also show that incubation with netrin-1increases translation of localized mRNA and synaptic strength in Aplysia sensory-motor neuron synapses. My results are most consistent with netrin-1 being release from the post-synaptic motor neuron and binding to DCC receptors on the sensory neuron to promote translation. Thus, my results show by using function-blocking DCC antibodies that netrin-1 acts as a retrograde signaling molecule from postsynaptic neuron to regulate presynaptic sensorin translation. Specifically, sensorin protein levels were decreased in sensory-motor neuron co-cultures exposed to blocking antibodies, but not in isolated sensory neurons. Also, netrin-1 enhances sensorin translation in isolated sensory neuron and sensory neurites contacting L11 non-target motor neuron, with increased phosphorylation of translation initiation factor eIF4E and also of 4EBP, which binds to and regulates the activity of eIF4E. These finding suggest that netrin-1 functions as a local cue to regulate gene expression at synapses.

Although my studies indicate that netrin-1 is a retrograde signal molecule that regulates presynaptic translation, many outstanding questions need to be addressed to confirm this hypothesis. In our previous results, postsynaptic calcium plays an important role in regulating presynaptic translation during long-term synaptic plasticity (Wang et al.,

2009). Thus, one question that needs to be studied is whether this release is regulated by postsynaptic Ca^{2+}. An additional question concerns the population of transcripts regulated by netrin-1/DCC signaling: does this signaling pathway regulate the translation of a subset of localized mRNAs, or does it globally regulate local translation? Are there additional local cues and receptors that regulate the translation of local mRNA?

Implications and future directions

Taken together, our findings show that a signaling pathway involved in axon guidance also functions to spatially restrict gene expression within neurons in a manner that regulates synapse formation. Decentralizing the control of gene expression to individual subcellular compartments enriches the adaptability and plasticity of the nervous system by enabling each compartment to change its proteome in response to local cues.

Compelling questions to address in future studies include analyze of how extracellular stimuli regulate the translation of specific transcripts and how new local translation contribute the function of neural circuits. An additional avenue of investigation concerns the coordinated regulation of protein synthesis and protein degradation, and the regulation of mRNA stability and decay during synapse formation and plasticity. Recent works suggest that non-coding RNA or miRNA may have local regulatory or structural roles (Kloc et al., 2005; Koebernic et al., 2010).

In the longer term, it will be informative to study of mRNA localization and the function of local protein synthesis in mammalian brain regions. While these processes

have been studied in the hippocampus and cerebral cortex, they may also modulate barin function and behavior in the amygdala, striatum and hypothalamus. It may have a role to modulate in brain function and behavior. Studies of mRNA localization and regulated translation may elucidate molecular mechanisms underlying neurological disorders such as intellectual disabilities and autism spectrum disorders.

REFERENCES

Bassell GJ, Z.H., Byrd AL, Femino AM, Singer RH, Taneja KL, Lifshitz LM, Herman IM, Kosik KS. (1998). Sorting of beta-actin mRNA and protein to neurites and growth cones in culture. J Neurosci *18*, 251-265.

Bianco A, D.M., Salter HK, Gatto G, Bullock SL. (2010). Bicaudal-D regulates fragile X mental retardation protein levels, motility, and function during neuronal morphogenesis. Curr Biol *20*, 1487-1492.

Bramham CR, W.D. (2007). Dendritic mRNA: transport, translation and function. Nat Rev Neurosci *8*, 776-789.

Chung S, T.P. (2010). Multiple Myo4 motors enhance ASH1 mRNA transport in Saccharomyces cerevisiae. J Cell Biol *189*, 755-767.

Dictenberg JB, S.S., Antar LN, Singer RH, Bassell GJ. (2008). A direct role for FMRP in activity-dependent dendritic mRNA transport links filopodial-spine morphogenesis to fragile X syndrome. Dev Cell *14*, 926-939.

Doyle M, K.M. (2011). Mechanisms of dendritic mRNA transport and its role in synaptic tagging. EMBO J *30*, 3540-3552.

Eberwine J, B.B., Kacharmina JE, Miyashiro K. (2002). Analysis of subcellularly localized mRNAs using in situ hybridization, mRNA amplification, and expression profiling. Neurochem Res *27*, 1065-1077.

Feig S, L.P. (1993). Pairing the cholinergic agonist carbachol with patterned Schaffer collateral stimulation initiates protein synthesis in hippocampal CA1 pyramidal cell dendrites via a muscarinic, NMDA-dependent mechanism. J Neurosci *13*, 1010-1021.

Glanzman DL, K.E., Schacher S. (1990). Target-dependent structural changes accompanying long-term synaptic facilitation in Aplysia neurons. Science *249*, 799-802.

Huber KM, K.M., Bear MF. (2000). Role for rapid dendritic protein synthesis in hippocampal mGluR-dependent long-term depression. Science *288*, 1254-1257.

Kang H, S.E. (1996). A requirement for local protein synthesis in neurotrophin-induced hippocampal synaptic plasticity. Science *273*, 1402-1406.

Kislauskis EH, Z.X., Singer RH. (1994). Sequences responsible for intracellular localization of beta-actin messenger RNA also affect cell phenotype. J Cell Biol *127*, 441-451.

Kloc M, W.K., Vargas D, Shirato Y, Bilinski S, Etkin LD. (2005). Potential structural role of non-coding and coding RNAs in the organization of the cytoskeleton at the vegetal cortex of Xenopus oocytes. Development *132*, 3445-3457.

Koebernick K, L.J., Arthur PK, Tarbashevich K, Pieler T. (2010). Elr-type proteins protect Xenopus Dead end mRNA from miR-18-mediated clearance in the soma. Proc Natl Acad Sci U S A *107*, 16148-16153.

Latham VM Jr, K.E., Singer RH, Ross AF. (1994). Beta-actin mRNA localization is regulated by signal transduction mechanisms. J Cell Biol *126*, 1211-1219.

Leung KM, v.H.F., Lin AC, Allison R, Standart N, Holt CE. (2006). Asymmetrical beta-actin mRNA translation in growth cones mediates attractive turning to netrin-1. Nat Neurosci *9*, 1247-1256.

Lyles, V., Zhao, Y., and Martin, K.C. (2006). Synapse formation and mRNA localization in cultured Aplysia neurons. Neuron *49*, 349-356.

Martin KC, C.A., Zhu H, Yaping E, Rose JC, Chen M, Bailey CH, Kandel ER. (1997). Synapse-specific, long-term facilitation of aplysia sensory to motor synapses: a function for local protein synthesis in memory storage. Cell *91*, 927-938.

Martin KC, Z.R. (2004). RNA trafficking and local protein synthesis in dendrites: an overview. J Neurosci *26*, 7131-7134.

Meer EJ, W.D., Kim S, Barr I, Guo F, Martin KC. (2012). Identification of a cis-acting element that localizes mRNA to synapses. Proc Natl Acad Sci U S A *109*, 4639-4644.

Moccia R, C.D., Lyles V, Kapuya E, E Y, Kalachikov S, Spahn CM, Frank J, Kandel ER, Barad M, Martin KC (2003). An unbiased cDNA library prepared from isolated Aplysia sensory neuron processes is enriched for cytoskeletal and translational mRNAs. J Neurosci *23*, 9409-9417.

Steward O, L.W. (1982). Preferential localization of polyribosomes under the base of dendritic spines in granule cells of the dentate gyrus. J Neurosci *2*, 284-291.

Steward O, W.P. (2001). A cellular mechanism for targeting newly synthesized mRNAs to synaptic sites on dendrites. Proc Natl Acad Sci U S A *98*, 7062-7068.

Sutton MA, S.E. (2006). Dendritic protein synthesis, synaptic plasticity, and memory. Cell *127*, 49-58.

Swanger SA, B.G. (2011). Making and breaking synapses through local mRNA regulation. Curr Opin Genet Dev *21*, 414-421.

Tang SJ, R.G., Kang H, Gingras AC, Sonenberg N, Schuman EM. (2002). A rapamycin-sensitive signaling pathway contributes to long-term synaptic plasticity in the hippocampus. Proc Natl Acad Sci U S A *99*, 467-472.

Tcherkezian J, B.P., Thomas F, Roux PP, Flanagan JG. (2010). Transmembrane receptor DCC associates with protein synthesis machinery and regulates translation. Cell *141*, 632-644.

Tiedge H, B.J. (1996). Translational machinery in dendrites of hippocampal neurons in culture. J Neurosci *16*, 7171-7181.

Wang, D.O., Kim, S.M., Zhao, Y., Hwang, H., Miura, S.K., Sossin, W.S., and Martin, K.C. (2009). Synapse- and stimulus-specific local translation during long-term neuronal plasticity. Science (New York, NY *324*, 1536-1540.

Yao J, S.Y., Wen Z, Bassell GJ, Zheng JQ. (2006). An essential role for beta-actin mRNA localization and translation in Ca2+-dependent growth cone guidance. Nat Neurosci *9*, 1265-1273.